



GE Nuclear Energy

9007030114 900627
PDR ADOCK 05000278
P PDC

SASR 90-50
DRF B11-00494
June 1990

PEACH BOTTOM ATOMIC POWER STATION,
UNIT 3 VESSEL SURVEILLANCE MATERIALS
TESTING AND FRACTURE TOUGHNESS ANALYSIS

Prepared by:

T. A. Caine

T. A. Caine, Senior Engineer
Materials Monitoring &
Structural Analysis Services

Verified by:

B. J. Branlund

B. J. Branlund, Engineer
Materials Monitoring &
Structural Analysis Services

Approved by:

S. Ranganath

S. Ranganath, Manager
Materials Monitoring &
Structural Analysis Services



GE Nuclear Energy

IMPORTANT NOTICE REGARDING
CONTENTS OF THIS REPORT
PLEASE READ CAREFULLY

This report was prepared by General Electric solely for the use of Philadelphia Electric Company. The information contained in this report is believed by General Electric to be an accurate and true representation of the facts known, obtained or provided to General Electric at the time this report was prepared.

The only undertakings of the General Electric Company respecting information in this document are contained in the contract between the customer and General Electric Company, as identified in the purchase order for this report and nothing contained in this document shall be construed as changing the contract. The use of this information by anyone other than the customer or for any purpose other than that for which it is intended, is not authorized; and with respect to any unauthorized use, General Electric Company makes no representation or warranty, and assumes no liability as to the completeness, accuracy, or usefulness of the information contained in this document.

CONTENTS

	Page
ABSTRACT	viii
ACKNOWLEDGMENTS	ix
1. INTRODUCTION	1-1
2. SUMMARY AND CONCLUSIONS	2-1
2.1 Summary of Results	2-1
2.2 Conclusions	2-5
3. SURVEILLANCE PROGRAM BACKGROUND	3-1
3.1 Capsule Recovery	3-1
3.2 RPV Materials and Fabrication Background	3-1
3.2.1 Fabrication History	3-1
3.2.2 Material Properties of RPV at Fabrication	3-2
3.2.3 Specimen Chemical Composition	3-2
3.2.4 Initial Reference Temperature	3-3
3.3 Specimen Description	3-5
3.3.1 Charpy Specimens	3-5
3.3.2 Tensile Specimens	3-6
4. PEAK RPV FLUENCE EVALUATION	4-1
4.1 Flux Wire Analysis	4-1
4.1.1 Procedure	4-1
4.1.2 Results	4-2
4.2 Determination of Lead Factors	4-3
4.2.1 Procedure	4-3
4.2.2 Results	4-4
4.3 Estimate of 32 EFPY Fluence	4-5
5. CHARPY V-NOTCH IMPACT TESTING	5-1
5.1 Impact Test Procedure	5-1
5.2 Impact Test Results	5-2
5.3 Irradiated Versus Unirradiated Charpy V-Notch Properties	5-3
5.4 Comparison to Predicted Shift	5-4
6. TENSILE TESTING	6-1
6.1 Procedure	6-1
6.2 Results	6-2
6.3 Irradiated Versus Unirradiated Tensile Properties	6-2
7. DEVELOPMENT OF OPERATING LIMITS CURVES	7-1
7.1 Background	7-1
7.2 Non-Beltline Regions	7-1
7.3 Core Beltline Region	7-2
7.4 Closure Flange Region	7-2
7.5 Core Critical Operation Requirements of 10CFR50, Appendix G	7-3

CONTENTS

	<u>Page</u>
7.6 Evaluation of Radiation Effects	7-4
7.6.1 Measured Versus Predicted Surveillance Shift	7-5
7.6.2 ART Versus EFPY	7-5
7.6.3 Fracture Toughness Conditions at 32 EFPY	7-5
7.7 Operating Limits Curves Valid to 32 EFPY	7-6
7.8 Reactor Operation Versus Operating Limits	7-6
8. REFERENCES	8-1

APPENDICES

A. IRRADIATED CHARPY SPECIMEN FRACTURE SURFACE PHOTOGRAPHS	A-1
B. UNIRRADIATED CHARPY SPECIMEN FRACTURE SURFACE PHOTOGRAPHS	B-1
C. BASIS FOR CONSERVATIVE RT_{NDT}	C-1

TABLES

<u>Table</u>	<u>Title</u>	<u>Page</u>
3-1	Chemical Composition of RPV Beltline Materials	3-8
3-2	Mechanical Properties of Beltline and Other Selected RPV Materials	3-9
3-3	Chemical Composition of Irradiated Surveillance Specimens	3-10
3-4	Identification of Unit 3 Surveillance Specimens	3-11
4-1	Summary of Daily Power History	4-6
4-2	Surveillance Capsule Flux and Fluence for Irradiation from 9/1/74 to 3/31/87	4-7
5-1	Vallecitos Riehle Charpy Machine Qualification Test Results Using NIST Standard Reference Specimens (Tested 3/5/90)	5-5
5-2	Charpy V-Notch Impact Test Results for Irradiated RPV Materials - Unit 3	5-6
5-3	San Jose Tinius-Olsen Charpy Machine Qualification Test Results Using NIST Standard Reference Specimens (Tested 5/14/90)	5-7
5-4	Charpy V-Notch Impact Test Results for Unirradiated RPV Materials - Unit 3	5-8
5-4	Significant Results of Irradiated and Unirradiated Charpy V-Notch Data for Unit 3	5-9
6-1	Tensile Test Results for Irradiated RPV Materials for Unit 3	6-3
6-2	Comparison of Unirradiated and Irradiated Tensile Properties at Room Temperature for Unit 3	6-4
7-1	Beltline Evaluation for Peach Bottom 3	7-7
7-2	Estimate of Upper Shelf Energy for Beltline Materials	7-8

ILLUSTRATIONS

<u>Figure</u>	<u>Title</u>	<u>Page</u>
2-1	Pressure-Temperature Curves Valid for 32 EFPY of Operation	2-6
3-1	Schematic of Identification on Basket Recovered from Unit 3	3-12
3-2	Schematic of the RPV Showing Identification of Vessel Beltline Plates and Welds	3-13
3-3	Fabrication Method for Base Metal Charpy Specimens	3-14
3-4	Fabrication Method for Weld Metal Charpy Specimens	3-15
3-5	Fabrication Method for HAZ Charpy Specimens	3-16
3-6	Fabrication Method for Base Metal Tensile Specimens	3-17
3-7	Fabrication Method for Weld Metal Tensile Specimens	3-18
3-8	Fabrication Method for HAZ Tensile Specimens	3-19
4-1	Schematic of Model for Two-Dimensional Flux Distribution Analysis	4-8
5-1	Irradiated Base Metal Impact Energy	5-10
5-2	Irradiated Weld Metal Impact Energy	5-11
5-3	Irradiated HAZ Impact Energy	5-12
5-4	Irradiated Base Metal Lateral Expansion	5-13
5-5	Irradiated Weld Metal Lateral Expansion	5-14
5-6	Irradiated HAZ Lateral Expansion	5-15
5-7	Comparison of Unirradiated and Irradiated Base Metal Impact Energy	5-16
5-8	Comparison of Unirradiated and Irradiated Weld Metal Impact Energy	5-17
5-9	Comparison of Unirradiated and Irradiated Base Metal Lateral Expansion	5-18
5-10	Comparison of Unirradiated and Irradiated Weld Metal Lateral Expansion	5-19

ILLUSTRATIONS

<u>Figure</u>	<u>Title</u>	<u>Page</u>
6-1	Typical Engineering Stress-Strain for Irradiated RPV Materials	6-5
6-2	Strength vs. Temperature for Irradiated Materials	6-6
6-3	Ductility vs. Temperature for Irradiated Materials	6-7
6-4	Fracture Location, Necking Behavior and Fracture Appearance for Irradiated Base Metal Tensile Specimens	6-8
6-5	Fracture Location, Necking Behavior and Fracture Appearance for Irradiated Weld Metal Tensile Specimens	6-9
6-6	Fracture Location, Necking Behavior and Fracture Appearance for Irradiated HAZ Tensile Specimens	6-10
7-1	ART of Limiting Beltline Material	7-9
7-2	Pressure-Temperature Curves Valid for 32 EFPY of Operation	7-10

ABSTRACT

A surveillance capsule was removed from the Peach Bottom Unit 3 reactor during the outage following Fuel Cycle 7. The capsule contained flux wires for neutron fluence measurement and Charpy and tensile test specimens for material property evaluation. Flux wire testing and the lead factor from previous computer analysis were used to establish the vessel peak flux location and magnitude. Charpy V-Notch impact testing and uniaxial tensile testing were performed to establish the properties of the irradiated surveillance materials. The irradiation effects were projected, based on Regulatory Guide 1.99, Revision 2, to conditions for 32 effective full power years (EFPY) of operation. The 32 EFPY conditions are predicted to be less severe than the limits in 10CFR50 Appendix G requiring provisions for vessel thermal annealing. Pressure-temperature operating limits curves valid to 32 EFPY were developed to 10CFR50 Appendix G requirements, accounting for irradiation shift per Regulatory Guide 1.99, Revision 2.

In conjunction with the surveillance capsule testing, unirradiated plate and weld Charpy specimens were tested to establish baseline curves. The irradiated Charpy data for the Unit 3 plate and weld specimens were compared to these unirradiated data to determine the shift in Charpy curves due to irradiation. The results are just above mean shift predictions, but below the upper bound predictions of the Regulatory Guide.

ACKNOWLEDGMENTS

The author gratefully acknowledges the efforts of the people mentioned below.

Flux wire testing was performed by G. C. Martin. Charpy testing was completed by G. P. Wozadlo and G. E. Dunning. Tensile specimen testing was done by S. B. Wisner and G. H. Henderson, and chemical composition analysis was performed by C. R. Judd.

1. INTRODUCTION

Part of the effort to assure reactor vessel integrity involves evaluation of the fracture toughness of the vessel ferritic materials. The key values which characterize a material's fracture toughness are the reference temperature of nil-ductility transition (RT_{NDT}) and the upper shelf energy (USE). These are defined in 10CFR50 Appendix G (Reference 1) and in Appendix G of the ASME Boiler and Pressure Vessel Code, Section XI (Reference 2). These documents contain requirements used to establish the pressure-temperature operating limits which must be met to avoid brittle fracture.

Appendix H of 10CFR50 (Reference 3) and ASTM E185 (Reference 4) establish the methods to be used for surveillance of the reactor vessel materials. The first vessel surveillance specimen capsule required by Reference 3 was removed from Unit 3 in June 1989. The capsule was sent to the GE Vallecitos Nuclear Center (VNC) for testing after exposure to seven fuel cycles of irradiation. The surveillance capsule contained flux wires for neutron flux monitoring and Charpy V-Notch impact test specimens and uniaxial tensile test specimens fabricated from materials from, or representative of, the vessel materials nearest the core (beltline). The impact and tensile specimens were tested to establish properties for the irradiated materials.

The results of the surveillance specimen testing are presented in this report. The irradiated material properties are compared to unirradiated properties from testing of archive specimens, also presented in this report. Predictions of the RT_{NDT} and USE at 32 EFPY are made for comparison with allowable values in Reference 1. Predictions of 32 EFPY properties were made based on Regulatory Guide 1.99, Revision 2 (Reference 5).

Operating limits curves for the Unit 3 reactor vessel are presented in this report. The curves account for current requirements of References 1 and 2. Geometric discontinuities and highly stressed regions, such as the feedwater nozzles and the closure flanges, are evaluated separately from the core beltline region. The operating limits developed consider the most limiting conditions of the discontinuity regions and the beltline region, so as to bound all operating conditions. The operating limits developed for the beltline region include irradiation shift, based on Reference 5 methods.

2. SUMMARY AND CONCLUSIONS

2.1 SUMMARY OF RESULTS

Surveillance capsule 1 was removed from Peach Bottom Unit 3 during the outage following Fuel Cycle 7 and shipped to VNC. The flux wires, Charpy V-Notch and tensile test specimens removed from the capsule were tested according to ASTM E185-82 (Reference 4). Revised operating limits curves were developed using the flux wire test results and the requirements and methods of 10CFR50 Appendix G (Reference 1) and Appendix G of ASME Code Section XI (Reference 2). The methods and results of the fracture toughness evaluation are presented in this report as follows:

- a. Section 3: Surveillance Program Background
- b. Section 4: Peak RPV Fluence Evaluation
- c. Section 5: Charpy V-Notch Impact Testing
- d. Section 6: Tensile Testing
- e. Section 7: Development of Operating Limits Curves

Photographs of fractured Charpy specimens are in Appendix A. The significant results of the evaluation are below:

- a. Capsule 1 was removed from the 30° azimuth position of the reactor. The capsule contained 9 flux wires: 3 copper (Cu), 3 iron (Fe), and 3 nickel (Ni). There were 36 Charpy V-Notch specimens in the capsule: 12 each of plate material, weld material and heat affected zone (HAZ) material. The 8 tensile specimens removed consisted of 3 plate, 2 weld and 3 HAZ metal specimens.

- b. The chemical compositions of the beltline materials were determined from data obtained from GE QA records or from correspondence with Babcock & Wilcox (B&W). The copper (Cu) and nickel (Ni) contents were determined for all heats of plate and weld material. The values for the limiting beltline plate are 0.15% Cu and 0.49% Ni. The limiting beltline weld values are 0.21% Cu and 0.21% Ni.
- c. Charpy and dropweight test results from the fabrication program materials certification testing were adjusted to be equivalent to test results done to current standards. The initial RT_{NDT} values for locations of interest in the vessel were determined. They are 10°F for the limiting beltline plate, -45°F for the limiting beltline weld (with $\sigma_I = 16.44^\circ F$), 10°F for the closure flange region, 50°F for the limiting nozzle and 54°F for the bottom head region.
- d. The flux wires were tested to determine the neutron flux at the surveillance capsule location. The fast flux (>1.0 MeV) measured was 6.8×10^8 n/cm²-sec. Based on the flux wire data, the surveillance specimens received a best estimate fluence of 1.6×10^{17} n/cm² at removal.
- e. The vessel inside surface lead factors were established using an analysis performed for Peach Bottom Unit 2 that combined two-dimensional and one-dimensional finite difference transport analysis. The flux peak occurs at an azimuthal location 25.5° from the vessel quadrant references. The lead factor for the surveillance capsules is 0.95 to the peak vessel inside surface location.

- f. The maximum accumulated neutron fluence at 32 EPFY was determined at the peak 1/4 T location, using the flux wire test results, the lead factor and the methods of Reference 5. The maximum 1/4 T vessel 32 EPFY fluence is 5.0×10^{17} n/cm².
- g. The surveillance Charpy V-Notch specimens were impact tested at temperatures selected to define the transition of the fracture toughness curves of the plate, weld, and HAZ materials. Measurements were taken of absorbed energy, lateral expansion and percentage shear. Fracture surface photographs of each specimen are presented in Appendix A. From absorbed energy and lateral expansion results for the plate and weld materials the following values were calculated: index temperatures for 30 ft-lb, 50 ft-lb, and 35-mil lateral expansion (MLE) values and USE. Similar test results were obtained for archive plate and weld Charpy specimens provided by PECO. The unirradiated specimen fracture surface photographs are presented in Appendix B.
- h. The curves of irradiated plate and weld specimen Charpy impact energies were compared to the corresponding unirradiated data to establish the 30 ft-lb, 50 ft-lb and 35 MLE index temperature irradiation shifts, and decreases in USE. The surveillance plate material showed an estimated 16°F shift and a 10% decrease in USE. The weld material estimated shift was also 16°F, with a decrease in USE of 9%.
- i. The irradiated tensile specimens were tested at room temperature (70°F), reactor operating temperature (550°F), and estimated onset to upper shelf temperature (160°F). The results tabulated for each specimen include yield and ultimate tensile strength, uniform and total elongation, and reduction of area.
- j. The irradiated plate and weld tensile test results for Unit 3 were compared to unirradiated data from the vessel fabrication test program records. The results generally showed increasing strength and decreasing ductility, consistent with expectations for irradiation embrittlement.

- k. As a part of the development of the pressure-temperature (P-T) operating limits curves, the irradiation shifts in RT_{NDT} were predicted, based on the methods of Regulatory Guide 1.99, Revision 2 (Reference 5). For information purposes, the measured shifts for the surveillance plate and weld materials were compared to the shifts predicted by Reference 5. The measured shift of 16°F in the plate material 30 ft-lb index, for a fluence of 1.6×10^{17} n/cm², is just above the predicted mean shift of 14°F, but is well below the upper limit shift prediction of 28°F. For the weld material, the measured shift of 16°F is slightly higher than the predicted mean shift of 15°F and well below the upper bound of 30°F.
- l. Data for prediction of most beltline material USE values were not available. Data for the surveillance materials and the longitudinal beltline welds were used to predict USE at 32 EFPY using the methods in Reference 5. The beltline transverse plate and weld USE values were predicted to be 78 ft-lb and 82 ft-lb, respectively, at 32 EFPY.
- m. P-T curves were developed for three reactor conditions: hydrostatic pressure test (Curve A), non-nuclear heatup and cooldown (Curve B), and core critical operation (Curve C). The curves are valid up to 32 EFPY of operation. The limiting regions of the vessel affecting the curves' shapes are the nozzle, bottom head and closure flange regions. The bolt preload and minimum permissible operating temperatures were determined to be 70°F. The predicted irradiation shifts for the Unit 3 beltline materials are low enough that the beltline is not predicted to be limiting through 32 EFPY of operation. The P-T curves for Unit 3 are shown in Figure 2-1.

2.2 CONCLUSIONS

The requirements of Reference 1 deal basically with vessel design life conditions and with limits of operation designed to prevent brittle fracture. Based on the evaluation of surveillance testing results, and the associated analyses, the following conclusions are made:

- a. The adjusted reference temperatures at 32 EFPY for the limiting beltline material of 71°F is below the Reference 1 allowable limit of 200°F, above which special analyses or provisions for annealing are required.
- b. The 32 EFPY values of USE could not be calculated for all beltline plates, but the 32 EFPY USE for the surveillance beltline plate, 78 ft-lb, and the lowest USE predicted for beltline welds, 82 ft-lb, are well above the Reference 1 allowable minimum of 50 ft-lb. The surveillance plate USE should be representative of the other beltline plates' USE values, so there is no need, based on USE values, for special analyses or provisions for annealing the Unit 3 vessel beltline.
- c. Examination of the normal and upset operating conditions expected for the reactor shows that the worst pressure-temperature conditions expected from unplanned temperature transients are acceptable relative to the limits in Figure 2-1. Therefore, the only operating conditions for which the operating limits are a concern are those involving operator interaction, such as pressure testing and initiation of core criticality.

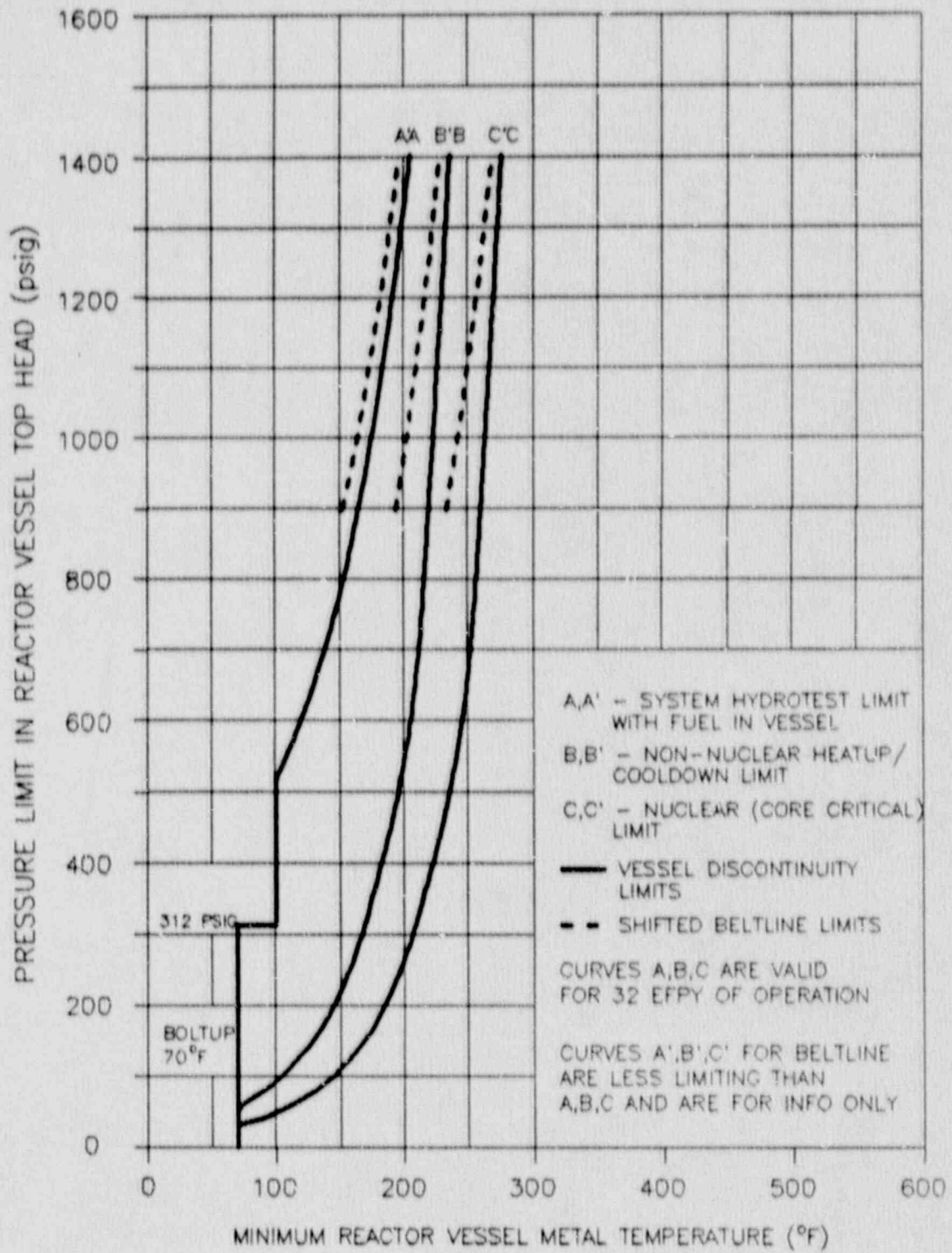


Figure 2-1. Pressure-Temperature Curves Valid for 32 EFPY of Operation

3. SURVEILLANCE PROGRAM BACKGROUND

3.1 CAPSULE RECOVERY

The Peach Bottom Unit 3 reactor was shut down in March, 1987. The accumulated thermal power output was 9.11×10^6 MWd or 7.57 EFPY. The reactor pressure vessel (RPV) originally contained three surveillance capsules, at 30°, 120° and 300° azimuths at the core midplane. The specimen capsules are held against the RPV inside surface by a spring loaded specimen holder. Each capsule receives equal irradiation because of core symmetry. In June 1989, Capsule 1 at 30° was removed. The capsule was cut from its holder assembly and shipped by cask to the GE Vallecitos Nuclear Center (VNC), where testing was performed.

Upon arrival at VNC, the capsule was examined for identification. The drilled hole binary code on the basket showed the reactor number of 27 and the capsule number of 1, as shown in Figure 3-1. The capsule contained three Charpy specimen packets and four tensile specimen tubes. Each tensile specimen tube contained two tensile specimens. Each Charpy specimen packet contained 12 plate, weld or HAZ Charpy specimens and 3 flux wires (one iron, one copper and one nickel) in a sealed helium environment.

3.2 RPV MATERIALS AND FABRICATION BACKGROUND

3.2.1 Fabrication History

The Peach Bottom 3 RPV is a 251 inch diameter BWR/4 design. Construction was begun by B&W to the Winter 1965 Addenda of the 1965 edition of the ASME Code. Chicago Bridge & Iron (CB&I) completed the vessel, generally to the 1968 edition of the ASME Code. The shell and head plate materials are ASME SA302, Grade B, low alloy steel (LAS), modified per Code Case 1339. The nozzles and closure flanges are ASTM A508 Class 2 LAS, modified per Code Case 1332-3, and the closure flange bolting materials are ASTM A540 Grade B23. The fabrication process employed double quench and temper heat treatment immediately after hot forming, then electroslag or submerged arc welding and post-weld heat treatment. The

post-weld heat treatment was typically for 30 hours at temperatures of $1125 \pm 25^\circ\text{F}$. The identification of plates and welds in the beltline region is shown in Figure 3-2.

3.2.2 Material Properties of RPV at Fabrication

Material certification records were retrieved from GE Quality Assurance (QA) records to determine chemical and mechanical properties of the vessel materials. In addition, data on the electroslag welds was obtained from the Unit 2 surveillance test report (Reference 6). Table 3-1 shows the chemistry data for the Unit 3 beltline materials.

Results of certification mechanical property tests performed during RPV fabrication were examined, specifically Charpy V-Notch and dropweight impact test results. Properties of the beltline materials and other locations of interest are presented in Table 3-2. The Charpy data collected were used to establish the RT_{NDT} values for each vessel component, as described in Subsection 3.2.4.

3.2.3 Specimen Chemical Composition

Samples were taken from the surveillance plate and weld tensile specimens after they were tested. Chemical analyses were performed using a Spectraspan III plasma emission spectrometer. Each sample was dissolved in an acid solution to a concentration of 40 mg steel per 40 ml solution. The spectrometer was calibrated for determination of Mn, Ni, Mo and Cu by diluting National Institute of Standards and Technology (NIST) Spectrometric Standard Solutions. The phosphorus calibration involved analysis of four reference materials from NIST with known phosphorus levels. Analysis accuracies are $\pm 0.003\%$ (absolute) for phosphorus and $\pm 5\%$ (relative) for other elements. The chemical composition results are given in Table 3-3 for the Unit 3 surveillance plate and weld materials. The results for the plate show reasonable agreement with corresponding data from fabrication records in Table 3-1. However, the surveillance weld chemistry results do not correspond to the results for the beltline electroslag weld heat, as would be expected from normal B&W practices. The surveillance weld is, however, representative of the beltline welds.

3.2.4 Initial Reference Temperatures

The requirements for establishing the vessel component RT_{NDT} values per the ASME Code prior to 1972 are summarized as follows:

- a. Test specimens shall be longitudinally oriented Charpy V-Notch specimens.
- b. At the RT_{NDT} , no impact test result shall be less than 25 ft-lb, and the average of three test results shall be at least 30 ft-lb.
- c. Pressure tests shall be conducted at a temperature at least 60°F above the acceptable RT_{NDT} for the vessel.

The current requirements for establishing RT_{NDT} are significantly different. For plants constructed to the ASME Code after Summer 1972, the requirements are as follows:

- a. Charpy V-Notch specimens shall be oriented normal to the rolling direction (transverse).
- b. RT_{NDT} is defined as the higher of the dropweight NDT or 60°F below the temperature at which Charpy V-Notch 50 ft-lb energy and 35 mils lateral expansion are met.
- c. Bolt-up in preparation for a pressure test or normal operation shall be performed at or above the RT_{NDT} or lowest service temperature (LST), whichever is greater.

Reference 1 states that for vessels constructed to a version of the ASME Code prior to the Summer 1972 Addendum, fracture toughness data and data analyses must be supplemented in an approved manner. GE has developed methods for analytically converting fracture toughness data for vessels constructed before 1972 to comply with current requirements. GE developed these methods from data in WRC Bulletin 217 (Reference 7) and from data collected to respond to NRC questions on FSAR submittals in the late 1970s.

These methods and example RT_{NDT} calculations for vessel plate, weld, weld HAZ, forging, and bolting material are summarized in the remainder of this subsection. Calculated RT_{NDT} values for selected RPV locations are given in Table 3-2.

For vessel plate material, the first step in calculating RT_{NDT} is to establish the 50 ft-lb transverse test temperature from longitudinal test specimen data. There are typically three energy values at a given test temperature. The lowest energy Charpy value is adjusted by adding 2°F per ft-lb energy to 50 ft-lb. For example, for the limiting Unit 3 beltline plate the test temperature and lowest Charpy energy from Table 3-2 is 44 ft-lb at +10°F for Heat C2773-2. The equivalent 50 ft-lb longitudinal test temperature is:

$$T_{50L} = 10^{\circ}\text{F} + [(50 - 44) \text{ ft-lb} * 2^{\circ}\text{F/ft-lb}] = 22^{\circ}\text{F}$$

The transition from longitudinal data to transverse data is made by adding 30°F to the test temperature. In this case, the 50 ft-lb transverse Charpy test temperature is $T_{50T} = 52^{\circ}\text{F}$. The RT_{NDT} is the greater of NDT or $(T_{50T} - 60^{\circ}\text{F})$. From Table 3-2, the NDT for Heat C2773-2 is 10°F, and $(T_{50T} - 60^{\circ}\text{F})$ is -8°F. Thus, the RT_{NDT} for that beltline plate is 10°F.

For vessel weld material, the Charpy V-Notch results are usually limiting in establishing RT_{NDT}. The 50 ft-lb test temperature is established as for the plate material, but the 30°F adjustment to convert longitudinal data to transverse data is not applicable to weld metal. In Reference 6, nine sets of Charpy curves for the electroslag weld heat used in Units 2 and 3 were evaluated to determine $(T_{50T} - 60^{\circ}\text{F})$ of -45°F. There are no NDT data available for the longitudinal electroslag welds. The GE procedure requires that, when no NDT is available, the resulting RT_{NDT} be -50°F or higher. In this example, $(T_{50T} - 60^{\circ}\text{F})$ is -45°F, so the RT_{NDT} is -45°F. Since the RT_{NDT} for the electroslag welds was based on statistical analysis of 9 curves, the value of σ_I discussed in Reference 6 is the standard deviation from the statistical analysis of the 9 curves, or 16.44°F.

For the vessel weld HAZ material, the RT_{NDT} is assumed to be the same as for the base material since ASME Code weld procedure qualification test requirements and post-weld heat treatment data indicate this assumption is valid.

For vessel forging material, such as nozzles and closure flanges the method for establishing RT_{NDT} is the same as for vessel plate material. For the recirculation inlet nozzles N2, the lowest Charpy data at 40°F is 30 ft-lb, and the NDT is 10°F. In this case, ($T_{50T} - 60°F$) is greater than NDT, so the RT_{NDT} is $[40 + (50-30)*2 + 30 - 60]$, or 50°F.

For bolting material, the current ASME Code requirements define the LST as the temperature at which transverse Charpy V-Notch energy of 45 ft-lb and 25 mils lateral expansion (MLE) are achieved. If the required Charpy results are not met, or are not reported, but the Charpy V-Notch energy reported is above 30 ft-lb, the requirements of the ASME Code at construction are applied, namely that the 30 ft-lb test temperature plus 60°F is the lowest service temperature (LST) for the bolting materials. Charpy data for the studs did not meet the 45 ft-lb, 25 MLE requirement, but 30 ft-lb energies were met at 10°F. Therefore, the bolting material LST is 70°F.

3.3 SPECIMEN DESCRIPTION

The surveillance capsule contained 36 Charpy specimens: base metal (12), weld metal (12), and HAZ (12). There were 8 tensile specimens: base metal (3), weld metal (2), and HAZ (3). The capsule contained 9 flux wires: 3 iron, 3 nickel and 3 copper. The chemistry and fabrication history for the Charpy and tensile specimens are described in this section.

3.3.1 Charpy Specimens

Charpy specimen fabrication is described in the vessel purchase specification (Reference 8). All specimen materials were specified to be beltline materials, but the chemistry test results indicate that the weld wire heat used is not the same as that in the Unit 3 beltline. It is, however, representative of the beltline electroslag welds.

The base metal specimens were cut from Heat C3103-1. The surveillance test plates received the same heat treatment as the fabrication specimens for Heat C3103-1, including the post-weld heat treatment for 30 hours at $1125^{\circ}\text{F} \pm 25^{\circ}\text{F}$. The method used to machine the specimens from the test plate is shown in Figure 3-3. Specimens were machined from the 1/4 T and 3/4 T positions in the plate, in the longitudinal orientation (long axis parallel to the rolling direction). The identifications of the base metal Charpy specimens recovered from the surveillance capsule are shown in Table 3-4.

The weld metal and HAZ Charpy specimens were fabricated by welding together two pieces of the surveillance test plate with a weld which was specified to be identical to the beltline longitudinal seam welds. The same weld procedure was used, but the actual weld wire heat and flux lot probably were not used in the vessel beltline welds, based on the results of the specimen chemistry tests. The welded test plate for the weld and HAZ Charpy specimens each received stress relief heat treatment at $1125^{\circ}\text{F} \pm 25^{\circ}\text{F}$ for 30 hours to simulate the fabrication specimen conditions. The weld specimens and HAZ specimens were fabricated as shown in Figures 3-4 and 3-5, respectively. The base metal orientation in the weld and HAZ specimens was longitudinal. The specimens were stamped on one end with the identifications shown in Table 3-4.

3.3.2 Tensile Specimens

Fabrication of the surveillance tensile specimens is described in Reference 8. The materials, and thus the chemical compositions and heat treatments for the base, weld and HAZ tensiles are the same as those for the corresponding Charpy specimens. The identifications of the base, weld, and HAZ tensile specimens are given in Table 3-4. A summary of the fabrication methods follows.

The base metal specimens were machined from material at the 1/4 T and 3/4 T depth. The specimens, oriented along the plate rolling direction, were machined to the dimensions shown in Figure 3-6. The gage section was tapered to a minimum diameter of 0.250 inch at the center. The weld metal

tensile specimen materials were cut from the welded test plates, as shown in Figure 3-7. The specimens were machined entirely from weld metal, scrapping material that might include base metal. The fabrication method for the HAZ tensile specimens is illustrated in Figure 3-8. The specimen blanks were cut from the welded test plates such that the gage section minimum diameters were machined at the weld fusion line. The finished HAZ specimens are approximately half weld metal and half base metal oriented along the plate rolling direction.

Table 3-1
CHEMICAL COMPOSITION OF RPV BELTLINE MATERIALS

Identification	Heat/Lot No.	Composition by Weight Percent							
		C	Mn	P	S	Si	Ni	Mo	Cu
Lower Shell Plates:									
6-146-1	C4689-2	0.21	1.27	0.011	0.016	0.25	0.56	0.60	0.12
6-146-3	C4684-2	0.22	1.41	0.013	0.016	0.24	0.58	0.55	0.13
6-146-7	C4627-1	0.22	1.32	0.015	0.016	0.25	0.57	0.56	0.12
Lower-Intermediate Shell Plates:									
6-139-10	C2773-2	0.22	1.30	0.012	0.018	0.24	0.49	0.48	0.15
6-139-11	C2775-1	0.21	1.34	0.010	0.018	0.19	0.46	0.46	0.13
6-139-12	C3103-1	0.21	1.35	0.011	0.016	0.24	0.60	0.47	0.14
Intermediate Shell Plates:									
6-146-5	C4608-1	0.23	1.30	0.011	0.015	0.24	0.55	0.55	0.12
6-146-4	C4689-1	0.21	1.27	0.011	0.016	0.25	0.56	0.60	0.12
6-146-2	C4654-1	0.23	1.38	0.010	0.015	0.24	0.55	0.56	0.11
Surveillance Plate:									
	C3103-1	see above							
Longitudinal Welds:									
D1,D2,D3, E1,E2,E3,F1,F2,F3	37C065	0.17	1.41	0.015	0.013	0.09	0.21	0.53	0.21
Lower to Lower-Intermediate Girth Weld:									
EE	3P4000, Linde 124 Flux Lot 3932	0.066	1.37	0.015	0.014	0.36	0.96	0.46	0.02
Intermediate to Lower-Intermediate Girth Weld:									
EF	IP4217, Linde 124 Flux Lot 3929	0.051	1.37	0.017	0.018	0.45	0.96	0.47	0.11
Surveillance Weld:									
		-	1.56	0.009	-	0.19	0.41	0.51	0.11

Table 3-2

MECHANICAL PROPERTIES OF BELTLINE AND OTHER SELECTED RPV MATERIALS

<u>Location</u>	<u>Ident. Number</u>	<u>Heat Number</u>	<u>Test Temp. (°F)</u>	<u>Charpy Energy (ft-lb)</u>	<u>NDT (°F)</u>	<u>T_{50T}-60 (°F)</u>	<u>RT_{NDT} (°F)</u>
<u>Beltline:</u>							
Lower Shell Plates	6-146-1	C4689-2	10	101,78,69	-10	-20	-10
	6-146-3	C4684-2	10	63,60,60	-20	-20	-20
	6-146-7	C4627-1	10	68,82,90	-20	-20	-20
Lower Intermediate Shell Plates	6-139-10	C2773-2	10	44,56,46	10	-8	10
	6-139-11	C2775-1	10	58,66,68	10	-20	10
	6-139-12	C3103-1	10	57,66,76	10	-20	10
Intermediate Shell Plates	6-146-5	C4608-1	10	82,108,90	10	-20	10
	6-146-4	C4689-1	10	60,96,105	10	-20	10
	6-146-2	C4654-1	10	55,77,78	10	-20	10
Longitudinal Welds	D1,D2,D3 E1,E2,E3 F1,F2,F3	37C065	see Reference 6 ($\sigma_I = 16.44^\circ\text{F}$)				-45
Lower to Lower-Int. Girth Weld	DE	3P4000	10	97,96,90	N/A	-50	-50
Lower-Int. to Int. Girth Weld	EF	IP4217	10	56,71,60	N/A	-50	-50
<u>Non-Beltline:</u>							
Upper Shell Plate	15-146-2	C4598-1	10	42,80,80	10	-4	10
Vessel Flange	48-146-1	ACN97	10	96,109,127	10	-20	10
Head Flange	209-139-2	AAL95	10	81,87,94	10	-20	10
Top Head Torus	202-139-11	C1982-1	10	45,60,90	10	-10	10
Bottom Head Torus	A2-146-4	B7255-2	40	81,28,64	40	54	54
Recirc Inlet N2	A7-139-15	EV9934	40	30,40,31	10	50	50

NOTE: N/A = not available

Table 3-3
 CHEMICAL COMPOSITION OF IRRADIATED SURVEILLANCE SPECIMENS

Identification	Composition by Weight Percent									
	C	Mn	P	S	Si	Ni	Mo	Cu		
Plate:										
A41	^a	1.45	0.007	-	0.24	0.62	0.50	0.13		
A46	-	1.48	0.007	-	0.22	0.64	0.52	0.13		
Weld:										
A4P	-	1.55	0.009	-	0.19	0.40	0.50	0.11		
A54	-	1.57	0.009	-	0.19	0.41	0.51	0.11		

^a A - mark denotes an element that was not evaluated.

Table 3-4

IDENTIFICATION OF UNIT 3 SURVEILLANCE SPECIMENS

Charpy Specimens^a

<u>Irradiated</u> <u>Base</u>	<u>Unirradiated</u> <u>Base</u>	<u>Irradiated</u> <u>Weld</u>	<u>Unirradiated</u> <u>Weld</u>	<u>Irradiated</u> <u>HAZ</u>
7P1	7PC	7TJ	7TE	A27
7LU	7LY	7TL	7U1	A1C
7T6	7MT	7UA	7U6	A1E
7TB	7MY	7TK	7U2	A1L
7MU	7P4	7UU	7U3	A1K
7M5	7M3	7TU	7TP	A3A
7PP	7M2	7UP	7TM	A22
7M7	7P7	7TD	7U4	A2E
7P2	7MD	A11	7TT	A23
7MJ	7PB	A15	7U5	A1D
7MB	7MM	7YD	7TY	A1J
7PY	7PD	A14	7U7	A2T

Tensile Specimens^a

<u>Irradiated</u> <u>Base</u>	<u>Irradiated</u> <u>Weld</u>	<u>Irradiated</u> <u>HAZ</u>
A41	A4P	A62
A4A	A54	A5M
A46		A5E

^a All specimen identifications include two dots.

3-12

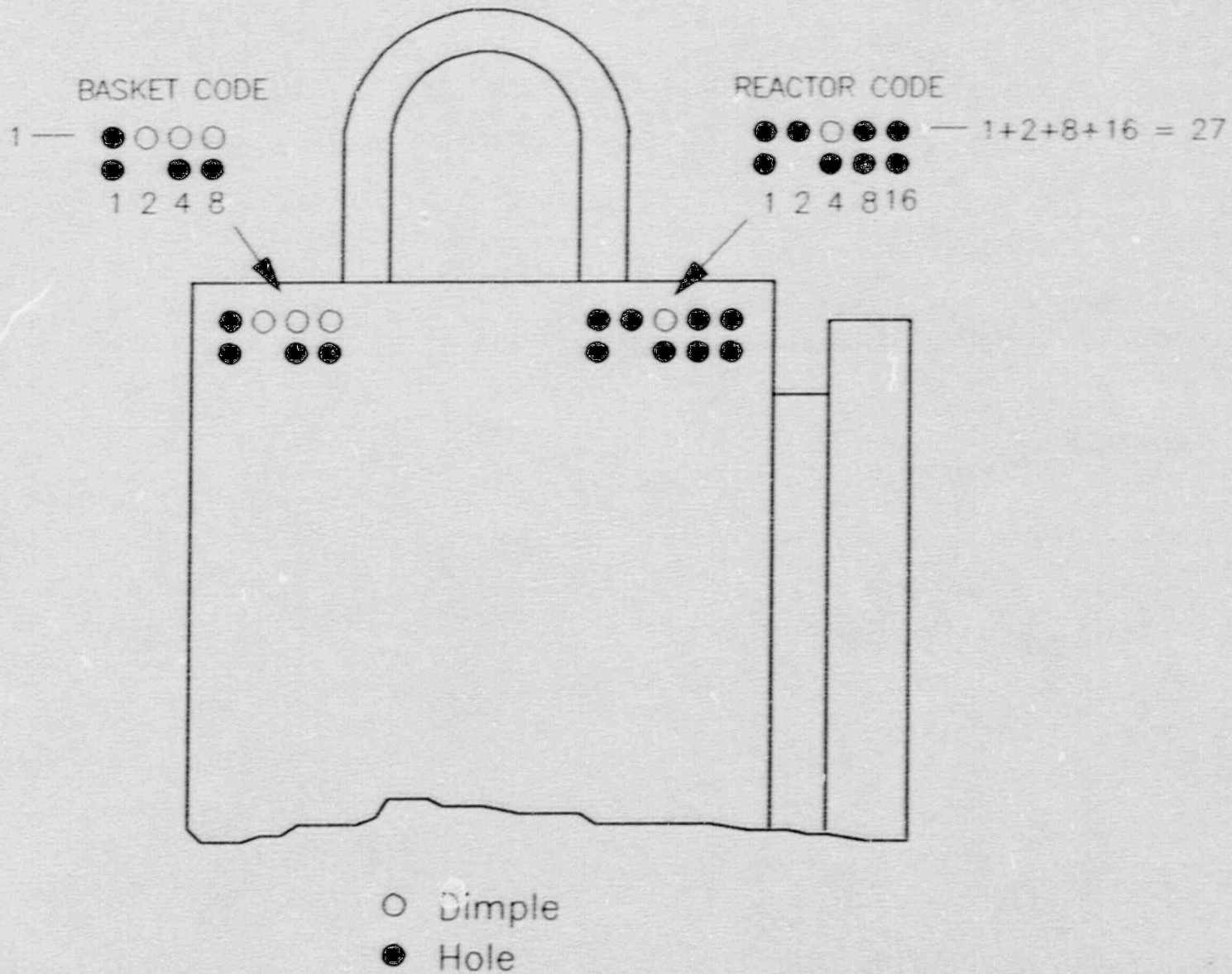


Figure 3-1. Schematic of Identification on Basket Recovered from Unit 3

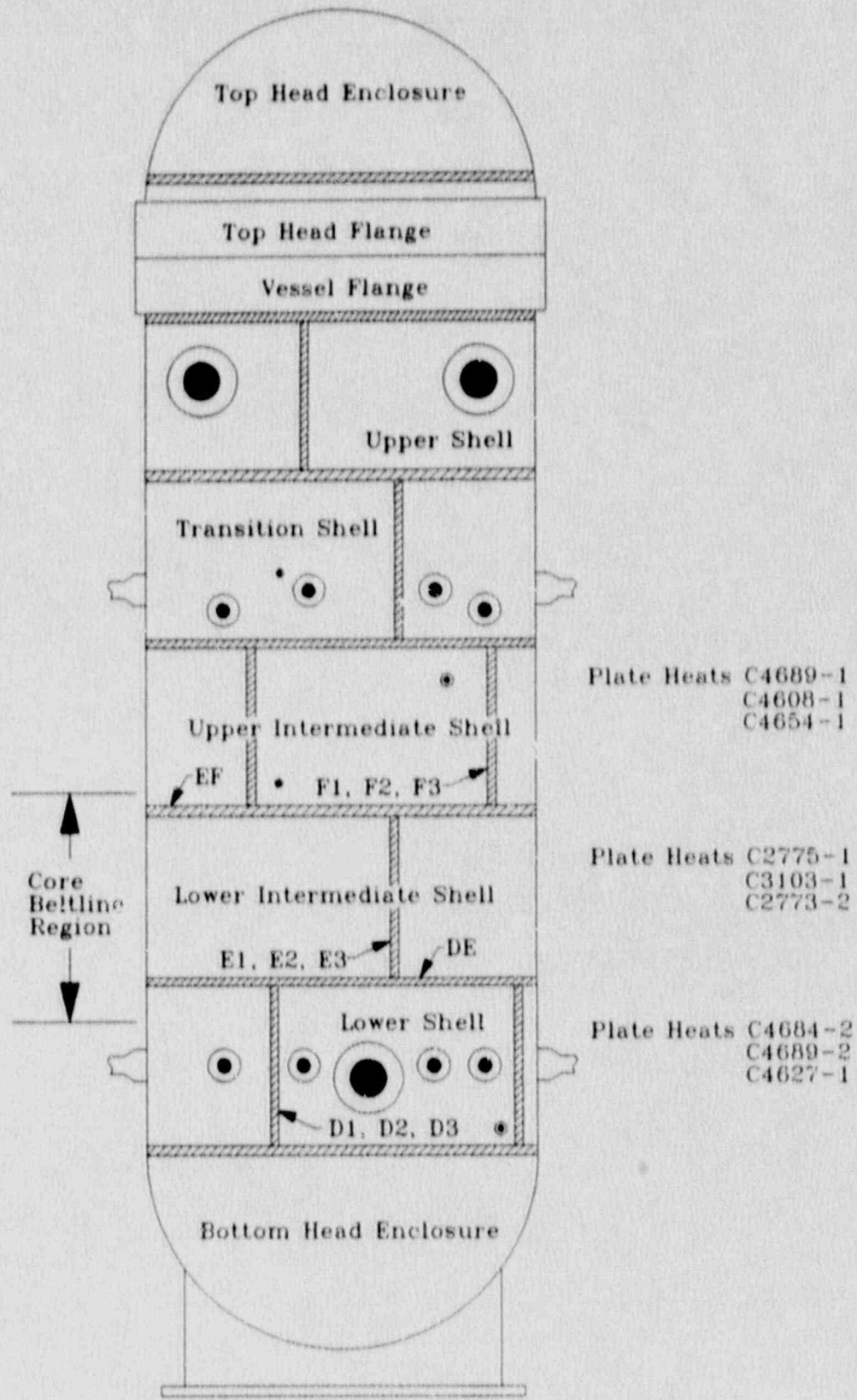


Figure 3-2. Schematic of the RPV Showing Identification of Vessel Beltline Plates and Welds

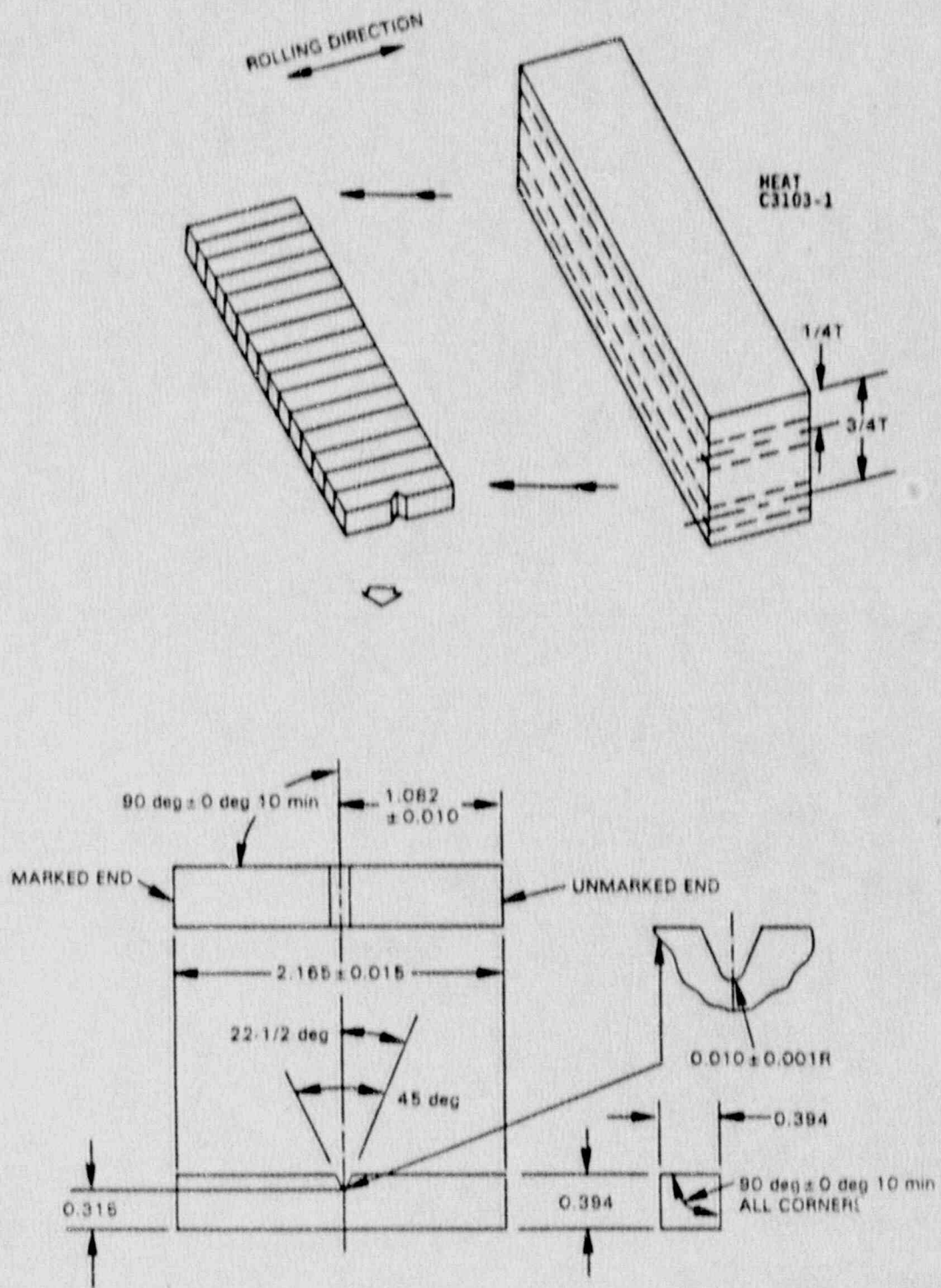


Figure 3-3. Fabrication Method for Base Metal Charpy Specimens

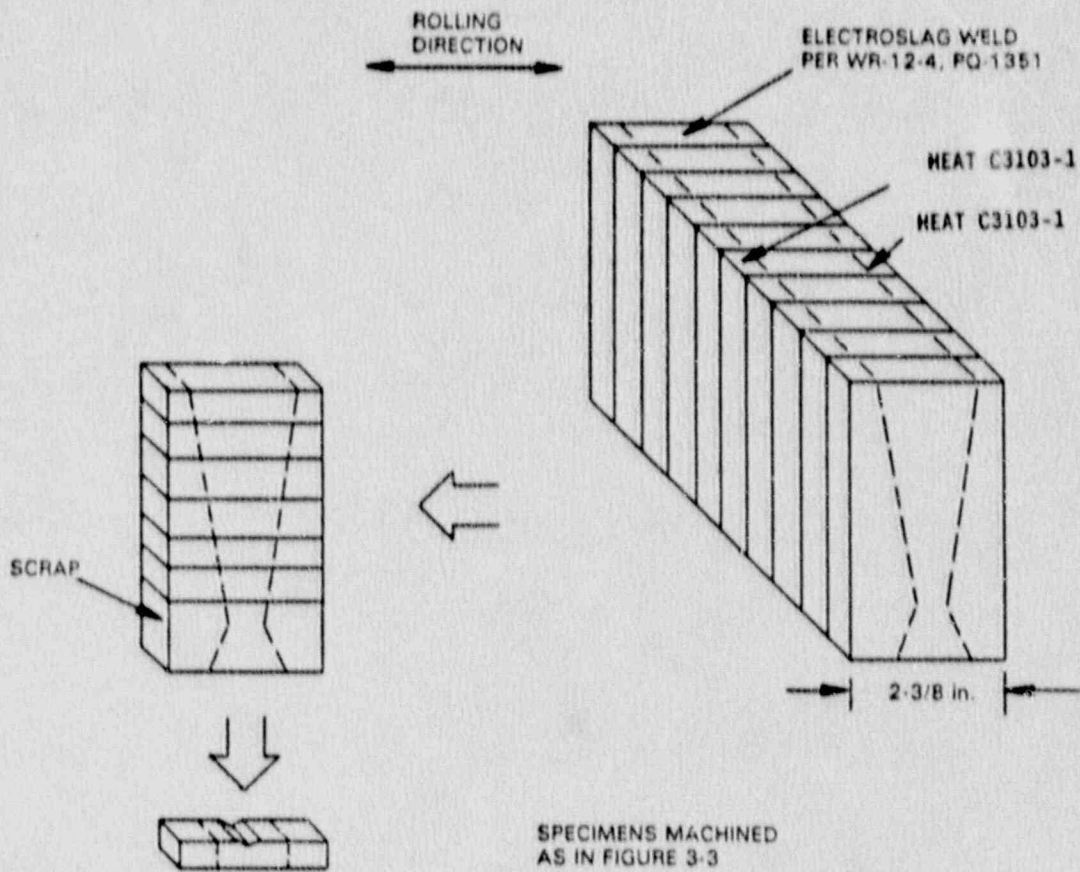


Figure 3-4. Fabrication Method for Weld Metal Charpy Specimens

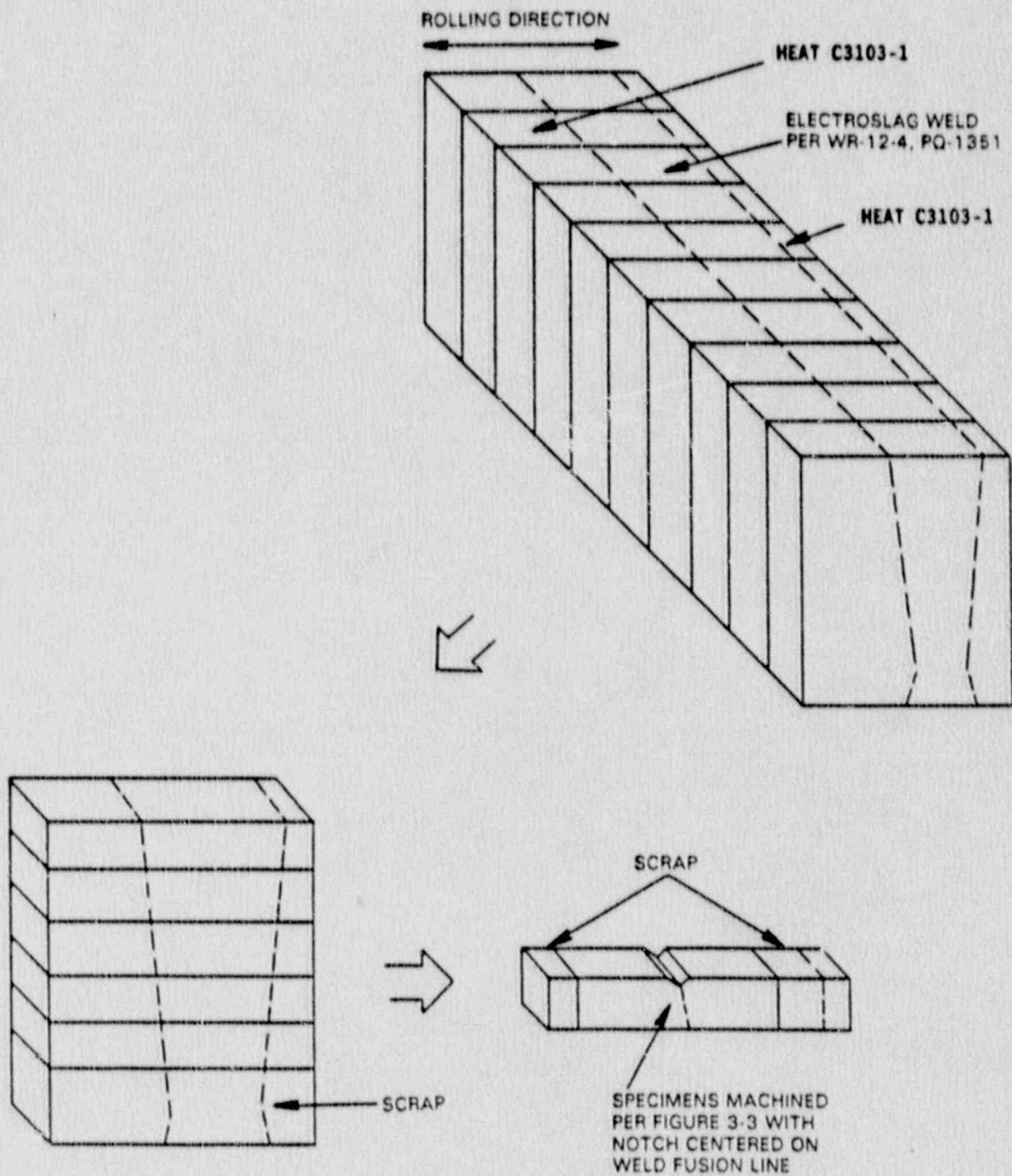


Figure 3-5. Fabrication Method for HAZ Charpy Specimens

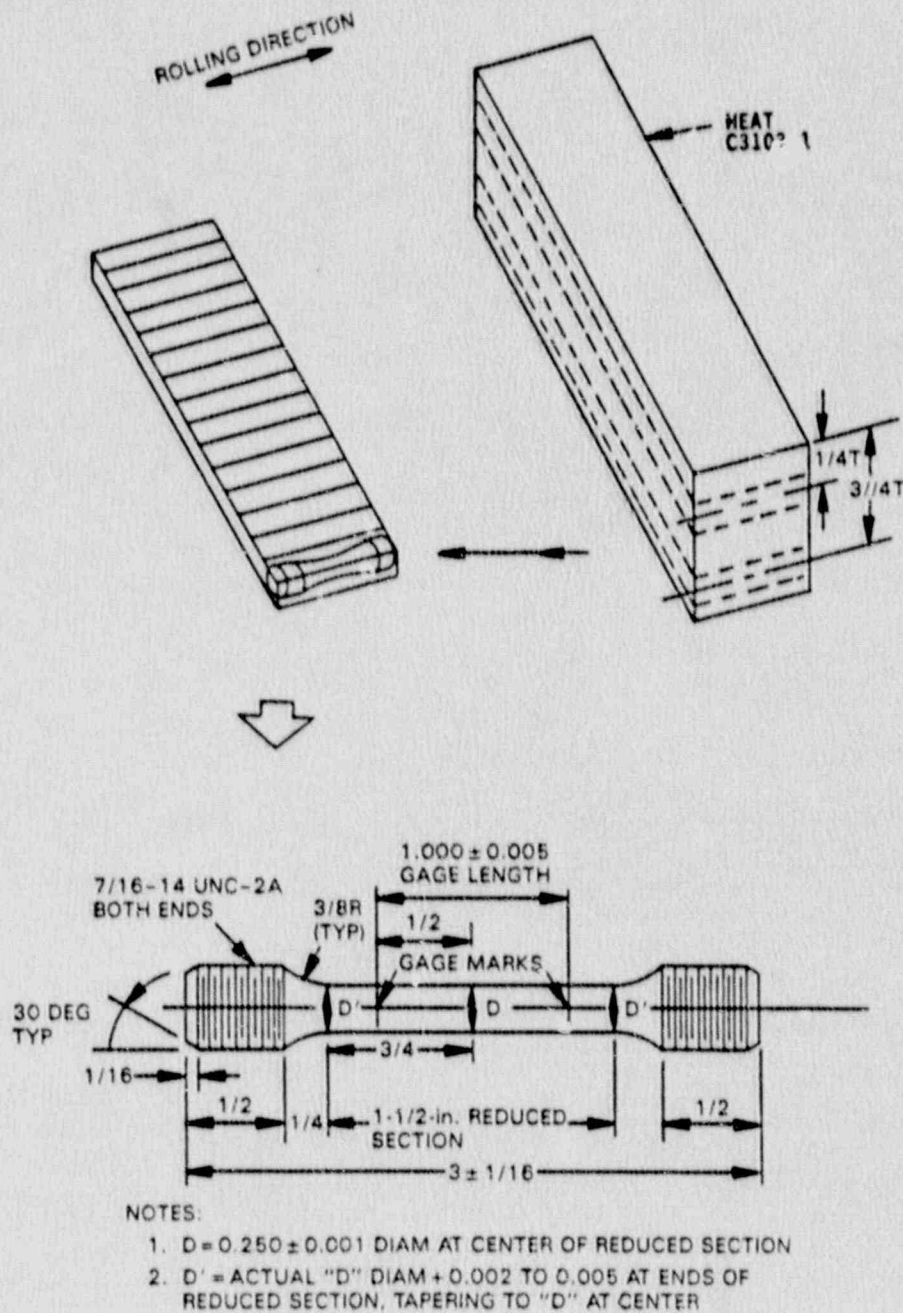


Figure 3-6. Fabrication Method for Base Metal Tensile Specimens

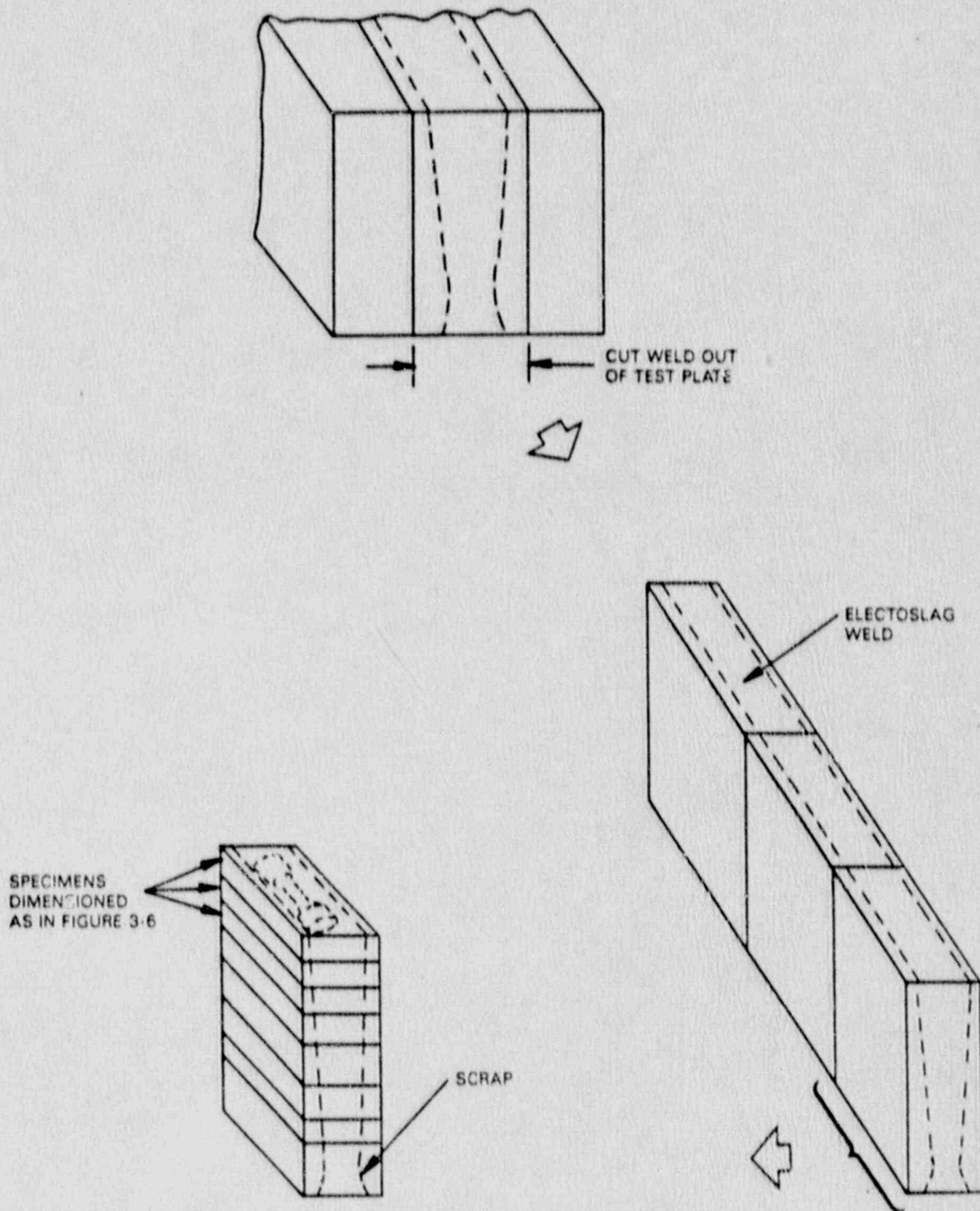


Figure 3-7. Fabrication Method for Weld Metal Tensile Specimens

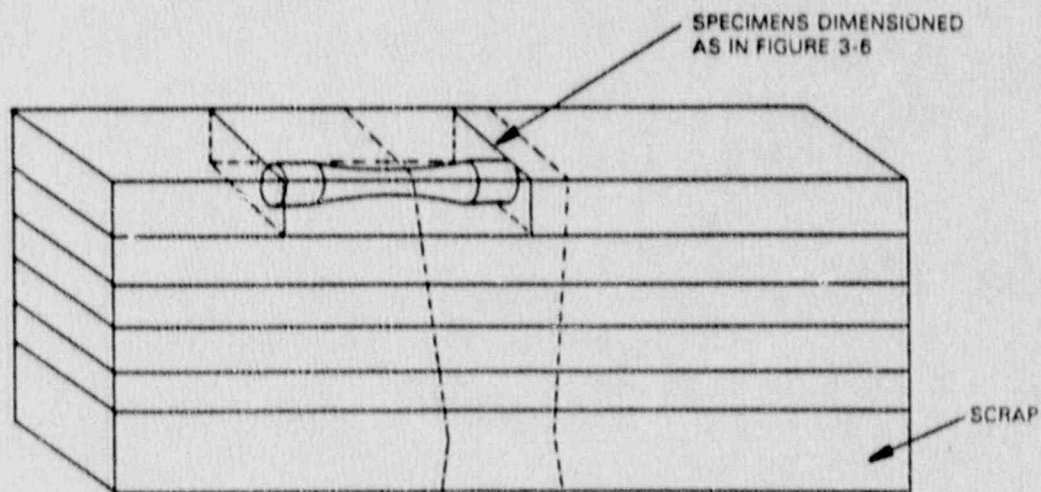
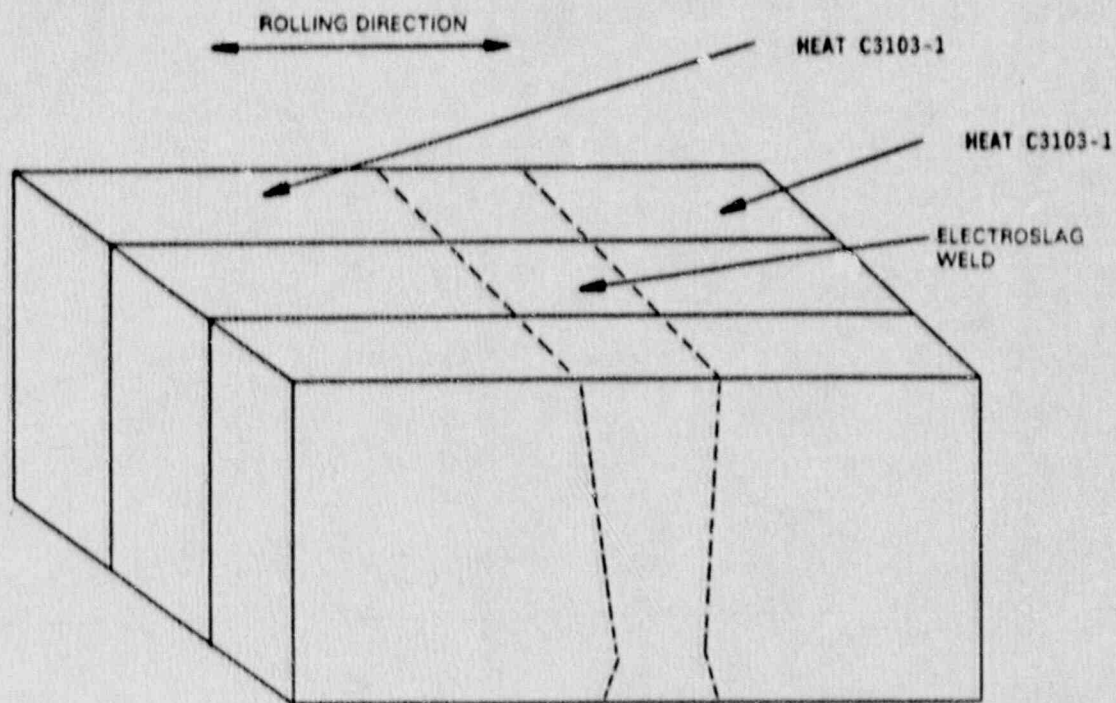


Figure 3-8. Fabrication Method for HAZ Tensile Specimens

4. PEAK RPV FLUENCE EVALUATION

Flux wires were analyzed to determine flux and fluence received by the surveillance capsule. An analysis combining two-dimensional and one-dimensional flux distribution computer calculations done for Peach Bottom Unit 2 (Reference 6) was evaluated to establish the location of peak vessel fluence and the lead factor of the Unit 3 surveillance capsule relative to the peak vessel location.

4.1 FLUX WIRE ANALYSIS

4.1.1 Procedure

The Unit 3 surveillance capsule contained 9 flux wires: three iron, three copper and three nickel. Each wire was removed from the capsule, cleaned with dilute acid, weighed, mounted on a counting card, and analyzed for its radioactivity content by gamma spectrometry. Each iron wire was analyzed for Mn-54 content and each copper wire for Co-60 at a calibrated 4-cm source-to-detector distance with 100-cc and 80-cc Ge(Li) detector systems. The nickel wire's radioactivity had decayed to such a low level that a meaningful analysis could not be done.

To properly predict the flux and fluence at the surveillance capsule from the activity of the flux wires, the periods of full and partial power irradiation and the zero power decay periods were considered. Operating days for each fuel cycle and the reactor average power fraction are shown in Table 4-1. Zero power days between fuel cycles are listed as well.

From the flux wire activity measurements and power history, reaction rates for Fe-54 (n,p) Mn-54 and Cu-63 (n, α) Co-60 were calculated. The >1 MeV fast flux reaction cross sections for the iron and copper wires were estimated to be 0.212 barn and 0.00374 barn, respectively. These values were obtained from measured cross section functions determined at GE's Vallecitos Nuclear Center from more than 65 spectral determinations for BWRs and for the General Electric Test Reactor using activation monitors and spectral unfolding techniques. These data functions are applied to BWR pressure vessel locations

based on water gap (fuel to vessel wall) distances. The cross sections for >0.1 MeV flux were determined from the measured 1-to-0.1 MeV cross section ratio of 1.6.

4.1.2 Results

The measured activity, reaction rate and determined full-power flux results for the surveillance capsule are given in Table 4-2. The >1 MeV flux value of 6.8×10^8 n/cm²-s from the flux wires was calculated by dividing the reaction rate measurement data by the appropriate cross sections. The corresponding fluence results, 1.6×10^{17} n/cm² (>1 MeV) was obtained by multiplying the full-power flux density values by the product of the total time of irradiation and the full power fraction, shown in Table 4-1.

Generally, for long-term irradiations, dosimetry results from copper flux wires are considered the most accurate because of Co-60's long half-life (5.27 years). The iron flux monitor reaction yielding the shorter half-life (312.1 day) Mn-54 gave results about 20% lower than the copper reaction. Because of the long decay period of this surveillance capsule, the nickel wire Co-58 activity (70.8 day half-life) was too low to be utilized. The major difference between the copper and iron wire results is due to differences between the local core power distribution near the surveillance capsule and the average core power, especially during the last two cycles. Therefore, the flux and fluence above are based only on the copper flux wire results.

The accuracies of the values in Tables 4-2 for a 2σ deviation are estimated to be:

- ± 5% for dps/g (disintegrations per second per gram)
- ± 12% for dps/nucleus (saturated)
- ± 30% for flux and fluence >1 MeV
- ± 40% for flux and fluence >0.1 MeV

Flux wires from Unit 3 were evaluated by General Electric in 1978. The >1 MeV flux value was 9.8×10^8 n/cm²-s. A re-evaluation in February 1980, using data from full neutron spectral determinations at the Browns Ferry 3 vessel, resulted in a revised >1 MeV flux of 7.1×10^8 n/cm²-s. Evaluation of the Unit 3 flux wire results from 1978 using current cross section information results in a flux of 8.2×10^8 n/cm²-s. The results from this study are lower, indicating that higher flux was incident on the vessel wall early in plant operation. Due to the accumulation of several cycles of typical operation and core power shape, the results from the copper flux wires analyzed in this report provide a reasonable, but conservative prediction of 32 EFPY fluence.

4.2 DETERMINATION OF LEAD FACTORS

The flux wires detect flux at a single location. The wires will therefore reflect the power fluctuations associated with the operation of the plant. However, the flux wires are not necessarily at the location of peak vessel flux. Lead factors are required to relate the flux at the wires' location to the peak flux. These lead factors are a function of the core and vessel geometry and of the distribution of bundles in the core. Lead factors were generated for the Unit 2 geometry in 1988, using a typical fuel cycle to determine power shape. Based on a review of core management and the similarity of the Unit 2 and 3 flux wire results (within 10%), it is appropriate to use the lead factors calculated in Reference 6 to compute the peak location flux for Unit 3. The methods used to calculate the lead factors in Reference 6 are discussed below.

4.2.1 Procedure

Determination of the lead factor for the RPV inside wall was made using a combination of one-dimensional and two-dimensional finite difference computer analysis. The two-dimensional analysis established the relative fluence in the azimuthal direction at the vessel surface. A series of one-dimensional analyses were done to determine the core height of the axial flux peak and its relationship to the surveillance capsule height. The combination of azimuthal and axial distribution results provides the ratio of

flux, or the lead factor, between the surveillance capsule location and the peak flux location.

The two-dimensional DOT IV computer program was used to solve the Boltzman transport equation using the discrete ordinate method on an (R, θ) geometry, assuming a fixed source. Eighth core symmetry was used with reflective boundary conditions at 0° and 45° . Neutron cross sections were determined for 26 energy groups, with angular scattering approximated by a third-order Legendre expansion. A schematic of the two-dimensional vessel model is shown in Figure 4-1. A total of 113 radial intervals and 45 azimuthal intervals was used. The model consists of an inner and outer core region, the shroud, water regions inside and outside the shroud, the vessel wall and the drywell. Flux as a function of azimuth was calculated, establishing the azimuth of the peak flux and its magnitude relative to the flux at the surveillance capsule azimuth of 30° .

The one-dimensional computer code (SN1D) was used to calculate radial flux distribution at several core elevations at the azimuth angle of 25.5° , where the azimuthal peak was determined to exist. The elevation of the peak flux was determined, as well as its magnitude relative to the flux at the surveillance capsule elevation.

4.2.2 Results

The two-dimensional calculation in Reference 6 indicated the flux to be a maximum 25.5° past the RPV quadrant references (0° , 90° , etc.). The peak closest to the 30° location of the surveillance capsules removed is at 25.5° . The distribution calculations establish the lead factor between the surveillance capsule location and the peak location at the inner vessel wall. This lead factor is 0.95. The fracture toughness analysis is based on a $1/4 T$ depth flaw in the beltline region, so the attenuation of the flux to that depth is considered. This attenuation is calculated according to the requirements in Regulatory Guide 1.99, Revision 2 (Reference 5), as shown in the next subsection.

4.3 ESTIMATE OF 32 EFPY FLUENCE

The inside surface fluence (f_{surf}) at 32 EFPY is determined from the best estimate of the measured flux from Table 4-2, using the lead factor in Section 4.2. The time period 32 EFPY, typically assumed for 40-year operation (80% capacity factor) is 1.01×10^9 seconds. The resulting 32 EFPY fluence value at the vessel inside surface is:

$$f_{\text{surf}} = (6.8 \times 10^8 \text{ n/cm}^2\text{-s})(1.01 \times 10^9 \text{ s})/0.95$$

$$f_{\text{surf}} = 7.2 \times 10^{17} \text{ n/cm}^2.$$

The 1/4 T fluence (f) is calculated according to the following equations from Reference 5:

$$f = f_{\text{surf}}(e^{-0.24x}) \quad (4-1)$$

where x = distance, in inches, from the inside surface to the 1/4 T depth.

The vessel beltline consists of the lower-intermediate and lower shell, both with a thickness of 6.125 inches. For the thickness of 6.125 inches, the corresponding depths x is 1.53 inches. Equation 4-1 evaluated for Unit 3 is:

$$f = 0.6925 f_{\text{surf}}$$

The 1/4 T value of 32 EFPY fluence is as follows:

$$f = 5.0 \times 10^{17} \text{ n/cm}^2$$

Table 4-1

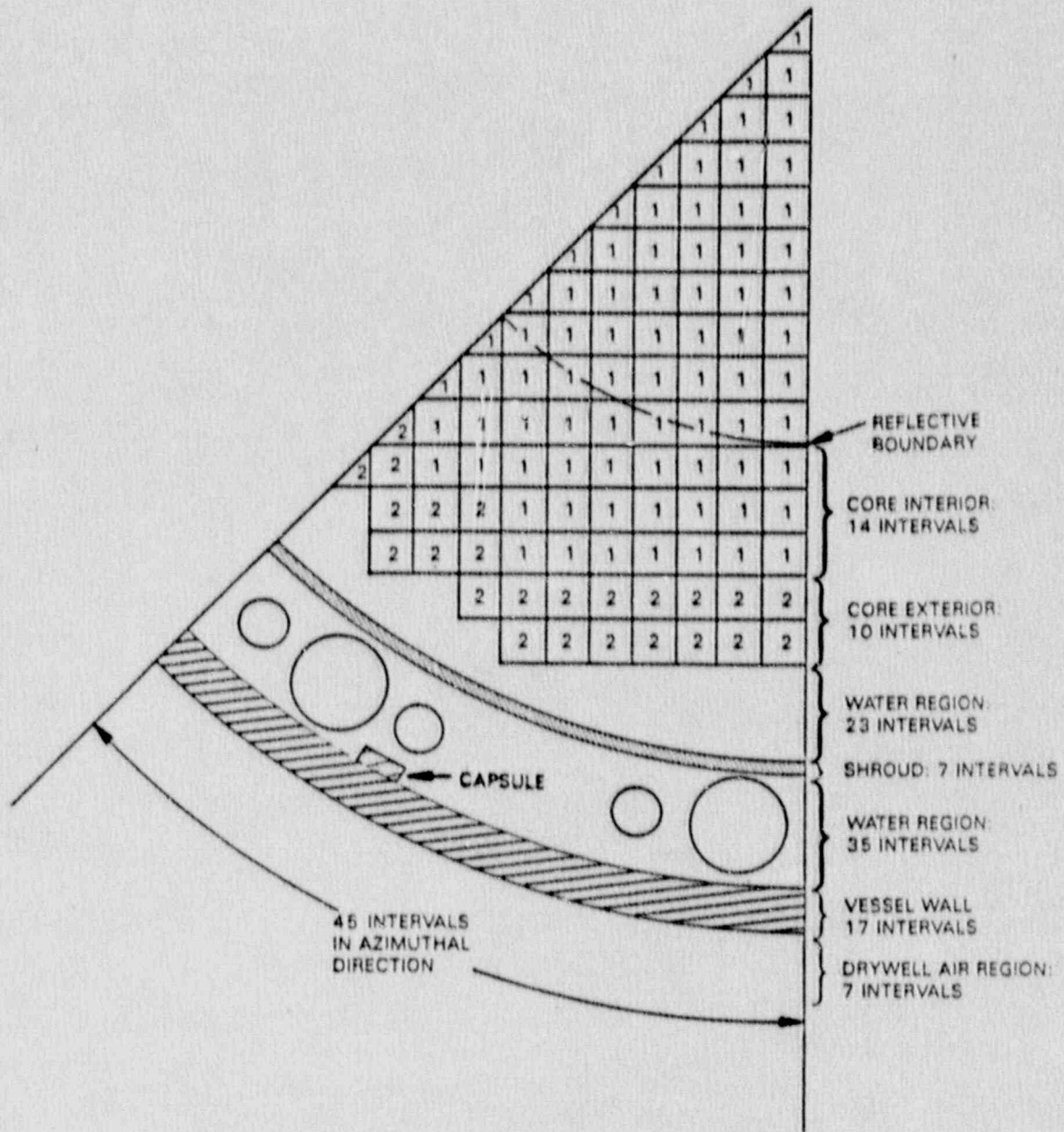
SUMMARY OF DAILY POWER HISTORY

<u>Cycle</u>	<u>Cycle Dates</u>	<u>Operating Days</u>	<u>Fraction of Full Power</u>	<u>Days Between Cycles</u>
1	9/1/74 - 12/24/76	846	0.603	108
2	4/12/77 - 4/1/78	355	0.779	48
3	5/20/78 - 9/15/79	484	0.844	51
4	11/6/79 - 3/7/81	488	0.793	229
5	10/23/81 - 2/13/83	479	0.903	243
6	10/15/83 - 7/15/85	640	0.772	228
7	3/1/86 - 3/31/87	<u>396</u>	<u>0.648</u>	
		3688	0.750 (average)	

Table 4-2
 SURVEILLANCE CAPSULE FLUX AND FLUENCE
 FOR IRRADIATION FROM 9/1/74 TO 3/31/87

Wire (Element)	Wire Weight (g)	dps/g Element (at end of Irradiation)	Reaction Rate [dps/nucleus (saturated)]	Full Power Flux ^a (n/cm ² ·s)		Fluence (n/cm ²)	
				>1 MeV	>0.1 MeV	>1 MeV	>0.1 MeV
Copper 65156	0.3630	7.63x10 ³	2.46x10 ⁻¹⁸				
Copper 65157	0.3697	8.15x10 ³	2.63x10 ⁻¹⁸				
Copper 65158	0.3691	7.86x10 ³	2.53x10 ⁻¹⁸				
		Average = 2.54x10 ⁻¹⁸		6.8x10 ⁸	1.1x10 ⁹	1.6x10 ¹⁷	2.6x10 ¹⁷
Iron 65156	0.1286	3.97x10 ⁴	1.15x10 ⁻¹⁶				
Iron 65157	0.1314	4.18x10 ⁴	1.21x10 ⁻¹⁶				
Iron 65158	0.1331	3.93x10 ⁴	1.14x10 ⁻¹⁶				
		Average = 1.16x10 ⁻¹⁶		5.5x10 ⁸	8.8x10 ⁸	1.3x10 ¹⁷	2.1x10 ¹⁷
				Values from this report (copper only) = 6.8x10 ⁸	1.1x10 ⁹	1.6x10 ¹⁷	2.6x10 ¹⁷

^a Full power of 3293 MW_t.



1 = CORE INTERIOR FUEL
2 = CORE EXTERIOR FUEL

Figure 4-1. Schematic of Model for Two-Dimensional Flux Distribution Analysis

5. CHARPY V-NOTCH IMPACT TESTING

The 36 Charpy specimens recovered from the Unit 3 surveillance capsule were impact tested at temperatures selected to establish the toughness transition and upper shelf of the irradiated RPV materials. Testing was conducted in accordance with ASTM E23-82 (Reference 9).

5.1 IMPACT TEST PROCEDURE

The testing machine used was a Riehle Model PL-2 impact machine serial number R-89916. The pendulum has a maximum velocity of 15.44 ft/sec and a maximum available hammer energy of 240 ft-lb.

The test apparatus and operator were qualified using NIST standard reference material specimens. The standards are designed to fail both at 70.5 ft-lb and 11.5 ft-lb at a test temperature of -40°F. According to Reference 9, the test apparatus averaged results must reproduce the NIST standard values within an accuracy of $\pm 5\%$ or ± 1.0 ft-lb, whichever is greater. The qualification of the Riehle machine and operator is summarized in Table 5-1. The calibration results for the low energy specimens are 0.4 ft-lb higher than the allowable variation in Reference 9. This is due to the occasional "kickback" of a broken specimen half contacting the hammer, which is only significant to the Charpy results at very low energies. Since the kickbacks have little effect on the results, especially compared to the typical scatter in the data, no correction to the test results was made.

Charpy V-Notch tests were conducted at temperatures between -40°F and 300°F. For tests below 70°F methanol was used as the cooling fluid. Between 70°F and 212°F, water was used as the temperature conditioning fluid. The specimens were heated in oil above 212°F. Cooling of the conditioning fluids was done with liquid nitrogen, and heating by an immersion heater. The fluids were mechanically stirred to maintain uniform temperatures. The fluid temperature was measured with a calibrated thermocouple. Once at test temperature, the specimens were manually transferred with centering tongs to the Riehle machine and impacted within 5 seconds.

For each Charpy V-Notch specimen the test temperature, energy absorbed, lateral expansion, and percent shear were evaluated. In addition, photographs were taken of each fracture surface pair. Lateral expansion and percent shear were measured according to Reference 9 methods. Percent shear was determined with method one of Subsection 11.2.4.3 of Reference 9, which involves measuring the length and width of the cleavage surface and locating the percent shear value from Tables 1 or 2 of Reference 9.

5.2 IMPACT TEST RESULTS

Twelve Charpy V-Notch specimens each of base, weld, and HAZ material were tested at temperatures (-40°F to 300°F) selected to define the toughness transition and upper shelf portions of the fracture toughness curves. The absorbed energy, lateral expansion, and percent shear data are listed for each material in Table 5-2. Plots of absorbed energy data for base, weld and HAZ materials are presented in Figures 5-1 through 5-3, respectively. Lateral expansion plots for base, weld and HAZ materials are presented in Figures 5-4 through 5-6, respectively. The fracture surface photographs and a summary of the test results for each specimen are contained in Appendix A.

The plate and weld data sets are fit with the hyperbolic tangent function developed by Oldfield for the EPRI Irradiated Steel Handbook (Reference 10):

$$Y = A + B * \text{TANH} [(T - T_0) / C],$$

where Y = impact energy or lateral expansion
T = test temperature, and
A, B, T₀ and C are determined by non-linear regression.

The TANH function is one of the few continuous functions with a shape characteristic of low alloy steel fracture toughness transition curves.

5.3 IRRADIATED VERSUS UNIRRADIATED CHARPY V-NOTCH PROPERTIES

As a part of the RPV surveillance test program, some Charpy V-Notch testing was performed. Data for the plate material specimens (Heat C3103-1) were recovered from QA records, but consisted only of three specimen tests at 10°F. For the surveillance weld, positive identification of the weld wire heat was not obtained from B&W. Therefore, unirradiated archive surveillance specimens were obtained from PECO and tested to establish the baseline needed to determine the irradiation shift.

To minimize personnel exposure, the unirradiated specimens were tested on the Tinius-Olsen Charpy test apparatus in San Jose (serial number 119037), with available hammer energy of 264 ft-lb and impact velocity of 16.8 ft/sec. The machine was calibrated with NIST specimens in May 1990. The calibration results, shown in Table 5-3, were within specifications.

Twelve each of plate and weld material specimens were tested at temperatures between -40°F and 300°F. Impact energy, lateral expansion and percent shear were determined with the same methods used for the irradiated specimens. The results are presented in Table 5-4. Photographs of specimen fracture surfaces are in Appendix B.

The impact energy and MLE data for the unirradiated materials were fit with the TANH function in the same manner as the irradiated data. The results for plate and weld impact energy are plotted in Figures 5-7 and 5-8, respectively, along with the corresponding irradiated data described in Section 5.2. The results for lateral expansion are plotted in Figures 5-9 and 5-10 for the plate and weld material, respectively.

The irradiated and unirradiated Charpy V-Notch data were used to estimate the values given in Table 5-5: 30 ft-lb, 50 ft-lb and 35 MLE index temperatures, and the USE for both irradiated materials and unirradiated materials, where available. Transition temperature shift values are determined as the change in the temperature at which 30 ft-lb impact energy is achieved, as required in Reference 4. Values were not determined for HAZ material because of the amount of scatter in the Charpy data, which is typical for that material.

5.4 COMPARISON TO PREDICTED SHIFT

The measured transition temperature shifts for the plate and weld materials were compared to the predictions calculated according to Regulatory Guide 1.99, Revision 2 (1.99). The 1.99 methods used to calculate shift are described in Section 7.6. The inputs for the surveillance plate and weld materials are as follows:

Plate: (based on Table 3-3 values)

Copper: 0.13%
Nickel: 0.63%
fluence: 1.6×10^{17} n/cm²

Weld: (based on Table 3-3 values)

Copper: 0.11%
Nickel: 0.41%
fluence: 1.6×10^{17} n/cm²

The chemistry factors (CF) are 91.8 for the plate and 102.5 for the weld. The fluence factor is 0.1495. The predicted shifts are, therefore, as follows:

	ΔRT_{NDT}	$\Delta RT_{NDT} + \text{Margin}$	Actual Test
Plate	13.7°F	27.4°F	16°F
Weld	15.3°F	30.6°F	16°F

The measured shifts of 16°F for both the plate and weld materials are slightly more than the mean prediction, and considerably less than the upper bound predictions of 1.99.

Table 5-1

VALLECITOS RIEHLE CHARPY MACHINE
 QUALIFICATION TEST RESULTS USING
 NIST STANDARD REFERENCE SPECIMENS
 (TESTED 3/5/90)

<u>Specimen Identification</u>	<u>Bath Medium</u>	<u>Test Temperature (°F)</u>	<u>Energy Absorbed (ft-lb)</u>	<u>Acceptable Range (ft-lb)</u>
MM-15 086	Methanol	-40	70.0	
MM-15 503	"	-40	69.0	
MM-15 364	"	-40	71.0	
MM-15 244	"	-40	67.5	
MM-15 326	"	-41	66.0	
		Average	68.7	70.5 ± 3.5
LL-18 105	Methanol	-40	12.5	
LL-18 246	"	-40	13.5	
LL-18 496	"	-41	13.5	
LL-18 1012	"	-40	12.5	
LL-18 040	"	-40	12.5	
		Average	12.9	11.5 ± 1.0

Table 5-2

CHARPY V-NOTCH IMPACT TEST RESULTS
FOR IRRADIATED RPV MATERIALS IN UNIT 3

<u>Specimen Identification</u>	<u>Test Temperature (°F)</u>	<u>Fracture Energy (ft-lb)</u>	<u>Lateral Expansion (mils)</u>	<u>Percent Shear (Method 1) (%)</u>
Base:				
7P1	-40	8.0	6	3
7LU	-30	8.0	11	7
7T6	-20	13.5	13	9
7TB	-10	15.5	14	8
7MU	0	43.5	34	16
7M5	20	46.0	42	22
7PP	40	65.0	50	23
7M7	80	112.0	88	73
7P2	120	102.5	70	67
7MJ	160	129.0	86	100
7MB	200	121.0	89	100
7PY	300	128.0	88	100
Weld:				
7TJ	-40	11.0	9	4
7TL	-20	18.0	16	3
7UA	-10	21.5	20	6
7TK	0	12.0	14	3
7UU	10	20.0	20	15
7TU	20	38.5	35	11
7UP	40	50.0	42	23
7TD	80	61.5	56	32
A11	120	80.5	73	75
A15	160	96.5	74	84
7YD	200	100.5	85	100
A14	300	98.0	81	100
HAZ:				
A27	-40	16.5	16	2
A1C	-30	23.5	20	12
A1E	-20	37.5	34	8
A1L	-10	41.5	31	16
A1K	0	21.5	21	19
A3A	20	83.0	60	40
A22	40	111.5	83	47
A2E	80	125.0	91	82
A23	120	99.0	70	81
A1D	160	103.0	87	100
A1J	200	107.0	88	100
A2T	300	162.0	86	100

Table 5-3

SAN JOSE TINIUS-OLSON CHARPY MACHINE
 QUALIFICATION TEST RESULTS USING
 NIST STANDARD REFERENCE SPECIMENS
 (TESTED 5/14/90)

<u>Specimen</u> <u>Identification</u>	<u>Bath</u> <u>Medium</u>	<u>Test</u> <u>Temperature</u> <u>(°F)</u>	<u>Energy</u> <u>Absorbed</u> <u>(ft-lb)</u>	<u>Acceptable</u> <u>Range</u> <u>(ft-lb)</u>
MM-16 307	Methanol	-40	71.0	
MM-16 465	"	-40	72.0	
MM-16 509	"	-40	75.0	
MM-16 552	"	-40	71.5	
MM-16 915	"	-40	73.0	
	Average		72.5	69.4 ± 3.5
LL-19 124	Methanol	-40	11.5	
LL-19 354	"	-40	11.5	
LL-19 411	"	-40	12.0	
LL-19 702	"	-40	10.5	
LL-19 925	"	-40	11.5	
	Average		11.4	11.9 ± 1.0

Table 5-4

CHARPY V-NOTCH IMPACT TEST RESULTS
FOR UNIRRADIATED RPV MATERIALS IN UNIT 3

<u>Specimen Identification</u>	<u>Test Temperature (°F)</u>	<u>Fracture Energy (ft-lb)</u>	<u>Lateral Expansion (mils)</u>	<u>Percent Shear (Method 1) (%)</u>
Base:				
7PC	-40	10.5	8.5	0
7LY	-40	24.5	16.5	0
7MT	-20	18.5	16.0	16
7MY	0	34.0	26.0	15
7P4	20	60.5	43.5	27
7M3	40	85.0	62.0	39
7M2	60	72.0	51.5	38
7P7	80	98.5	70.0	67
7MD	120	117.5	86.5	83
7PB	160	130.0	81.0	100
7MM	200	130.0	80.0	100
7PD	300	143.5	83.0	100
Weld:				
7TE	-40	6.5	3.0	0
7U1	-20	17.5	15.5	6
7U6	0	29.0	20.5	11
7U2	0	48.0	41.5	15
7U3	20	39.5	30.5	14
7TP	40	56.5	46.0	22
7TM	60	44.0	39.0	39
7U4	80	54.0	40.5	41
7TT	120	92.0	70.0	77
7U5	160	101.0	77.0	100
7TY	200	106.5	80.0	100
7U7	300	104.0	79.0	100

Table 5-5

SIGNIFICANT RESULTS OF IRRADIATED AND
UNIRRADIATED CHARPY V-NOTCH DATA FOR UNIT 3

<u>Material</u>	<u>Index Temperature (°F)</u>			Upper Shelf ^a
	<u>E-30 ft-lb</u>	<u>E-50 ft-lb</u>	<u>MLE-35 mil</u>	Energy
				(ft-lb)
				<u>L/T</u>
Unirradiated Plate	-14	17	12	137/ 89
Irradiated Plate	<u>2</u>	<u>23</u>	<u>13</u>	<u>123/ 80</u>
Difference	16	6	1	14/ 9 (10%)
Unirradiated Weld	2	47	34	110
Irradiated Weld	<u>18</u>	<u>54</u>	<u>33</u>	<u>100</u>
Difference	16	7	-1	10 (9%)

^a Longitudinal (L) USE is from the data shown in Figures 5-7 and 5-8. Transverse (T) plate USE is taken as 65% of the longitudinal USE, according to Reference 11. L/T USE values are equal for weld metal, which has no orientation effect.

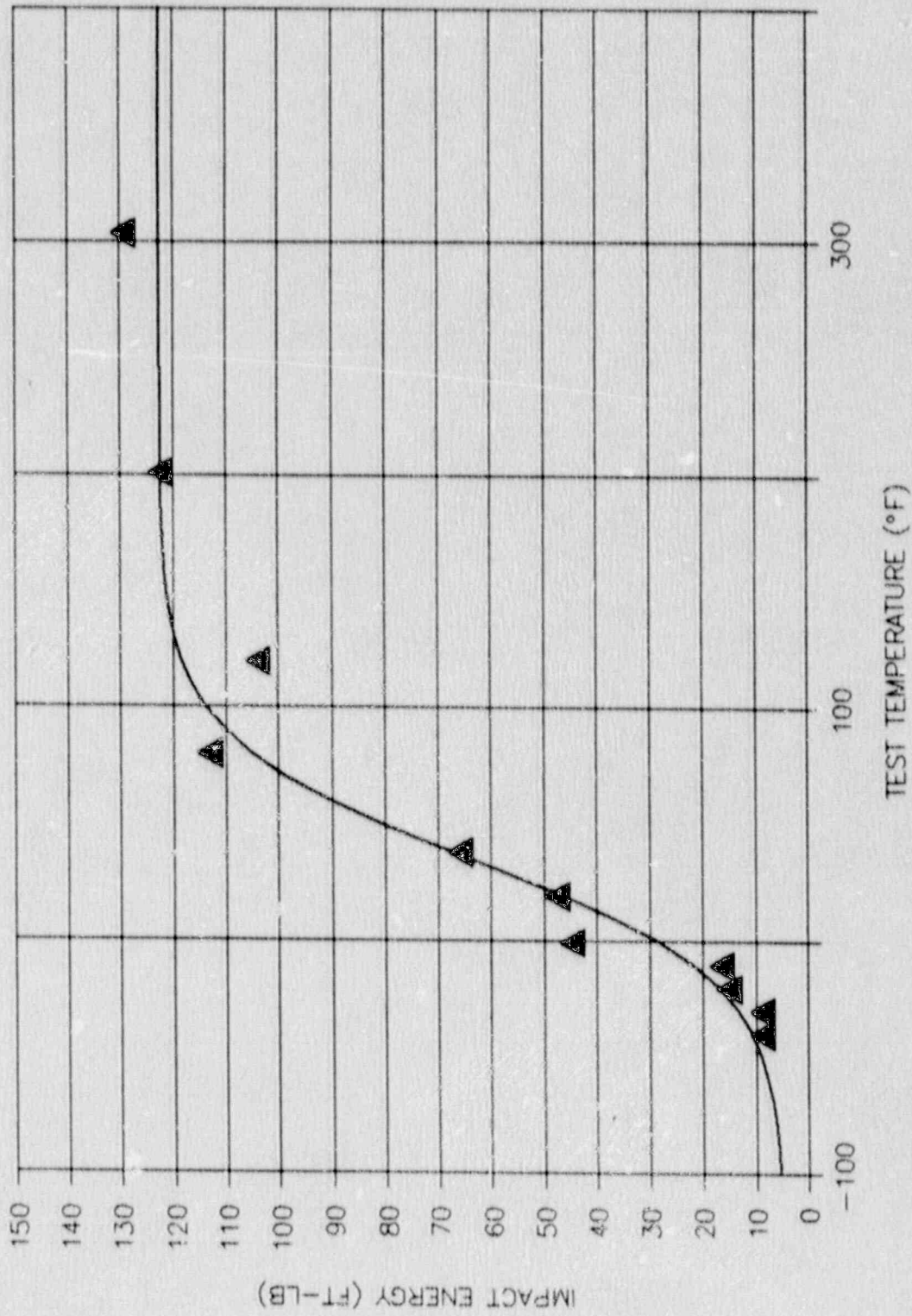


Figure 5-1. Irradiated Base Metal Impact Energy

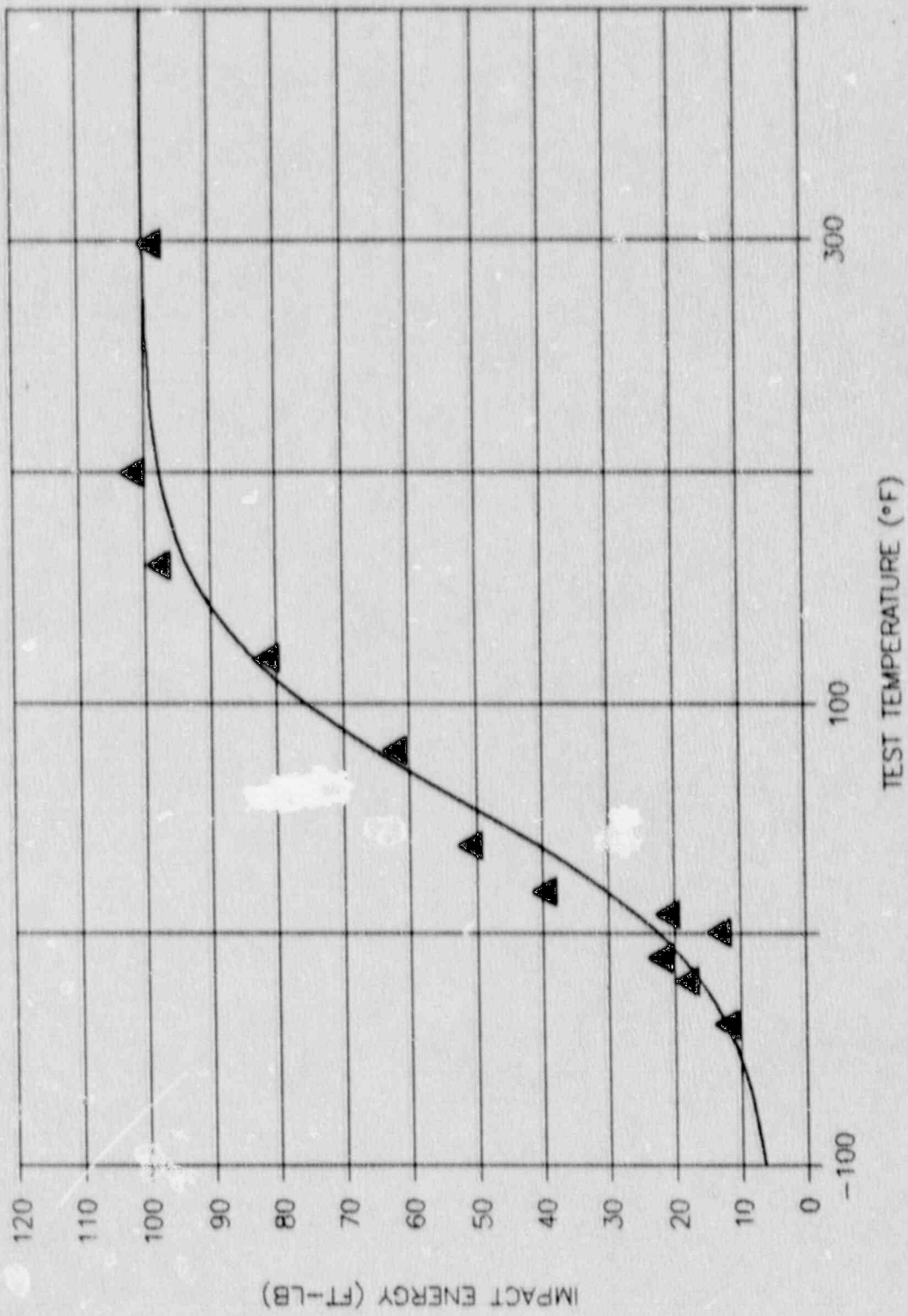


Figure 5-2. Irradiated Weld Metal Impact Energy

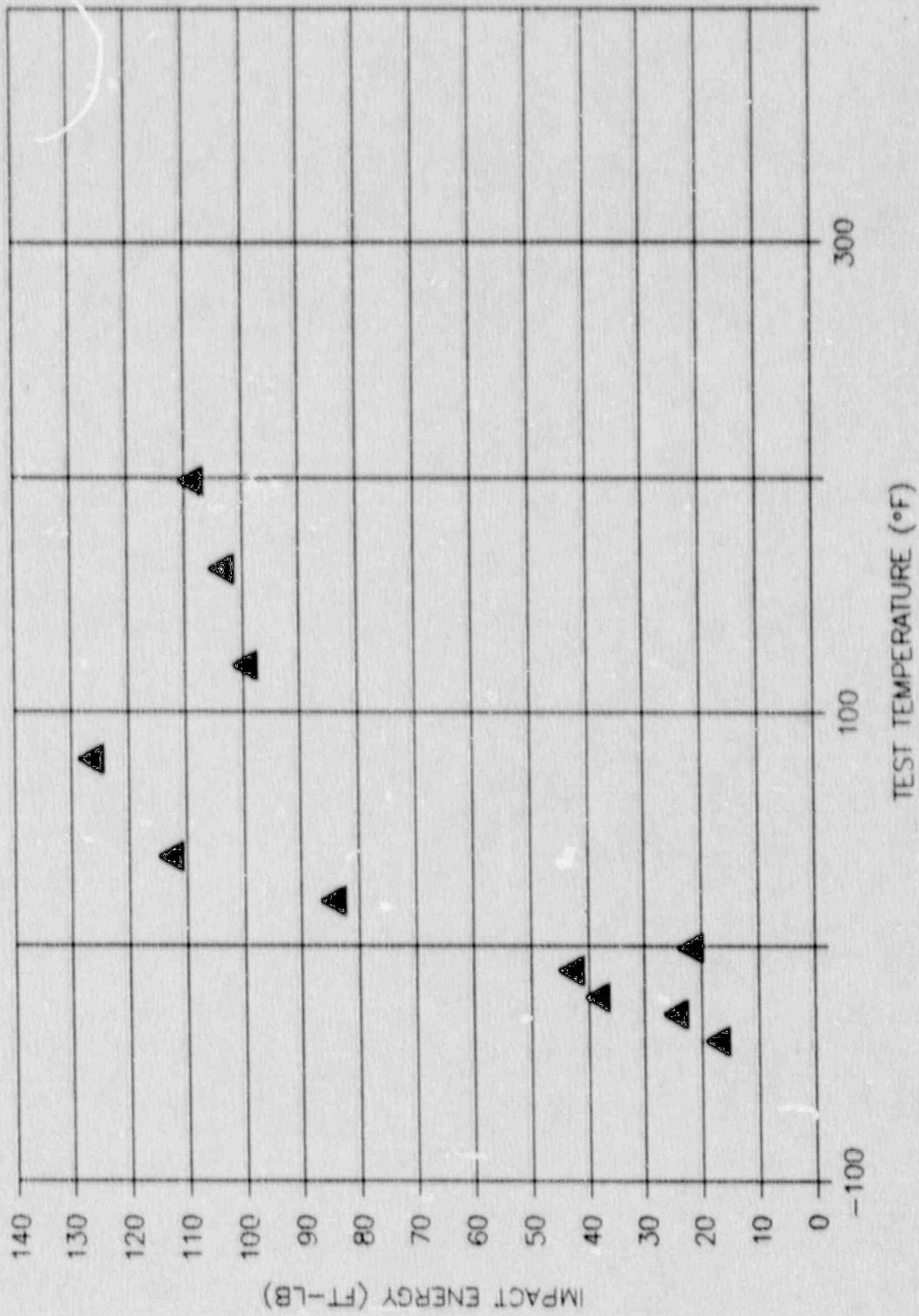


Figure 5-3. Irradiated HAZ Impact Energy

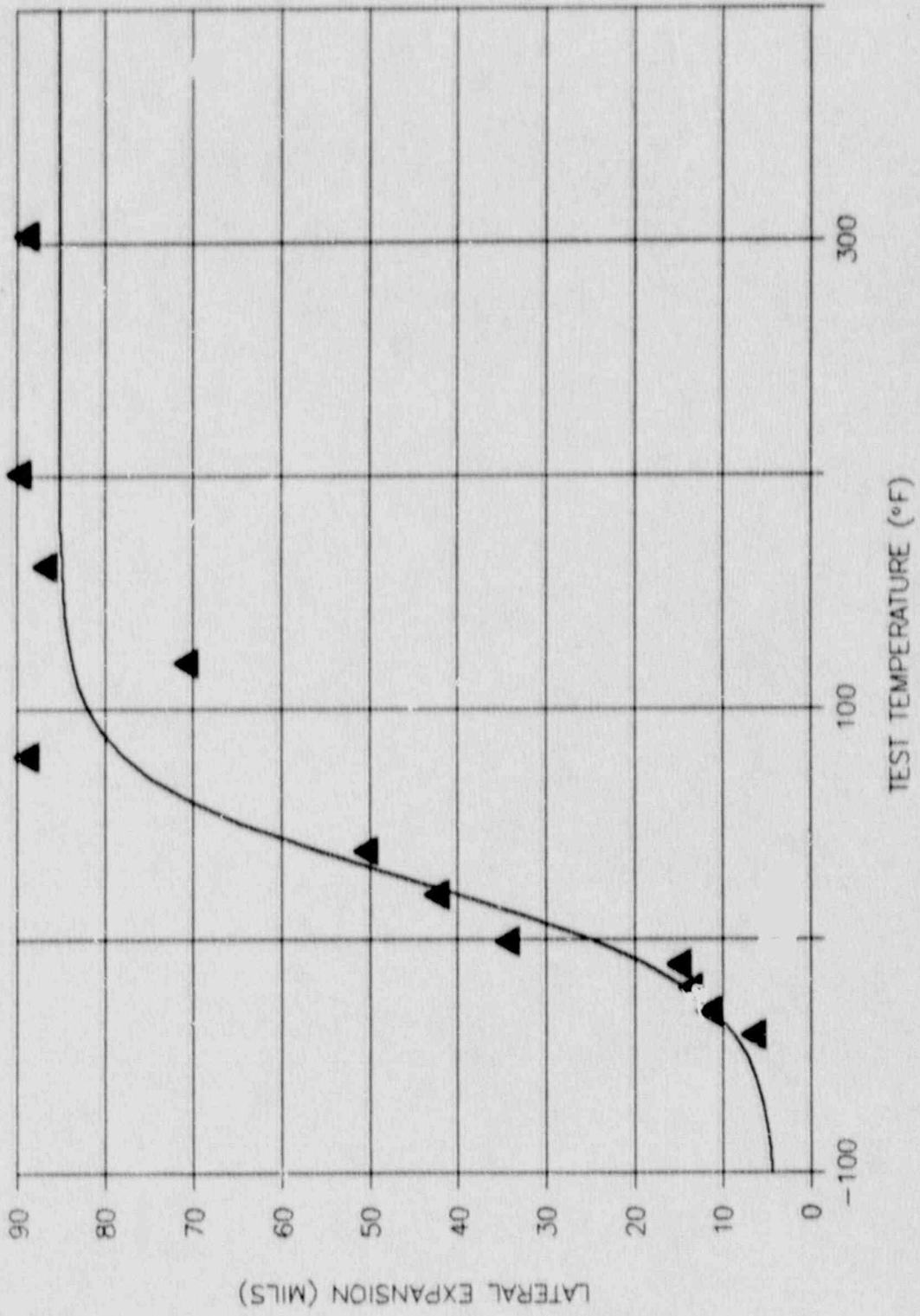


Figure 5-4. Irradiated Base Metal Lateral Expansion

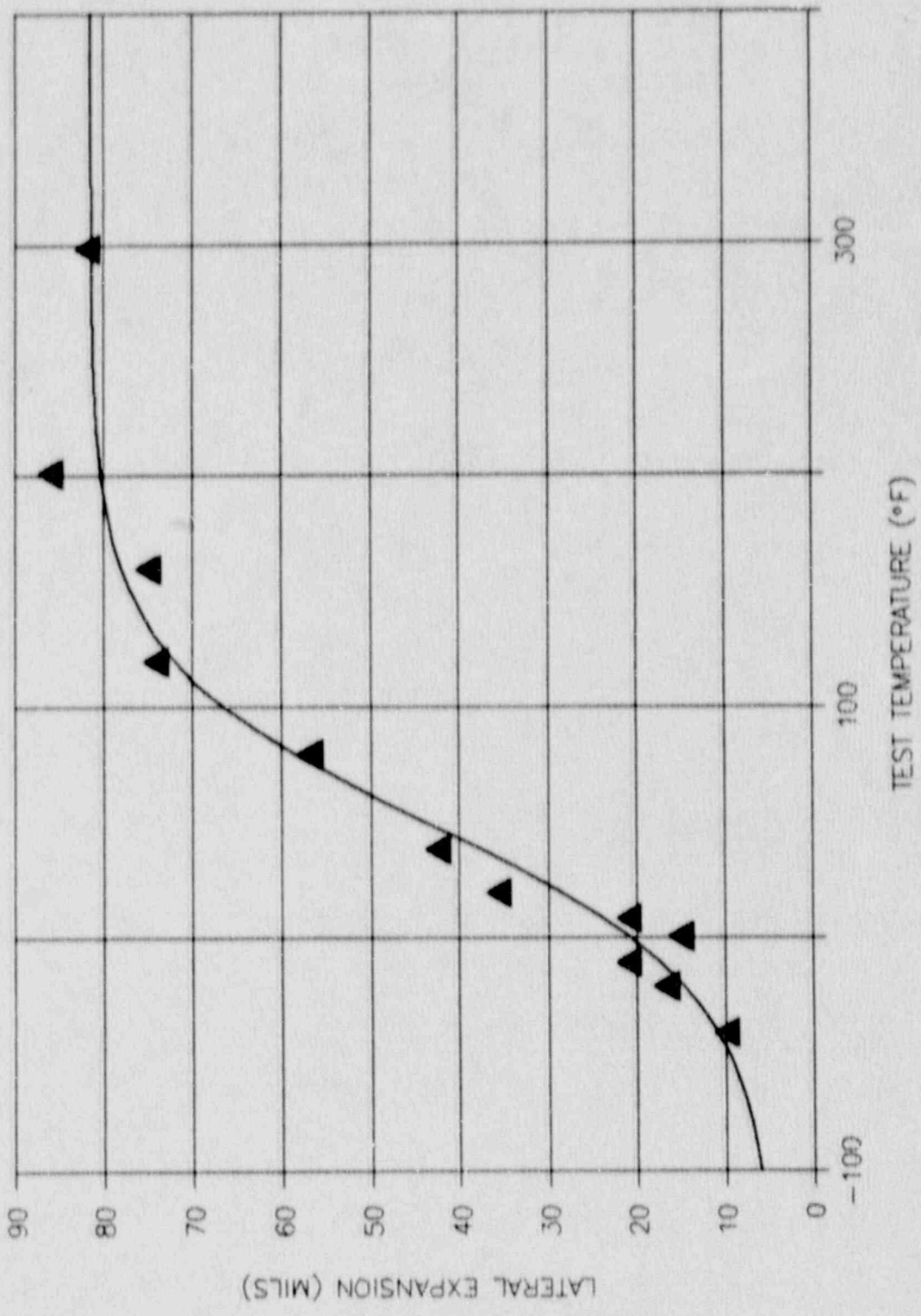


Figure 5-5. Irradiated Weld Metal Lateral Expansion

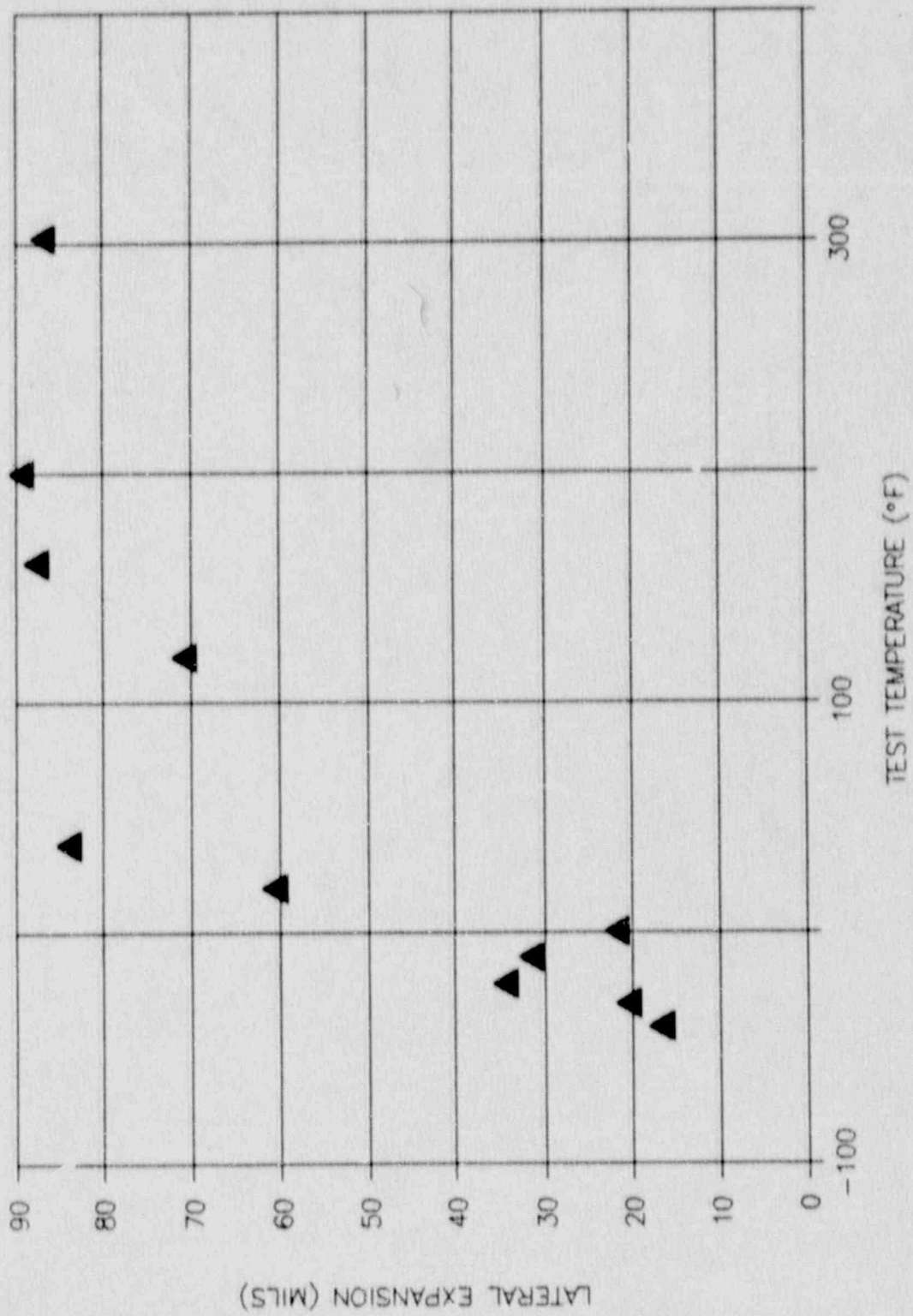


Figure 5-6. Irradiated HAZ Lateral Expansion

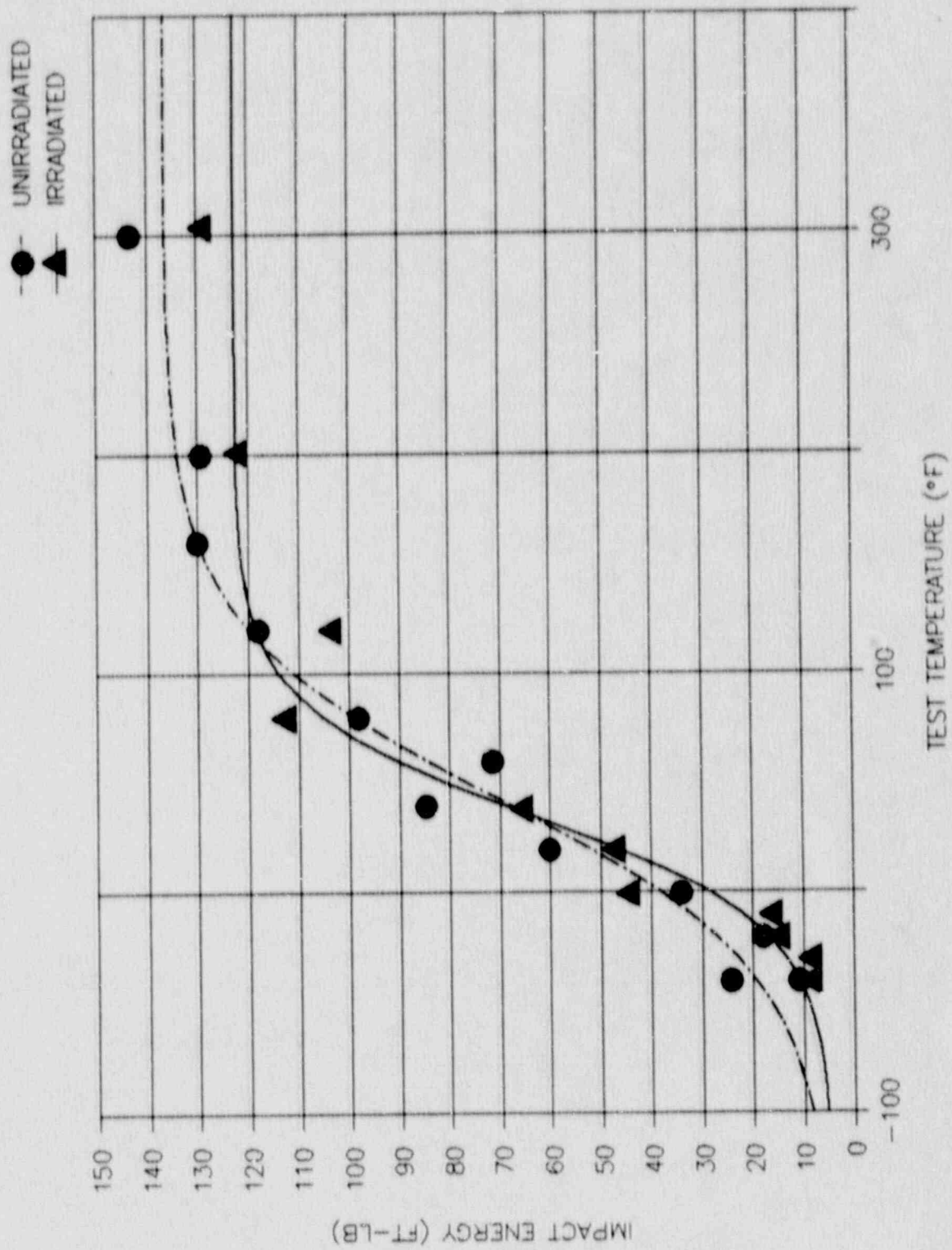


Figure 5-7. Comparison of Unirradiated and Irradiated Base Metal Impact Energy

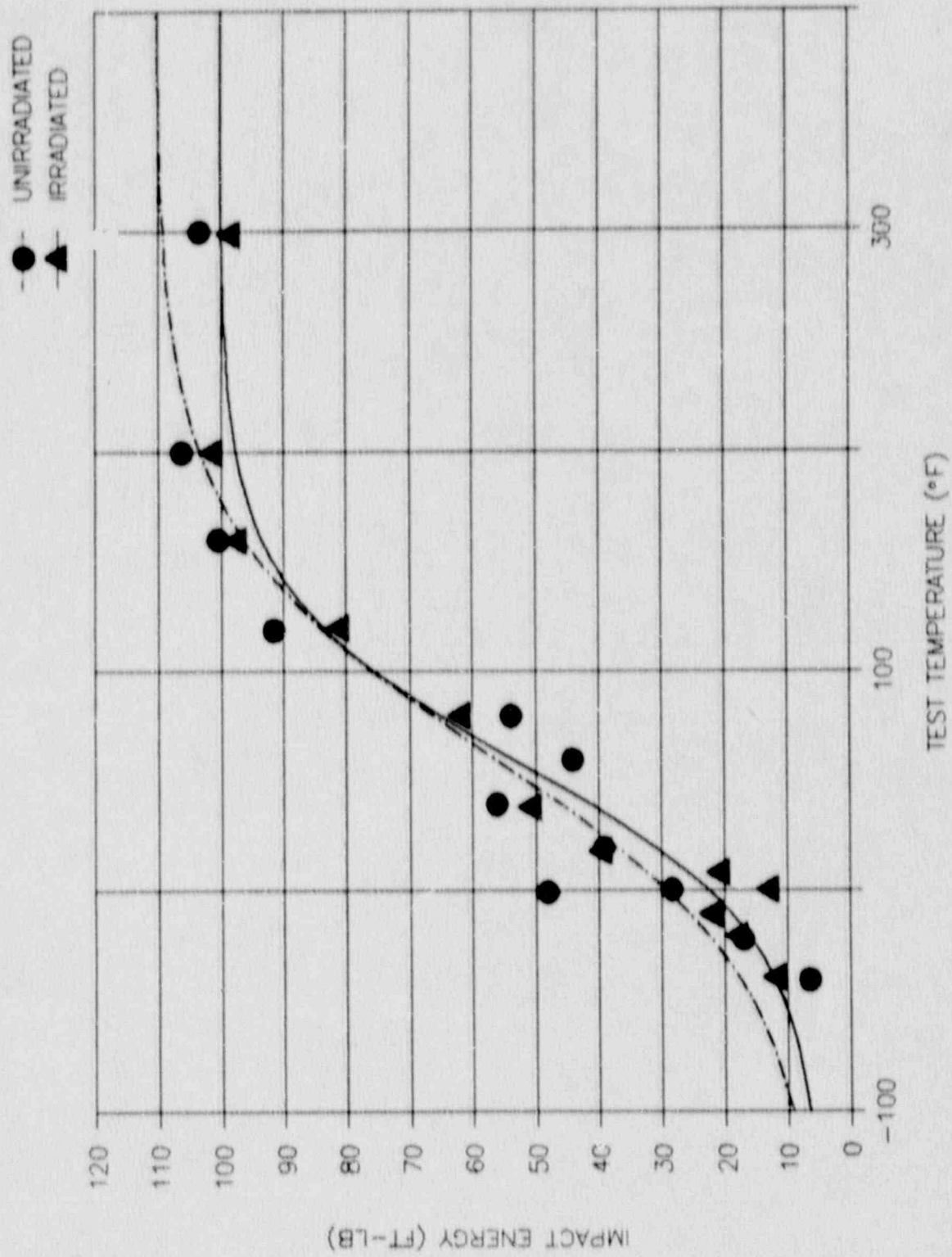


Figure 5-8. Comparison of Unirradiated and Irradiated Weld Metal Impact Energy

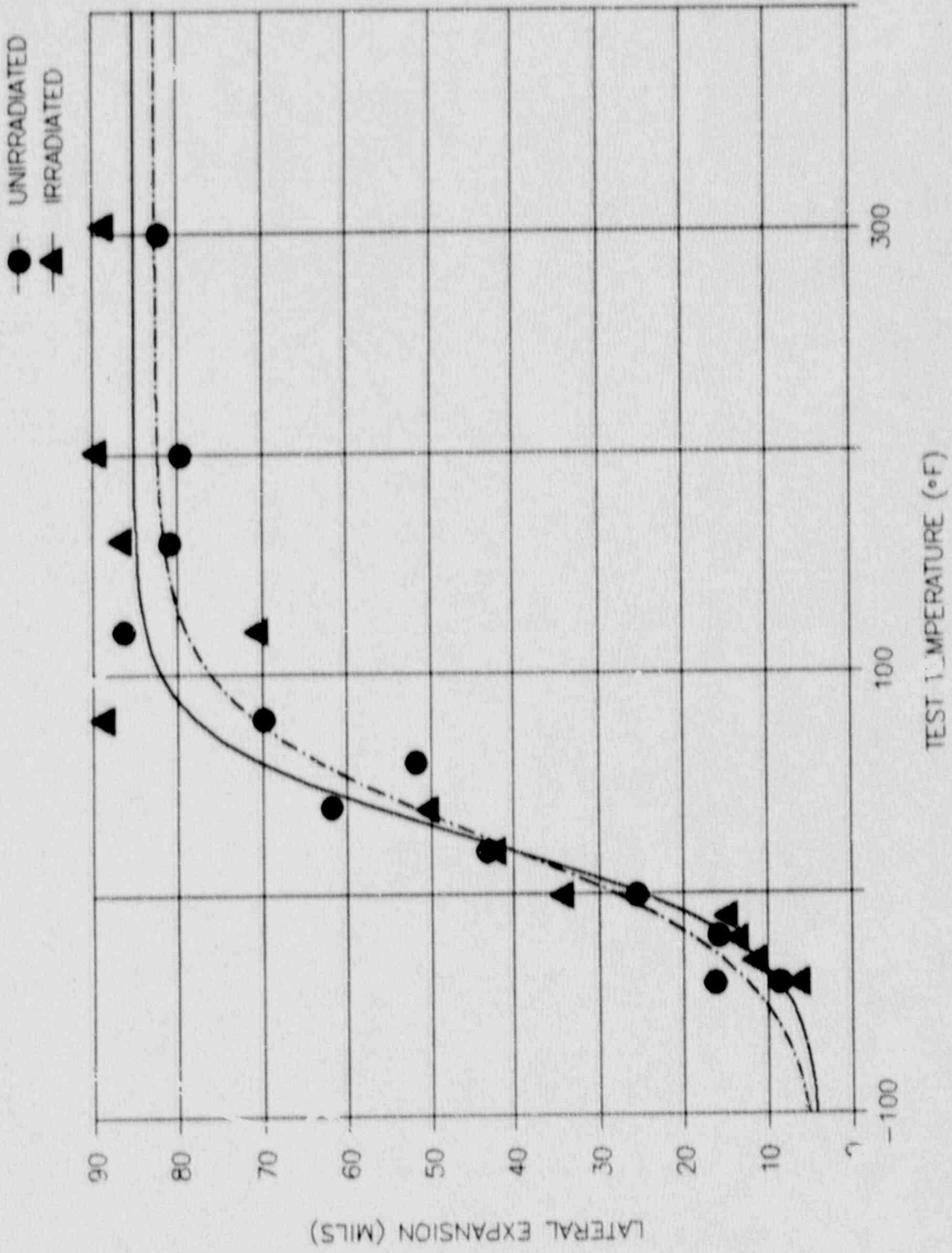


Figure 5-9. Comparison of Unirradiated and Irradiated Base Metal Lateral Expansion

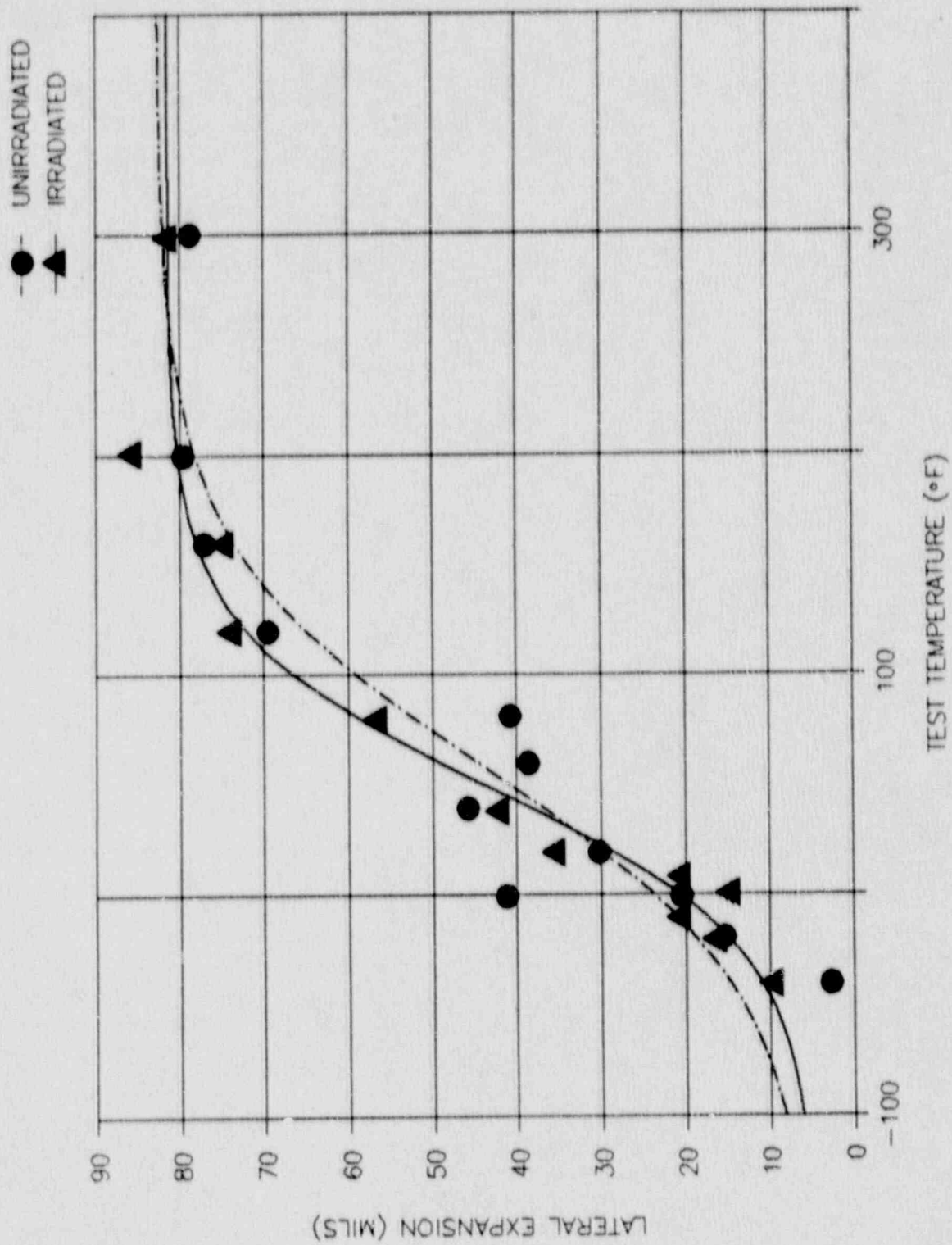


Figure 5-10. Comparison of Unirradiated and Irradiated Weld Metal Lateral Expansion

6. TENSILE TESTING

Eight round bar tensile specimens were recovered from the Peach Bottom Unit 3 surveillance capsule and tested. Uniaxial tensile tests were conducted in air at room temperature (70°F), RPV operating temperature (550°F), and onset of upper shelf temperature (160°F). The tests were conducted in accordance with ASTM E8-81 (Reference 12).

6.1 PROCEDURE

All tests were conducted using a screw-driven Instron test frame equipped with a 20-kip load cell and special pull bars and grips. Heating was done with a Satec resistance clamshell furnace centered around the specimen load train. The test temperature was monitored and controlled by a chromel-alumel thermocouple spot-welded to an Inconel clip that was friction-clipped to the surface of the specimen at its midline. Before the elevated temperature tests, a profile of the furnace was conducted at the test temperature of interest using an unirradiated steel specimen of the same geometry. Thermocouples were spot-welded to the top, middle, and bottom of a central 1 inch gage of this specimen. In addition, the clip-on thermocouple was attached to the midline of the specimen. When the target temperatures of the three thermocouples were within $\pm 5^\circ\text{F}$ of each other, the temperature of the clip-on thermocouple was noted and subsequently used as the target temperature for the irradiated specimens.

All tests were conducted at a calibrated crosshead speed of 0.005 inch/min until well past yield, at which time the speed was increased to 0.05 inch/min until fracture.

The test specimens were machined with a minimum diameter of 0.250 inch at the center of the gage length. The yield strength (YS) and ultimate tensile strength (UTS) were calculated by dividing the nominal area (0.0491 in²) into the 0.2% offset load and into the maximum test load, respectively. The values listed for the uniform and total elongations were obtained from plots that recorded load versus specimen extension and are based on a 1.0 inch gage length. Reduction of area (RA) values were determined from post-test measurements of the necked specimen diameters using a calibrated blade micrometer and employing the following formula:

$$RA = 100\% * (A_0 - A_f)/A_0$$

After testing, each broken specimen was photographed end-on, showing the fracture surface, and lengthwise, showing the fracture location and necking.

6.2 RESULTS

Irradiated tensile test properties of Yield Strength (YS), Ultimate Tensile Strength (UTS), Reduction of Area (RA), Uniform Elongation (UE), and Total Elongation (TE) are presented in Table 6-1. A stress-strain curve for a 550°F base metal irradiated specimen is shown in Figure 6-1. This curve is typical of the stress-strain characteristics of all the tested specimens. The data in Table 6-1 are shown graphically in Figures 6-2 and 6-3. As can be seen from Figures 6-2 and 6-3, the base, weld and HAZ materials generally follow the trend of decreasing properties with increasing temperature. Photographs of the fracture surfaces and necking behavior are given in Figures 6-4 through 6-6.

6.3 IRRADIATED VERSUS UNIRRADIATED TENSILE PROPERTIES

Unirradiated tensile test data, shown in Table 6-2, were recovered from QA records for surveillance plate Heat C3103-1. The unirradiated data provide average values of YS, UTS, RA, and TE at room temperature. These were compared to the irradiated plate specimen RT data to determine the irradiation effect. The trends of increasing YS and UTS and of decreasing RA, characteristic of irradiation embrittlement, are seen. The increasing TE seen may be due to different reference gage lengths for the tests.

Table 6-1

TENSILE TEST RESULTS FOR IRRADIATED RPV MATERIALS
FOR UNIT 3

<u>Specimen Number</u>	<u>Test Temp (°F)</u>	<u>Yield^a Strength (ksi)</u>	<u>Ultimate Strength (ksi)</u>	<u>Uniform Elongation (%)</u>	<u>Total Elongation (%)</u>	<u>Reduction of Area (%)</u>
Base:						
A41	68	74.0	96.0	14.5	29.5	66.6
A4A	160	68.9	90.4	13.0	27.3	69.9
A46	550	67.3	95.6	14.0	26.9	59.6
Weld:						
A4P	66	64.2	86.9	15.0	29.7	68.6
A54	550	60.0	83.4	12.5	24.5	60.7
HAZ:						
A62	68	67.0	88.5	13.8	27.4	67.6
A5M	160	63.6	84.2	13.5	28.8	68.3
A5E	550	61.5	83.8	10.6	23.0	64.2

^a Yield Strength is determined by 0.2% offset.

Table 6-2

COMPARISON OF UNIRRADIATED AND IRRADIATED
TENSILE PROPERTIES AT ROOM TEMPERATURE
FOR UNIT 3

	Yield Strength <u>(ksi)</u>	Ultimate Strength <u>(ksi)</u>	Total Elongation <u>(%)</u>	Reduction of Area <u>(%)</u>
Plate:				
Unirradiated	71.3	91.5	28.1	71.6
Irradiated	74.0	96.0	29.5	66.6
Difference ^a	3.8%	4.9%	5.0%	-7.0%

^a Difference = [(Irradiated - Unirradiated)/Unirradiated] * 100%

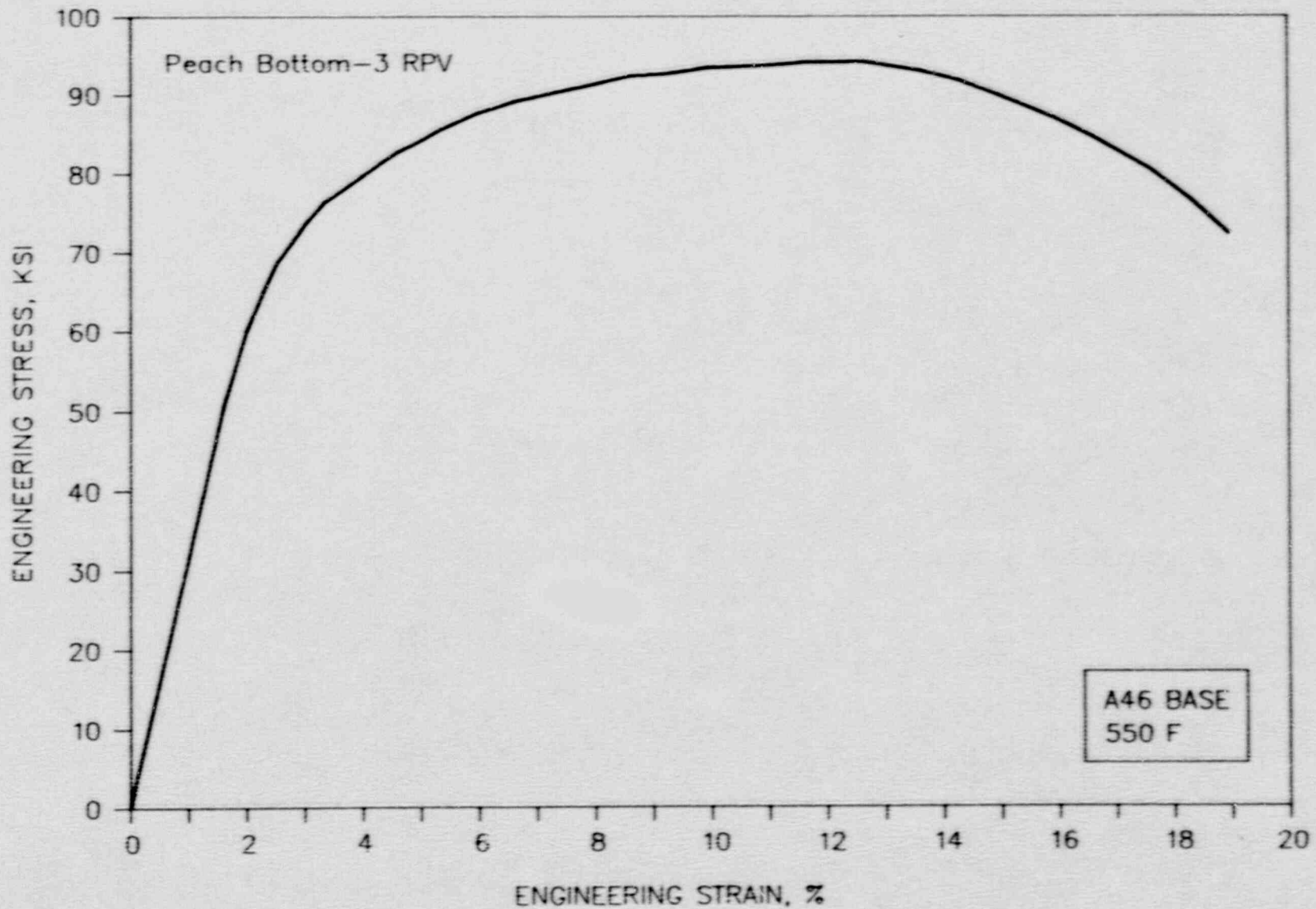


Figure 6-1. Typical Engineering Stress-Strain for Irradiated RPV Materials

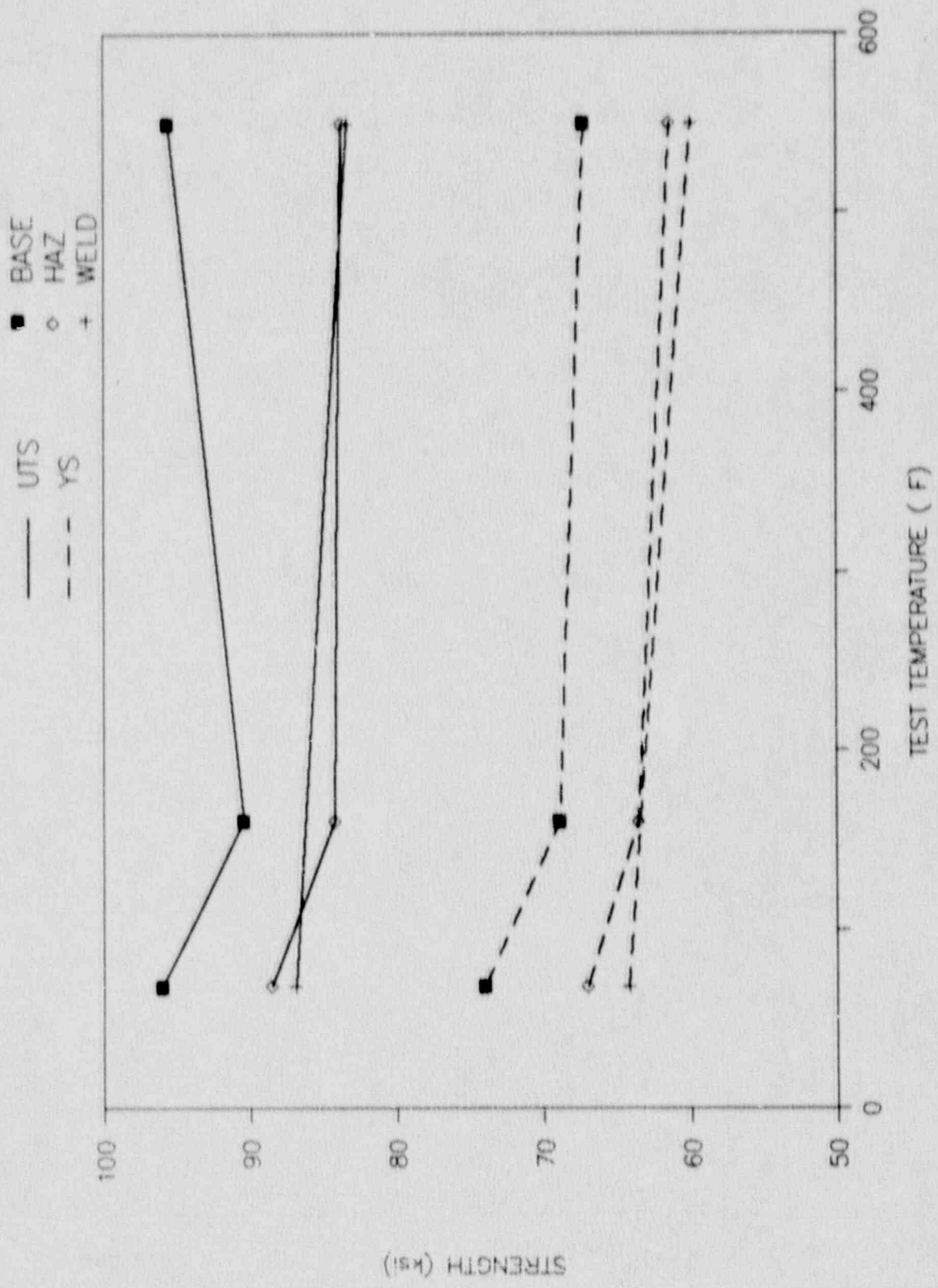


Figure 6-2. Strength vs. Temperature for Irradiated Materials

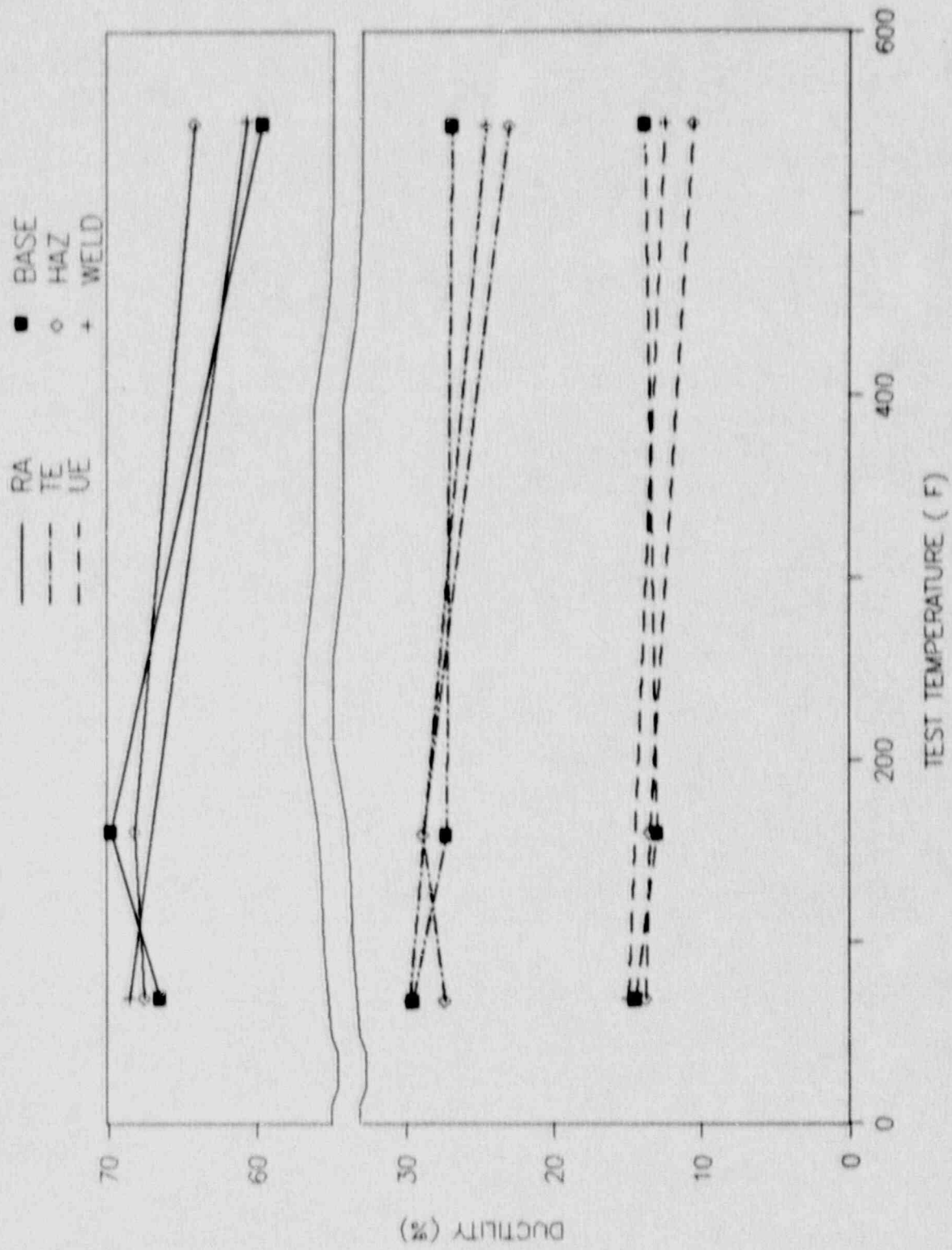
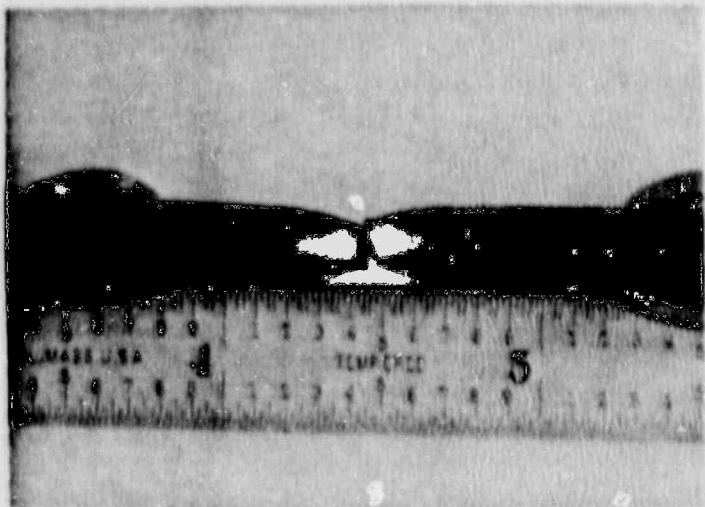
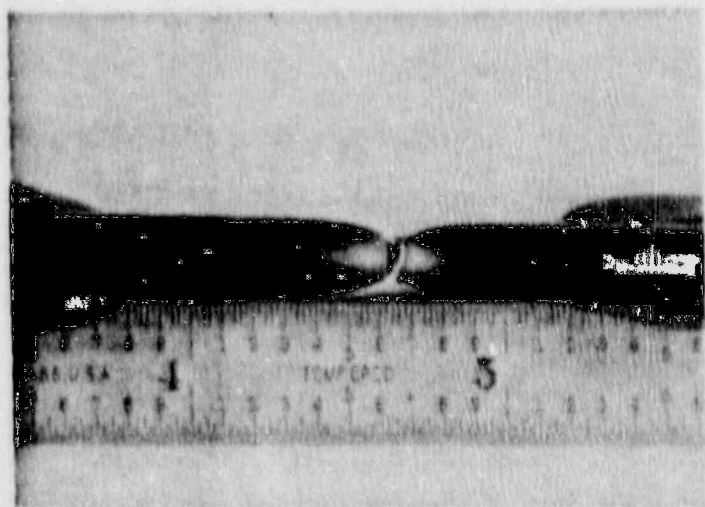
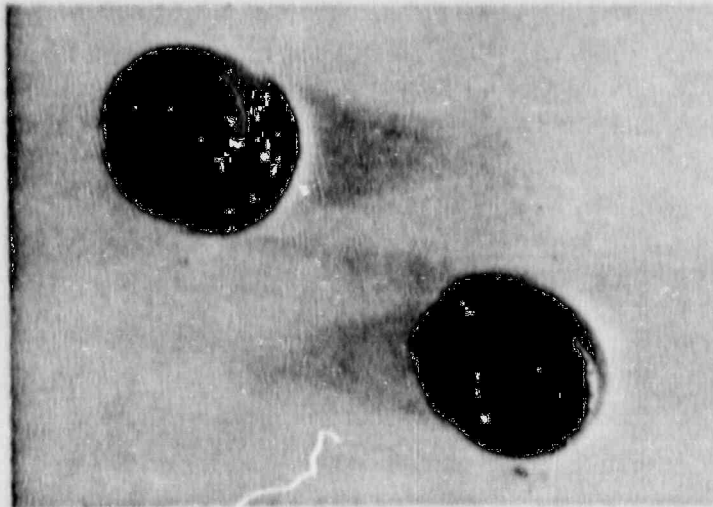


Figure 6-3. Ductility vs. Temperature for Irradiated Materials



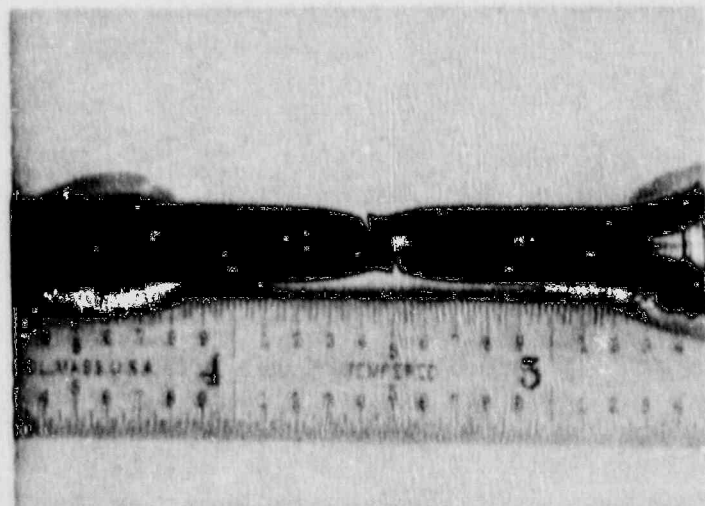
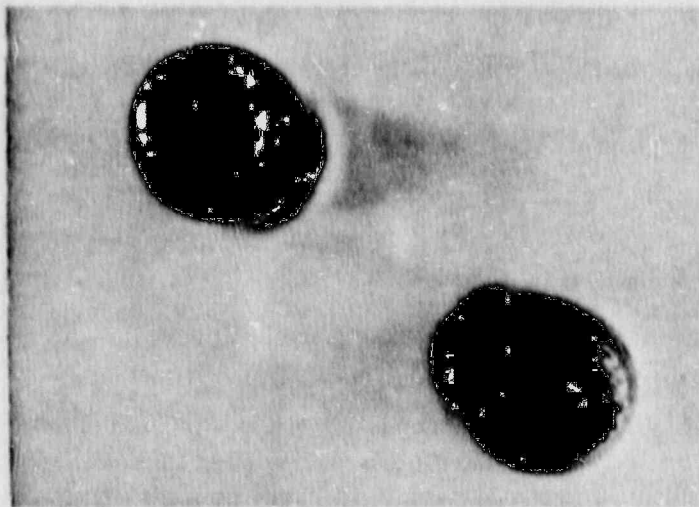
A41

68°F



A4A

160°F



A46

550°F

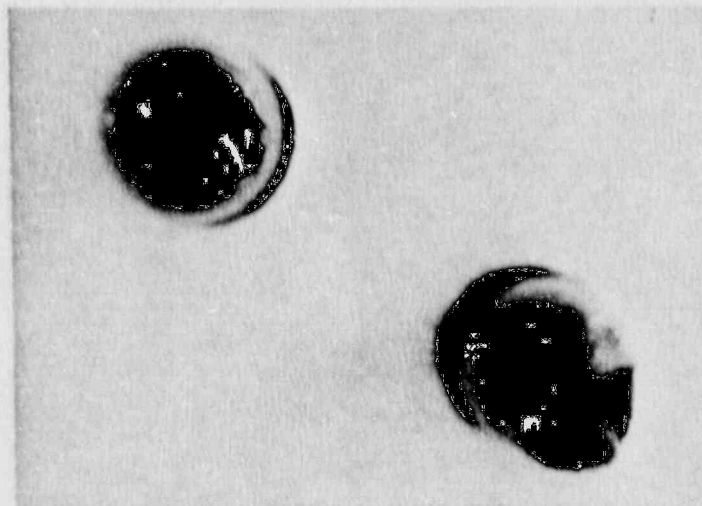
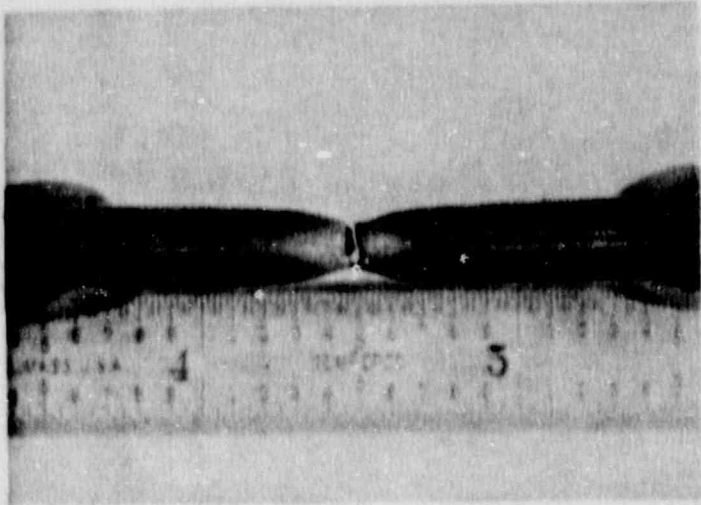
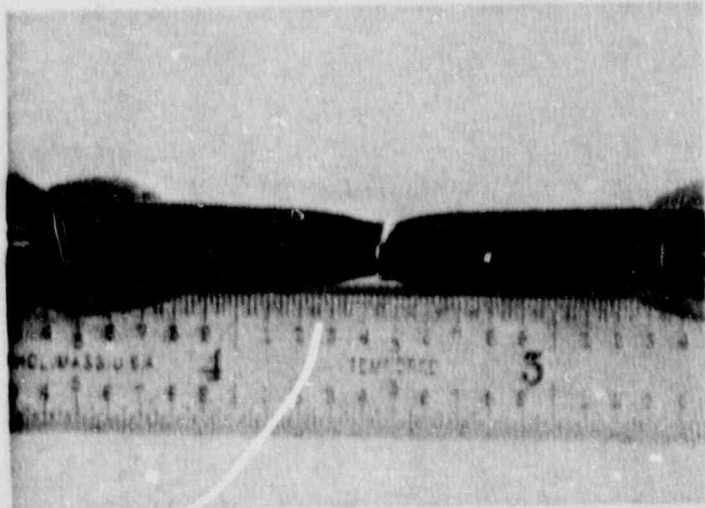
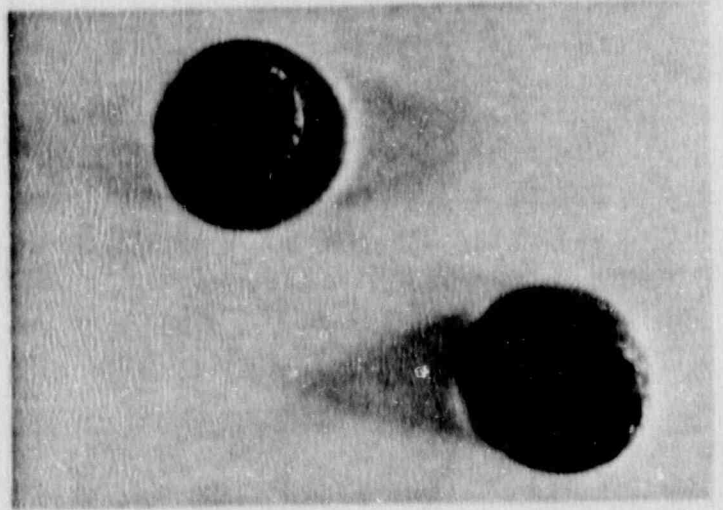


Figure 6-4. Fracture Location, Necking Behavior, and Fracture Appearance for Irradiated Base Metal Tensile Specimens



A4P

66°F



A54

550°F

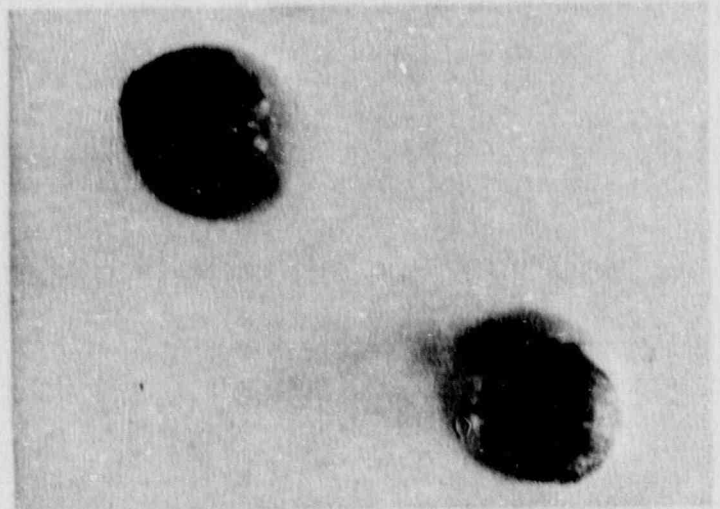
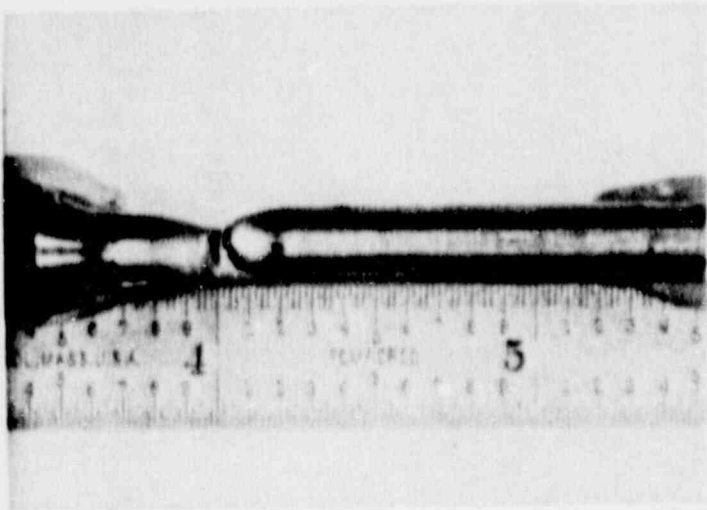
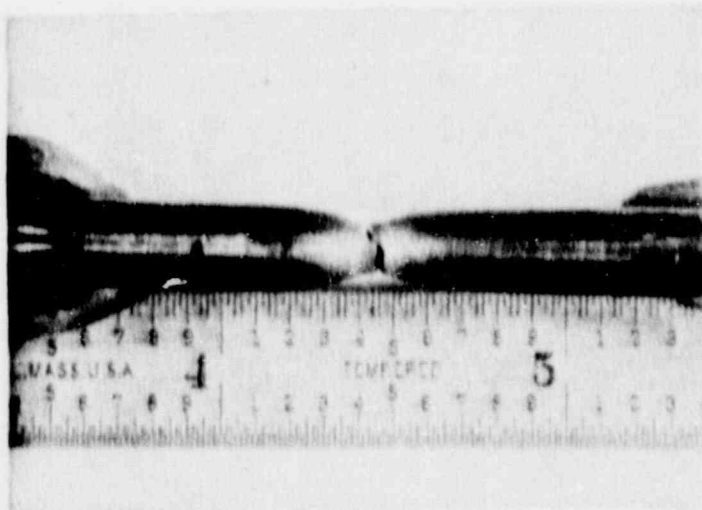
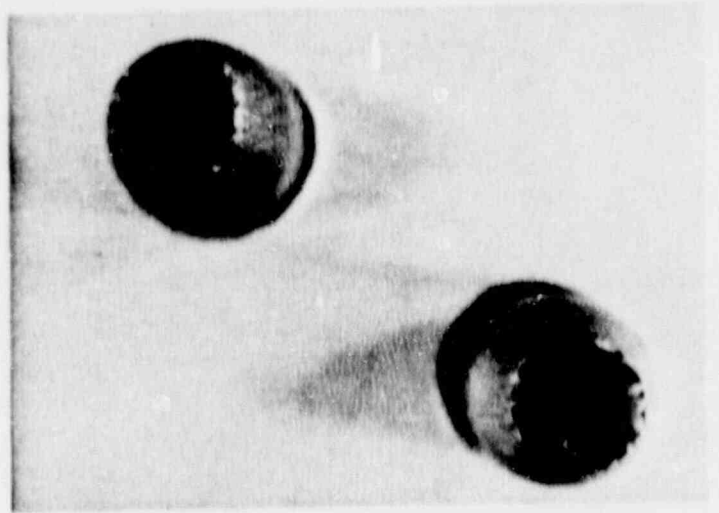


Figure 6-5. Fracture Location, Necking Behavior, and Fracture Appearance For Irradiated Weld Metal Tensile Specimens



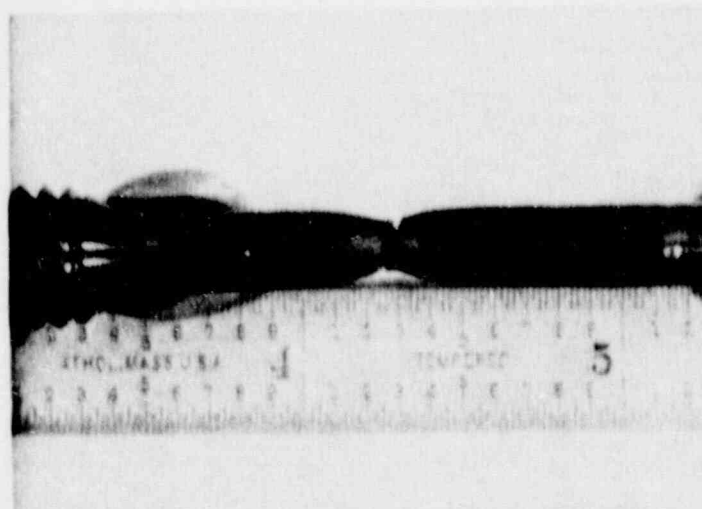
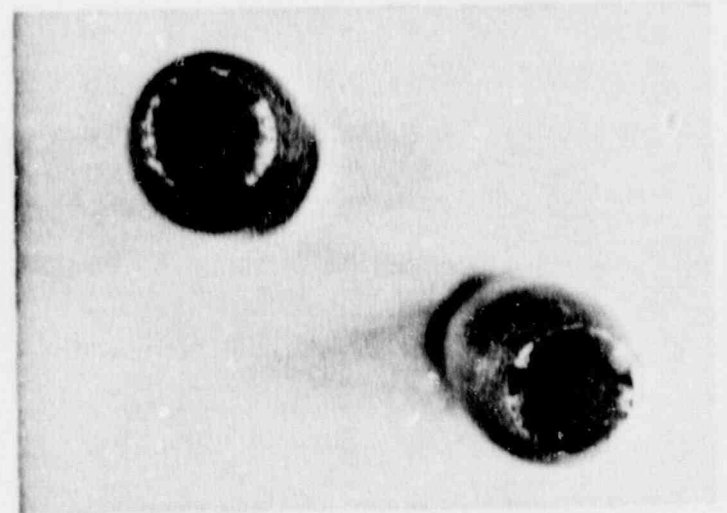
A62

68°F



A5M

160°F



A5E

550°F

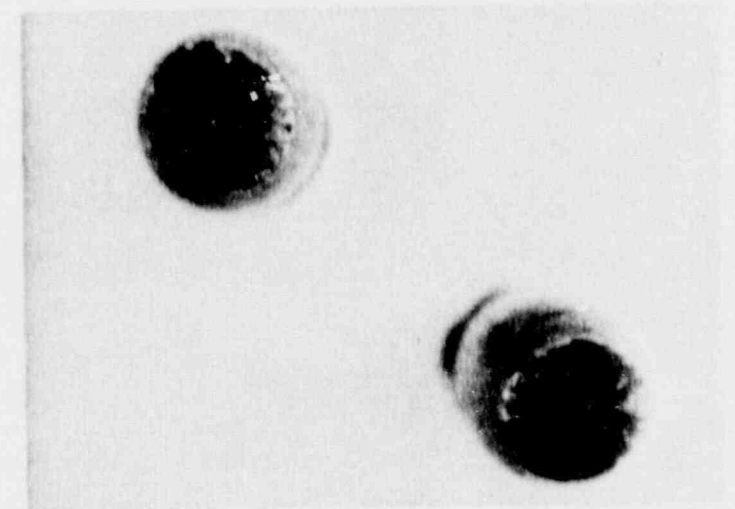
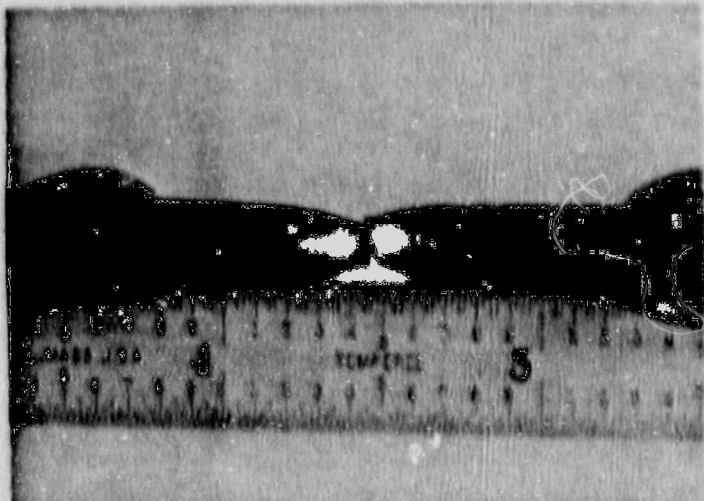
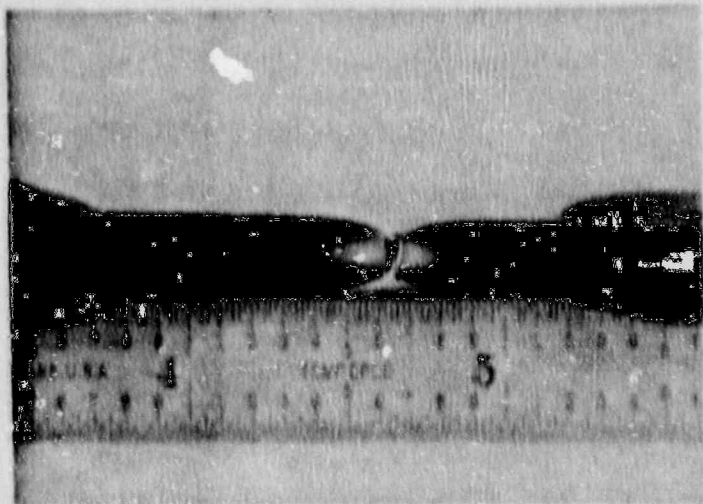
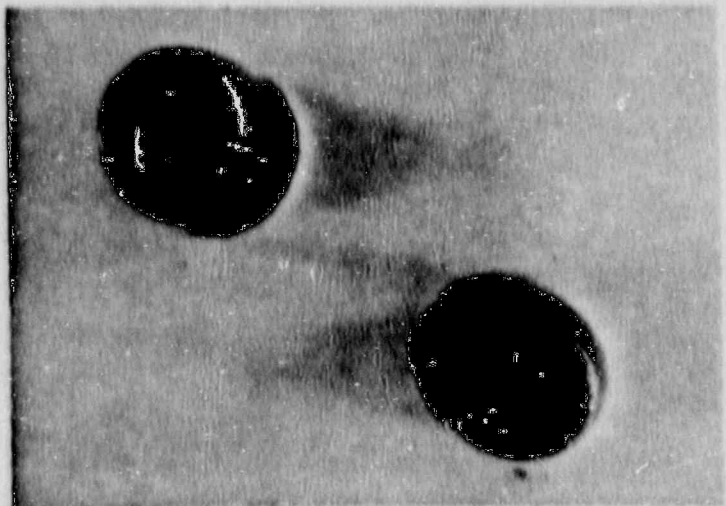


Figure 6-6. Fracture Location, Necking Behavior, and Fracture Appearance for Irradiated HAZ Tensile Specimens



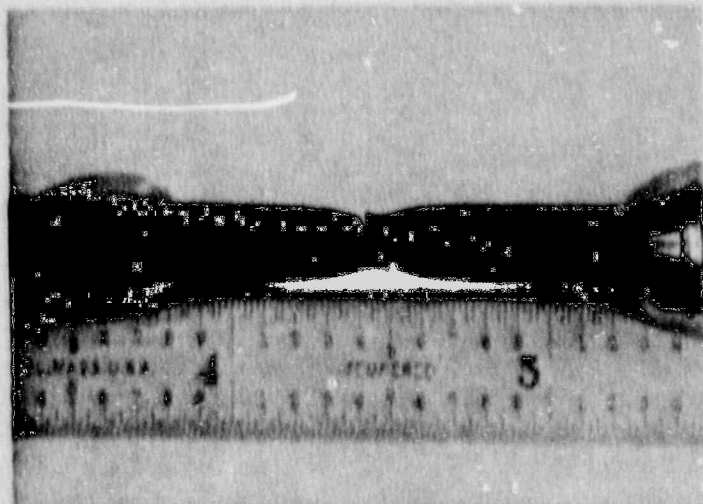
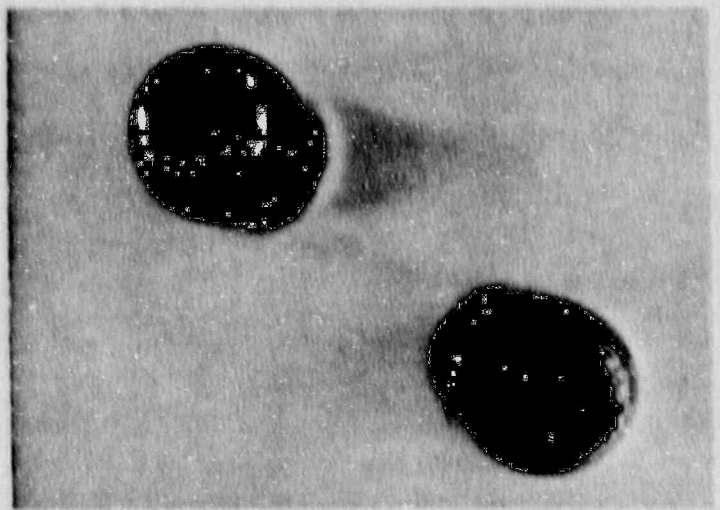
A41

68°F



A4A

160°F



A46

550°F

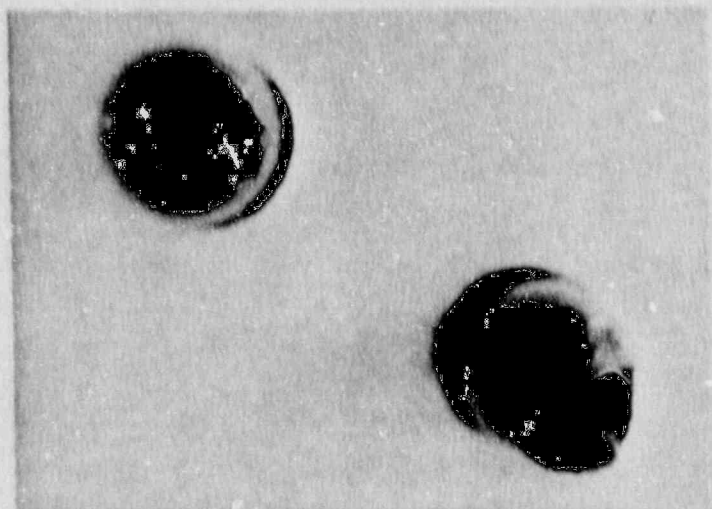
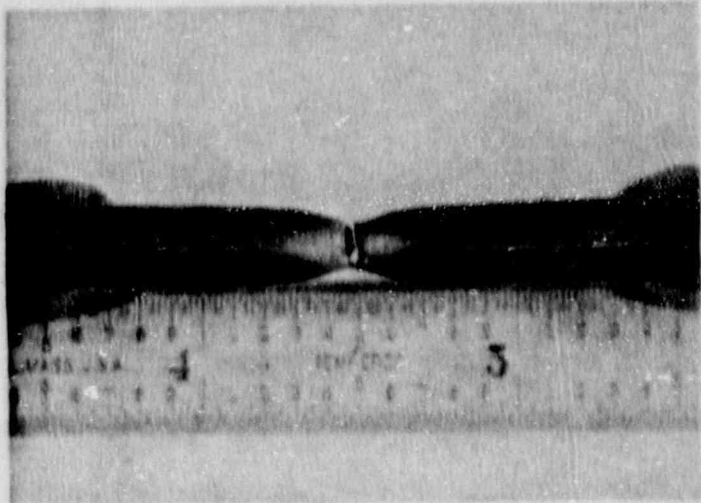
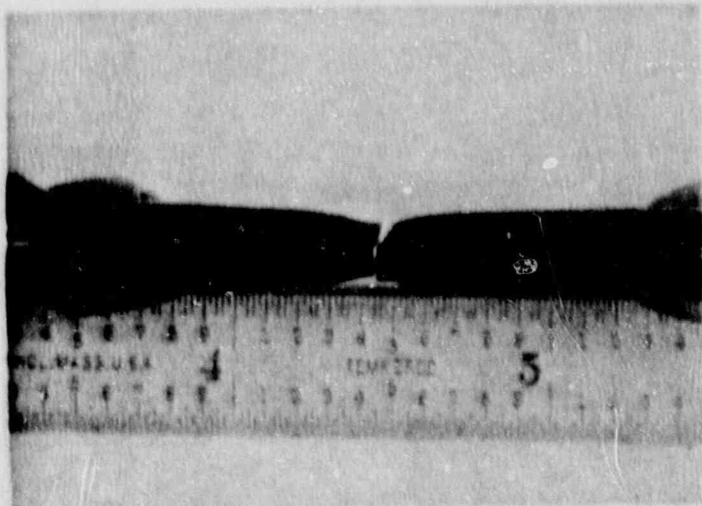
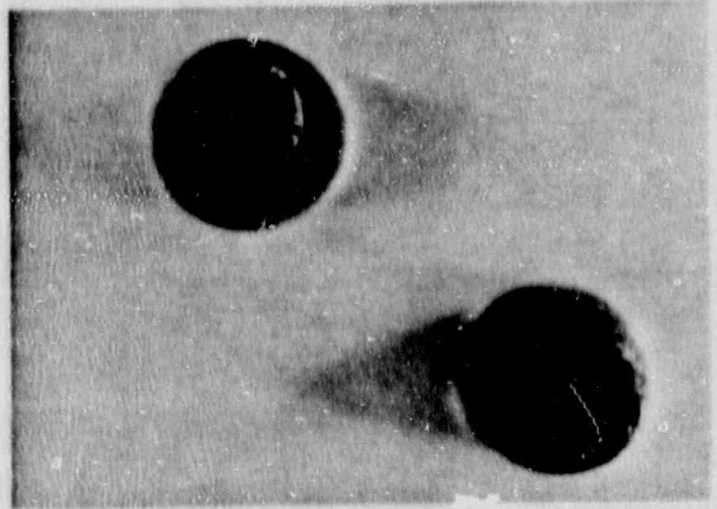


Figure 6-4. Fracture Location, Necking Behavior, and Fracture Appearance for Irradiated Base Metal Tensile Specimens



A4P

66°F



A54

550°F

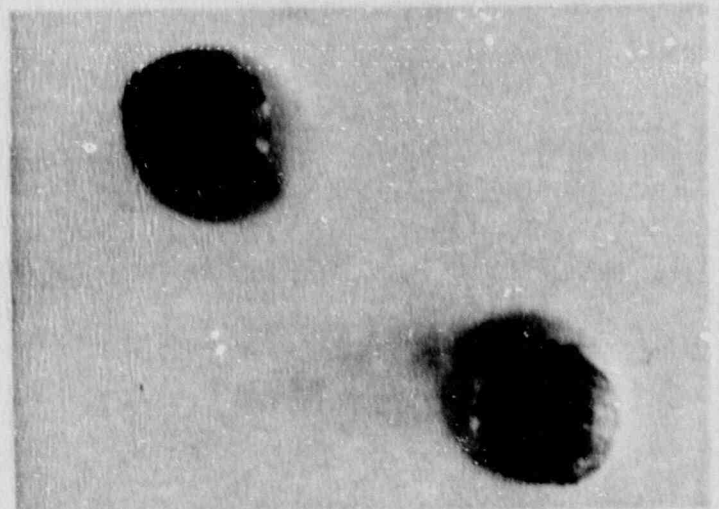
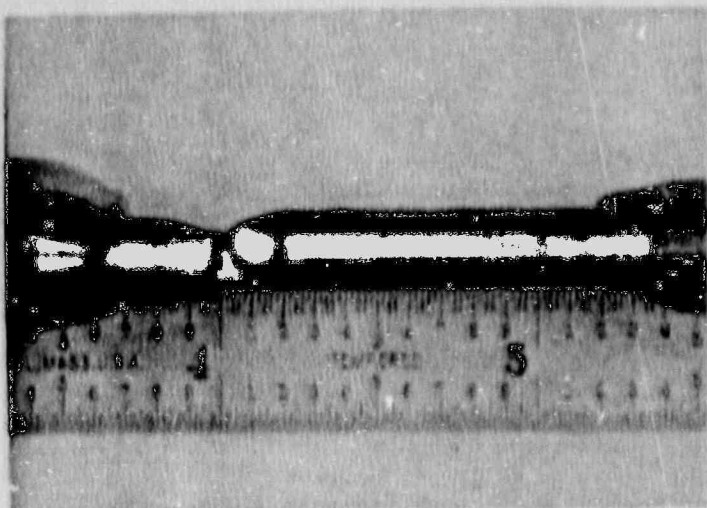
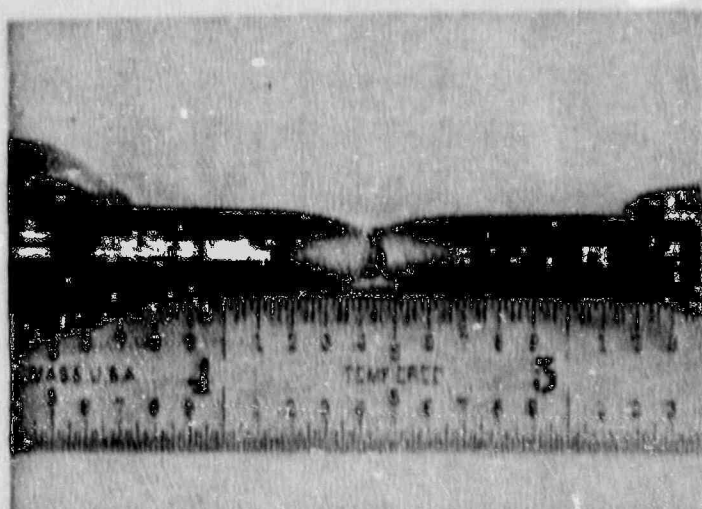
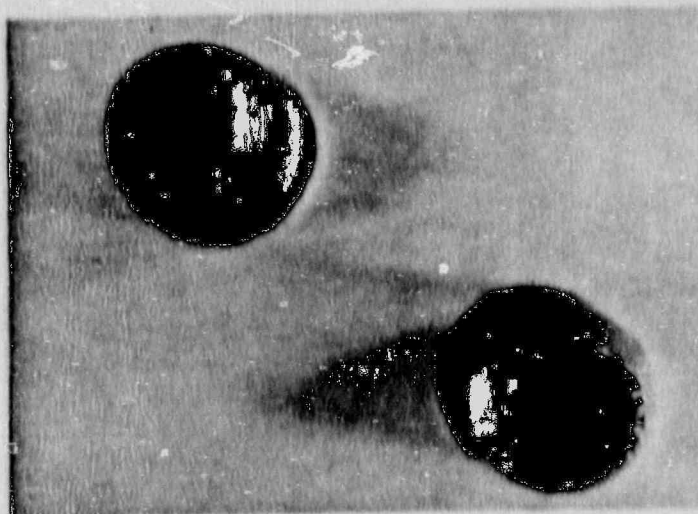


Figure 6-5. Fracture Location, Necking Behavior, and Fracture Appearance For Irradiated Weld Metal Tensile Specimens



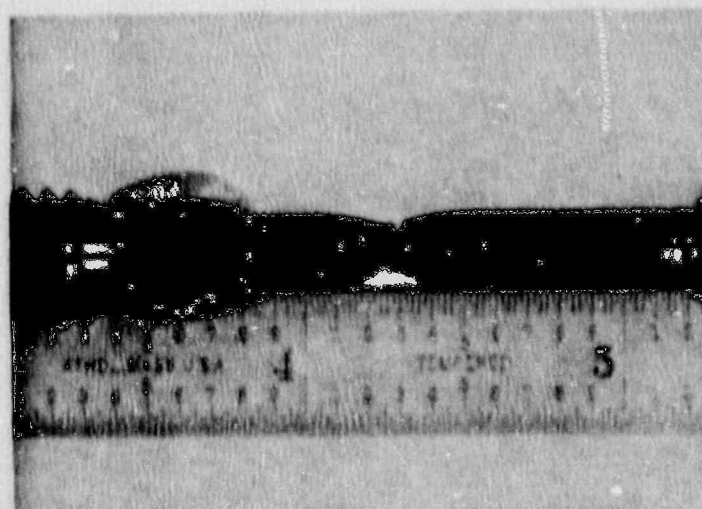
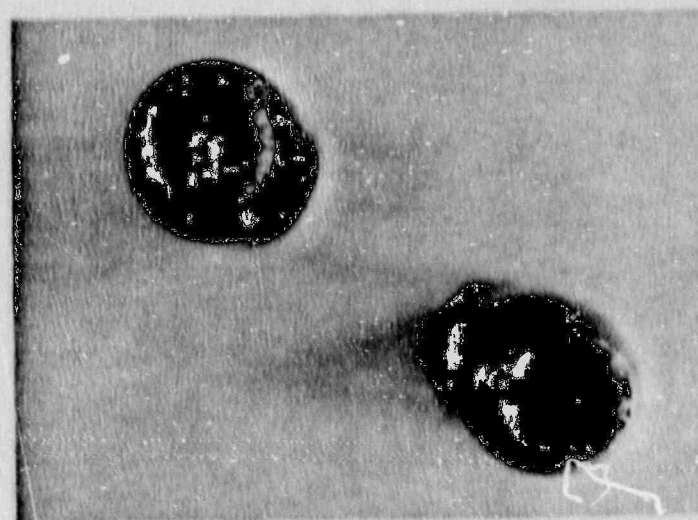
A62

68°F



A5M

160°F



A5E

550°F

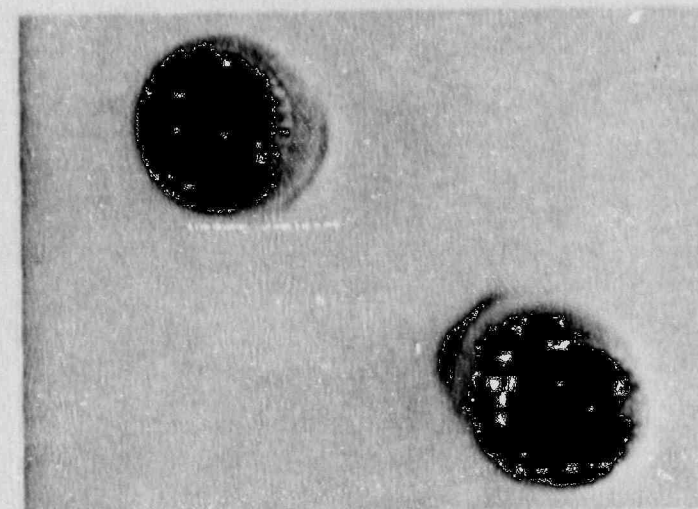


Figure 6-6. Fracture Location, Necking Behavior, and Fracture Appearance for Irradiated HAZ Tensile Specimens

7. DEVELOPMENT OF OPERATING LIMITS CURVES

7.1 BACKGROUND

Operating limits for pressure and temperature are required for three categories of operation: (a) hydrostatic pressure tests and leak tests, referred to as Curve A; (b) non-nuclear heatup/cooldown and low-level physics tests, referred to as Curve B; and (c) core critical operation, referred to as Curve C. There are three vessel regions that affect the operating limits: the closure flange region, the core beltline region, and the remainder of the vessel, or non-beltline regions. The closure flange region limits are controlling at lower pressures primarily because of Reference 1 requirements. The non-beltline and beltline region operating limits are evaluated according to procedures in References 1 and 2, with the beltline region minimum temperature limits increasing as the vessel is irradiated.

7.2 NON-BELTLINE REGIONS

Non-beltline regions are those locations that receive too little fluence to cause any RT_{NDT} increase. Non-beltline components include the nozzles, the closure flanges, some shell plates, top and bottom head plates and the control rod drive (CRD) penetrations. Detailed stress analyses of the non-beltline components, considering operating transients with relatively high pressures and low temperatures, were performed for the BWR/6, specifically for use in developing pressure-temperature (P-T) limits. The analyses bounded all mechanical loadings and thermal transients anticipated. Detailed stresses were used according to Reference 2 to develop plots of allowable pressure (P) versus temperature relative to the reference temperature ($T - RT_{NDT}$). These results are applicable to the Unit 3 vessel components, since the non-beltline geometries are not significantly different from BWR/6 configurations and the mechanical and thermal loadings are comparable.

The non-beltline region results were established by adding the highest RT_{NDT} for the non-beltline discontinuities to the P versus (T - RT_{NDT}) curves for the most limiting BWR/6 components, which are the CRD penetration and feedwater nozzle. Table 3-2 has the limiting RT_{NDT} values applicable to the feedwater nozzle limits and to the CRD penetration limits. They are 50°F for the feedwater nozzle limits, based on the RT_{NDT} of the recirculation inlet nozzles, and 54°F for the CRD penetration limits, based on the RT_{NDT} of the bottom head torus plates.

7.3 CORE BELTLINE REGION

As the beltline fluence increases during operation, the beltline P-T limit curves shift to the right by an amount discussed in Subsection 7.6. Depending on the amount of shift, the beltline curves may or may not become more limiting than the non-beltline curves at some time during plant life. The stress intensity factors calculated for the beltline region according to Reference 2 procedures are based on a combination of pressure and thermal stresses. The pressure stresses were calculated using thin-walled cylinder equations. Thermal stresses were calculated assuming the through-wall temperature distribution of a flat plate subjected to a 100°F/hr thermal gradient. The adjusted RT_{NDT} (ART) values calculated in Subsection 7.6 for the limiting beltline materials were used to adjust the P versus (T - RT_{NDT}) values from Figure G-2210-1 of Reference 2. ART is the initial RT_{NDT} plus the shift in RT_{NDT} due to irradiation.

7.4 CLOSURE FLANGE REGION

References 1 and 2 have several requirements that affect the P-T curves, based on the RT_{NDT} values in the closure flange region. As stated in Paragraph G-2222(c) of Reference 2, for application of full bolt preload and reactor pressure up to 20% of preservice hydrostatic test pressure (312 psig), the closure flange region metal temperature must be at RT_{NDT} or greater. The GE practice, however, is to recommend ($RT_{NDT} + 60^\circ\text{F}$) for bolt preload, for two reasons:

- a. The original ASME Code of construction required ($RT_{NDT} + 60^{\circ}F$);
and
- b. The highest stressed region during boltup is the closure flange region, and the flaw size assumed in that region (0.24 inches) is less than $1/4 T$. This flaw size is detectable using ultrasonic testing (UT) techniques. In fact, References 13 and 14 report that a flaw in the closure flange region of 0.09 inches can be reliably detected using UT.

For Unit 3, ($RT_{NDT} + 60^{\circ}F$) of the closure region materials is $70^{\circ}F$, because the RT_{NDT} values for the upper shell plates, top head plates and flanges are all $10^{\circ}F$, and the LST of the closure studs is $70^{\circ}F$. Therefore, the bolt preload temperature used in developing the P-T curves was $70^{\circ}F$.

Reference 1, Paragraph IV.A.2, sets requirements on minimum temperature when pressure is above 312 psig. The requirements are based on the RT_{NDT} of the closure region. Curve A temperature must be no less than ($RT_{NDT} + 90^{\circ}F$) and Curve B temperature no less than ($RT_{NDT} + 120^{\circ}F$). The Curve A requirement causes a $30^{\circ}F$ shift at 312 psig on the P-T curves. The Curve B requirement is not seen on Curve B, because the non-beltline part of the curve is more limiting.

7.5 CORE CRITICAL OPERATION REQUIREMENTS OF 10CFR50, APPENDIX G

Curve C, the core critical operation curve, is developed from the requirements of Reference 1, paragraph IV.A.3. Essentially paragraph IV.A.3 requires that Curve C be $40^{\circ}F$ above any Curve A or B limits. Curve B is more limiting than Curve A, so Curve C is Curve B plus $40^{\circ}F$. Curve C initiates at zero pressure at ($RT_{NDT} + 60^{\circ}F$), based on an exception for BWRs in Paragraph IV.A.3, allowing critical operation at temperatures below the hydrostatic pressure (Curve A at 1100 psig) test temperature. This exception is valid only when water level is within the normal range and pressure is below 312 psig.

7.6 EVALUATION OF RADIATION EFFECTS

The impact on adjusted reference temperature (ART) due to irradiation in the beltline materials is determined according to the methods in Reference 5, as a function of neutron fluence and the element contents of copper (Cu) and nickel (Ni). The specific relationship from Reference 5 is:

$$\text{ART} = \text{Initial RT}_{\text{NDT}} + \text{Shift} + \text{Margin} \quad (7-1)$$

where:

$$\text{Shift} = [\text{CF}] * f(0.28 - 0.10 \log f) \quad (7-2)$$

$$\text{Margin} = 2 * (\sigma_I^2 + \sigma_{\Delta}^2)^{1/2} \quad (7-3)$$

CF = chemistry factor from Tables 1 or 2 of Reference 5,

f = 1/4 T fluence (n/cm²) divided by 10¹⁹,

σ_I = standard deviation on initial RT_{NDT},

σ_{Δ} = standard deviation on RT_{NDT} shift, is 28°F for welds and 17°F for base material, except that σ_{Δ} need not exceed 0.50 times the Shift value.

The limiting beltline plate and weld are determined based on the Cu-Ni content and initial RT_{NDT} of the materials. Calculations to determine 32 EFPY ART values, and thus the limiting beltline materials, are summarized in Table 7-1. The results show that a lower-intermediate shell plate, Heat C2773-2, is the most limiting beltline material.

One input to the Reference 5 calculations not shown in Table 7-1 is σ_I . As determined in Reference 6, the longitudinal electroslag welds have $\sigma_I = 16.44^\circ\text{F}$. For all the other beltline materials, where RT_{NDT} values were determined from measured Charpy data, $\sigma_I = 0^\circ\text{F}$. The basis for using $\sigma_I = 0^\circ\text{F}$ is discussed in more detail in Appendix C.

7.6.1 Measured Versus Predicted Surveillance Shift

Section 5 of this report compares the measured shift for the plate surveillance specimens with predicted shifts for the surveillance plate material based on the method shown in Equation 7-2. Reference 5 states that surveillance data may be used in place of Equations 7-2 and 7-3 when two sets of credible data are available. This is only the first set of data for Unit 3. Therefore, determinations of ART for the purposes of developing P-T curves are based on Reference 5 predictions.

7.6.2 ART Versus EFPY

Equations 7-1 through 7-3 were evaluated for the beltline plate and weld metals. Table 7-1 shows the 32 EFPY fluence at the vessel 1/4 T locations to be 5.0×10^{17} n/cm². Calculations of the plate and weld ART values at 32 EFPY show that Heat C2773-2 is the most limiting material throughout plant life. Figure 7-1 shows the ART for Heat C2773-2 as a function of full power years of operation, through 32 EFPY.

7.6.3 Fracture Toughness Conditions at 32 EFPY

Paragraph IV.B of Reference 1 sets limits on the ART and on the upper shelf energy (USE) of the beltline materials. The ART must be less than 200°F, and the USE must be above 50 ft-lb. Based on Table 7-1, the ART values at 32 EFPY of 71°F or less are acceptable.

Calculations of 32 EFPY USE, using Reference 5 methods, were done for the surveillance plate and the beltline welds, and are summarized in Table 7-2. The fabrication data for the other beltline plates did not include USE data, so general conclusions for those plates are drawn based on the results for the surveillance plate. The surveillance plate data are longitudinal so the equivalent transverse USE of the plate material is taken as 65% of the longitudinal USE, according to Reference 11. The weld metal USE has no transverse/longitudinal correction because weld metal has no orientation effect. The longitudinal weld initial USE was computed in Reference 6, based on data for nine weld prolongations. The girth weld initial USE is based on Charpy data taken at only 10°F, so the girth weld

results are conservative. Extrapolating to the 32 EFPY fluence according to Reference 5, the lowest predicted transverse USE values for the plate and weld materials are 78 ft-lb and 82 ft-lb, respectively. While there may be some variation in the initial USE values of the beltline plates, the moderate copper levels and the relatively low fluence at 32 EFPY, considered in conjunction with the results for Heat C3103-1, indicate that the 32 EFPY USE will be above 50 ft-lb for all beltline plates.

Based on the above results, it is expected that the beltline materials will have 32 EFPY USE above 50 ft-lb, as required in Reference 1. Since USE and ART requirements are met, irradiation effects are not severe enough to necessitate additional analyses or preparations for RPV annealing.

7.7 OPERATING LIMITS CURVES VALID TO 32 EFPY

Figure 7-2 shows P-T curves for Unit 3, valid to 32 EFPY. The P-T curves are developed by considering the requirements applicable to the non-beltline, beltline and closure flange regions. In reviewing the shifted beltline curves, it was determined that the non-beltline curves are still limiting at 32 EFPY. Therefore, barring any changes due to future surveillance data or revisions to regulations, the P-T curves shown in Figure 7-2 will apply for operation through 32 EFPY.

7.8 REACTOR OPERATION VERSUS OPERATING LIMITS

For most reactor operating conditions, pressure and temperature are at saturation conditions, which are well into the acceptable operating area (to the right of the P-T curves). The most severe unplanned transient relative to the P-T curves is an upset condition consisting of several transients which result in a SCRAM. The worst combination of pressure and temperature during this postulated event is 1180 psig with temperatures in the lower head of 250°F. In this case, the core is not critical, so the non-nuclear heatup/cooldown curve applies (Curve B). As seen for Curve B in Figure 7-2, at 1180 psi the minimum transient temperature of 250°F lies in the acceptable operating area. Therefore, violation of the P-T curves is only a concern in cases where operator interaction occurs, such as during pressure testing and initiation of criticality.

Table 7-1

BELTLINE EVALUATION FOR PEACH BOTTOM 3

Shell
Thickness = 6.125 inches

Fluence:

Peak I.D. fluence = 7.2E+17
Peak 1/4 T fluence = 5.0E+17

COMPONENT	I.D.	HEAT OR HEAT/LOT	%Cu	%Ni	CF	Initial FTndt	32 Delta	EFPY RTndt	Margin	32 EPFY Shift	32 EPFY ART
PLATES:											
Lower Shell	6-146-1	C4689-2	0.12	0.56	82.2	-10		24.0	24.0	48.0	38.0
Lower Shell	6-146-3	C4684-2	0.13	0.58	90.4	-20		26.4	26.4	52.8	32.8
Lower Shell	6-146-7	C4627-1	0.12	0.57	82.4	-20		24.1	24.1	48.2	28.2
Low-Int Shell	6-139-10	C2773-2	0.15	0.49	104	10		30.4	30.4	60.8	70.8
Low-Int Shell	6-139-11	C2775-1	0.13	0.46	86.8	10		25.4	25.4	50.7	60.7
Low-Int Shell	6-139-12	C3103-1	0.14	0.6	100	10		29.2	29.2	58.5	68.5
Intermediate	6-146-5	C4608-1	0.12	0.55	82	10		24.0	24.0	47.9	57.9
Intermediate	6-146-4	C4689-1	0.12	0.56	82.2	10		24.0	24.0	48.0	58.0
Intermediate	6-146-2	C4654-1	0.11	0.55	73.5	10		21.5	21.5	43.0	53.0
WELDS:											
Lower Long.	D1,D2,D3	37C065	0.21	0.21	109.3	-45		31.9	45.8	77.8	32.8
Low-Int Long.	E1,E2,E3	37C065	0.21	0.21	109.3	-45		31.9	45.8	77.8	32.8
Intermediate	F1,F2,F3	37C065	0.21	0.21	109.3	-45		31.9	45.8	77.8	32.8
Lower to Low-Int Girth	DE	3P4000,Linde 124 Flux Lot 3932	0.02	0.96	27	-50		7.9	7.9	15.8	34.2
Low-Int to Intermed. Girth	EF	IP4217,Linde 124 Flux Lot 3929	0.11	0.96	147.2	-50		43.0	43.0	86.0	36.0

Table 7-2

ESTIMATE OF UPPER SHELF ENERGY FOR BELTLINE MATERIALS

<u>Identification</u>	<u>% Cu</u>	32 EFPY ^a		Upper Shelf (ft-lb)	
		<u>Decrease</u>	<u>in USE</u>	<u>Longitudinal/Transverse</u>	<u>Unirradiated</u>
Surveillance Plate:					
C3103-1	0.14	11%		137/89	122/79
Beltline Plate (highest copper):					
	0.15	12%		137/89	120/78
Longitudinal Welds:					
37C065	0.21	17.5%		99	82
Lower to Lower-Intermediate Girth Weld:					
3P4000	0.02	8%		97 ^b	89
Lower-Intermediate to Intermediate Girth Weld:					
IP4217	0.11	12.5%		71 ^b	62

^a USE decrease percentages based on 32 EFPY fluence of 5.0×10^{17} n/cm²

^b Values are highest Charpy energy from tests at 10°F.

Plate Heat C2773-2

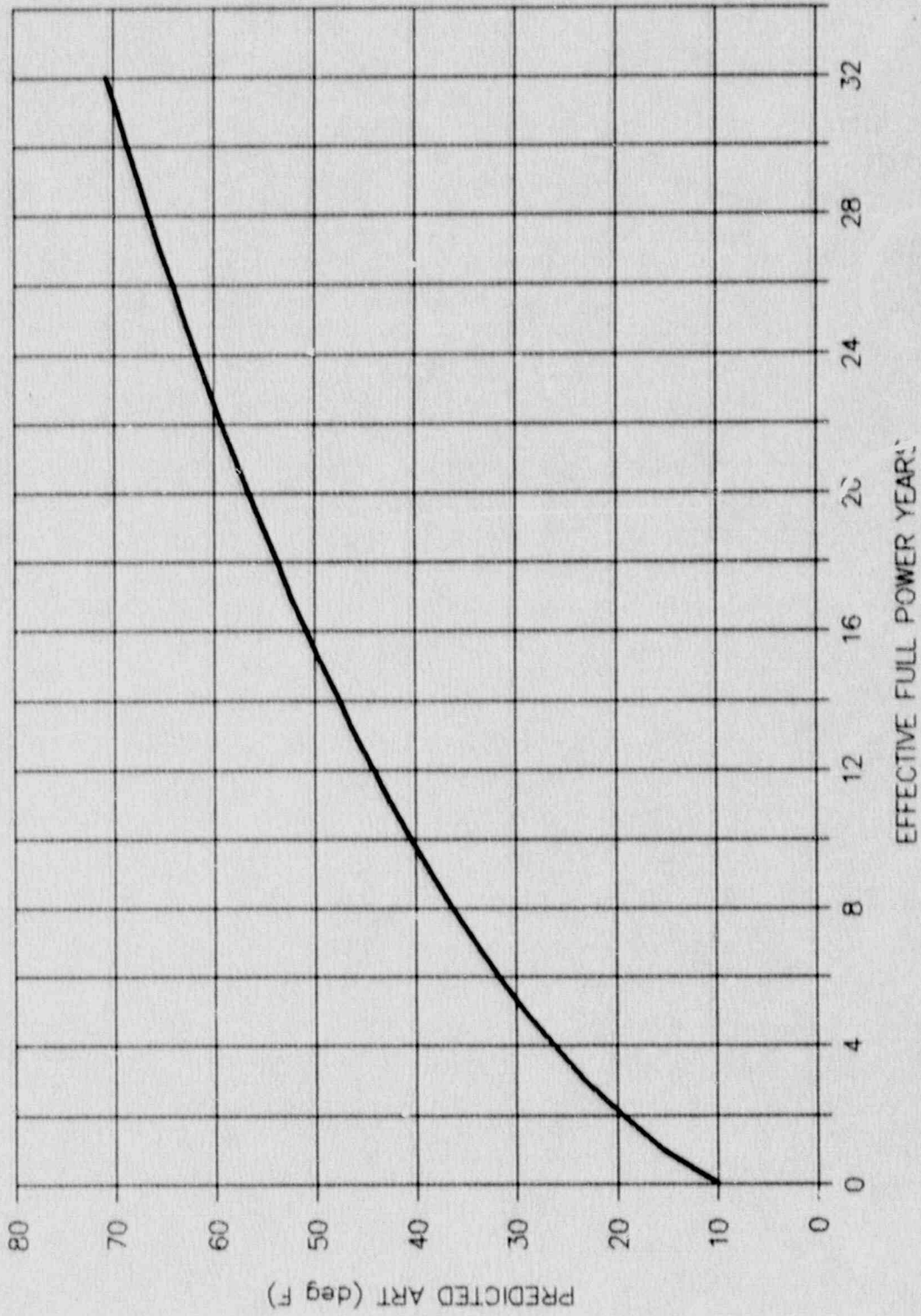


Figure 7-1. ART of Limiting Beltline Material

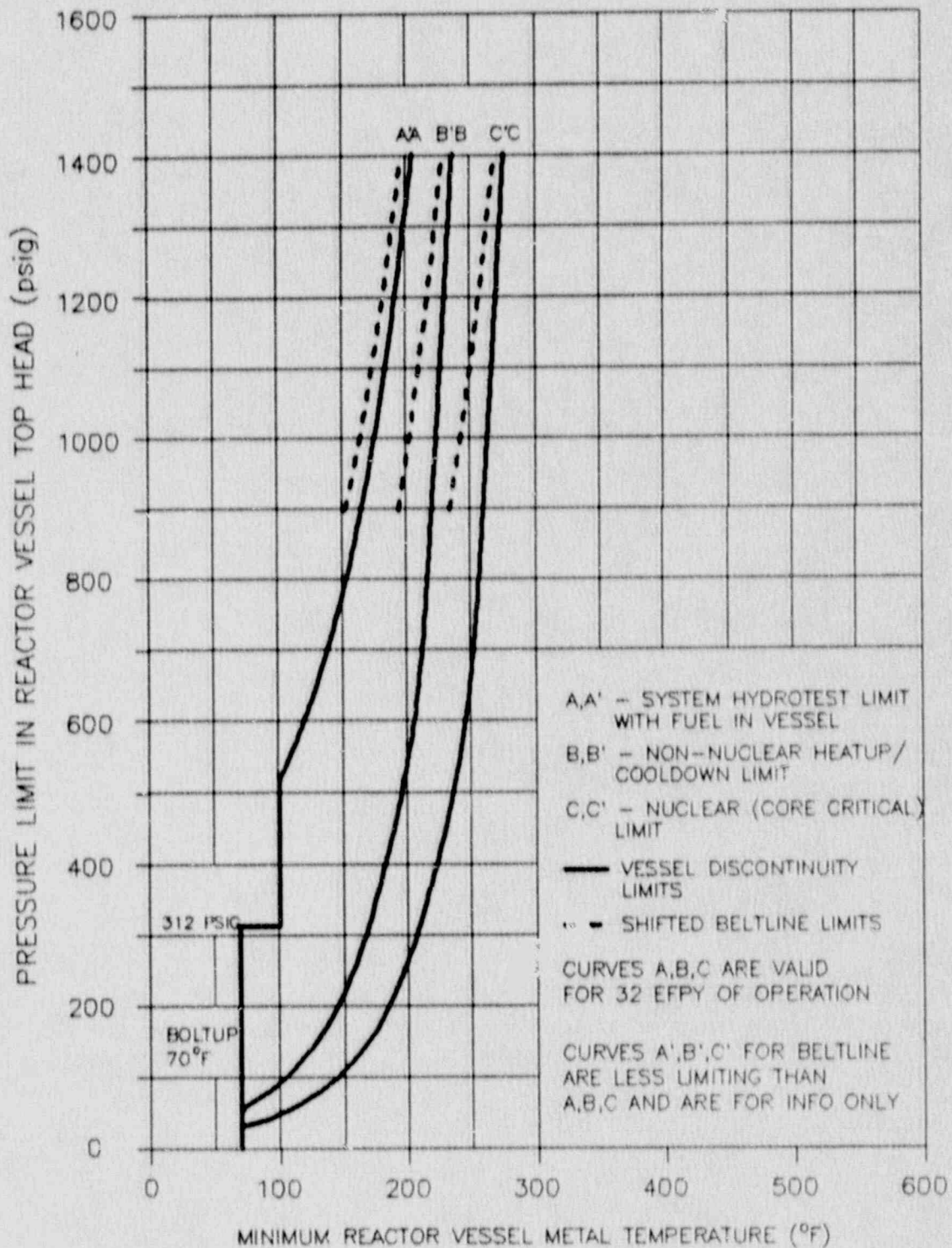


Figure 7-2. Pressure-Temperature Curves Valid for 32 EFY of Operation

8. REFERENCES

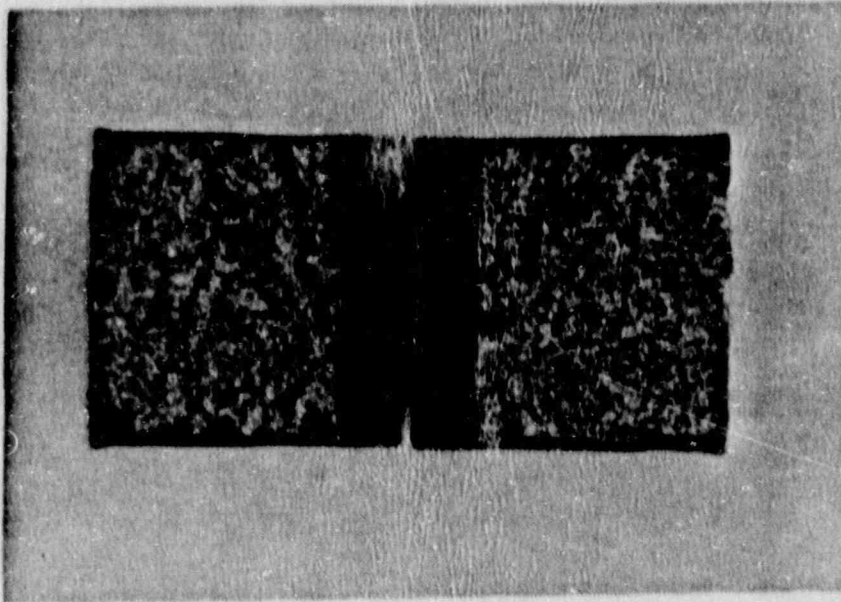
1. "Fracture Toughness Requirements," Appendix G to Part 50 of Title 10 of the Code of Federal Regulations, July 1983.
2. "Protection Against Non-Ductile Failure," Appendix G to Section XI of the 1989 ASME Boiler & Pressure Vessel Code.
3. "Reactor Vessel Material Surveillance Program Requirements," Appendix H to Part 50 of Title 10 of the Code of Federal Regulations, July 1983.
4. "Conducting Surveillance Tests for Light Water Cooled Nuclear Power Reactor Vessels," Annual Book of ASTM Standards, E185-82, July 1982.
5. "Radiation Embrittlement of Reactor Vessel Materials," USNRC Regulatory Guide 1.99, Revision 2, May 1988.
6. Caine, T. A., "Peach Bottom Unit 2 Surveillance Testing and Fracture Toughness Analysis," GE Report SASR 88-24, May 1988.
7. Hodge, J. M., "Properties of Heavy Section Nuclear Reactor Steels," Welding Research Council Bulletin 217, July 1976.
8. "Reactor Pressure Vessel," GE Purchase Specification 21A1111, Revision 9, August 1970.

9. "Standard Methods for Notched Bar Impact Testing of Metallic Materials," Annual Book of ASTM Standards, E23-82, March 1982.
10. "Nuclear Plant Irradiated Steel Handbook," EPRI Report NP-4797, September 1986.
11. "Fracture Toughness Requirements," USNRC Branch Technical Position MTEB 5-2, Revision 1, July 1981.
12. "Standard Methods of Tension Testing of Metallic Materials," Annual Book of ASTM Standards, E8-81.
13. "Ultrasonic Examination for Cracks in the Top Head Flange," CBI Nuclear, Development Report 74-9047, December 1975.
14. "Ultrasonic Examination for Cracks in the Shell Flange," CBI Nuclear, Development Report 74-9056, November 1975.

APPENDIX A

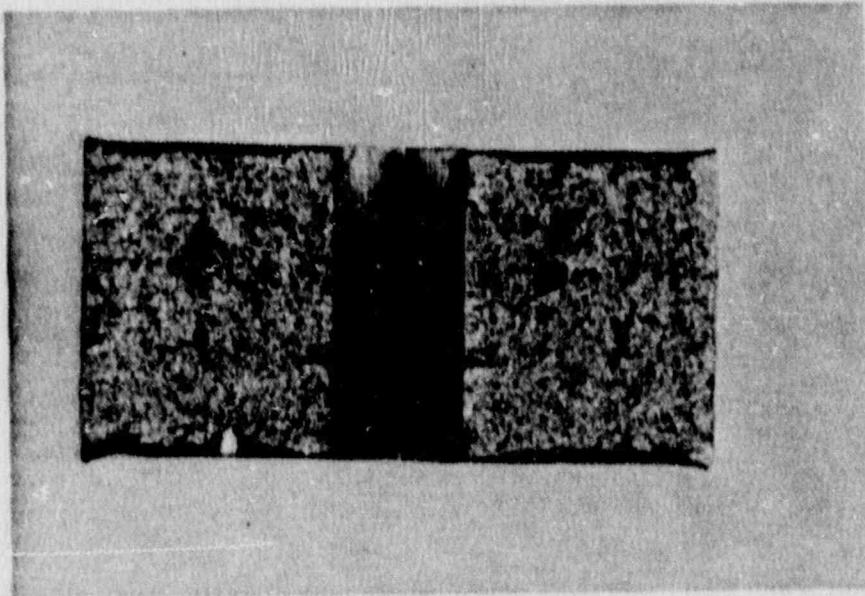
IRRADIATED CHARPY SPECIMEN FRACTURE SURFACE PHOTOGRAPHS

Photographs of each Charpy specimen fracture surface were taken per the requirements of ASTM E185-82. The pages following show the fracture surface photographs along with a summary of the Charpy test results for each specimen. The photographs are arranged with the materials in the order of base, weld and HAZ.



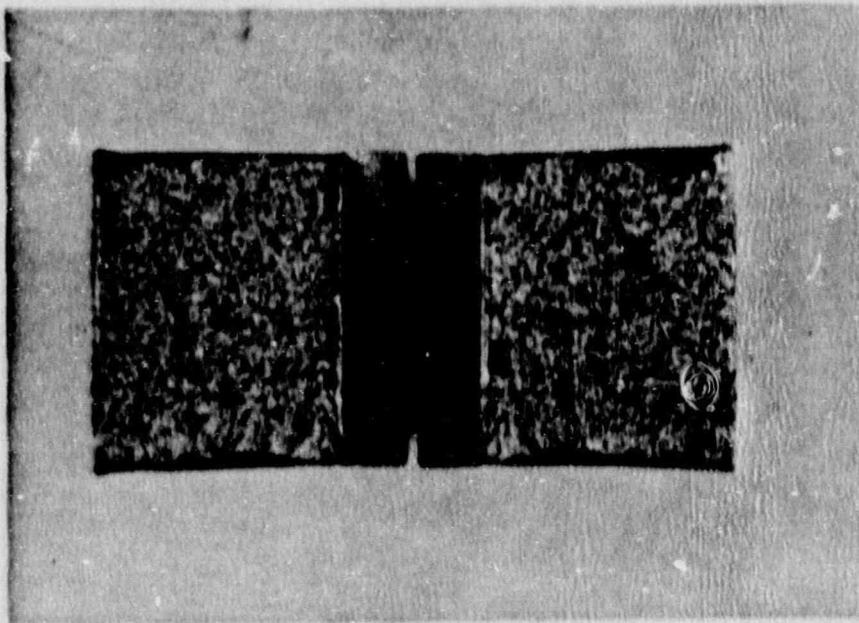
BASE: 7P1
TEMP: -40°F
ENERGY: 8.0 ft-lb

MLE: 6
% SHEAR: 3



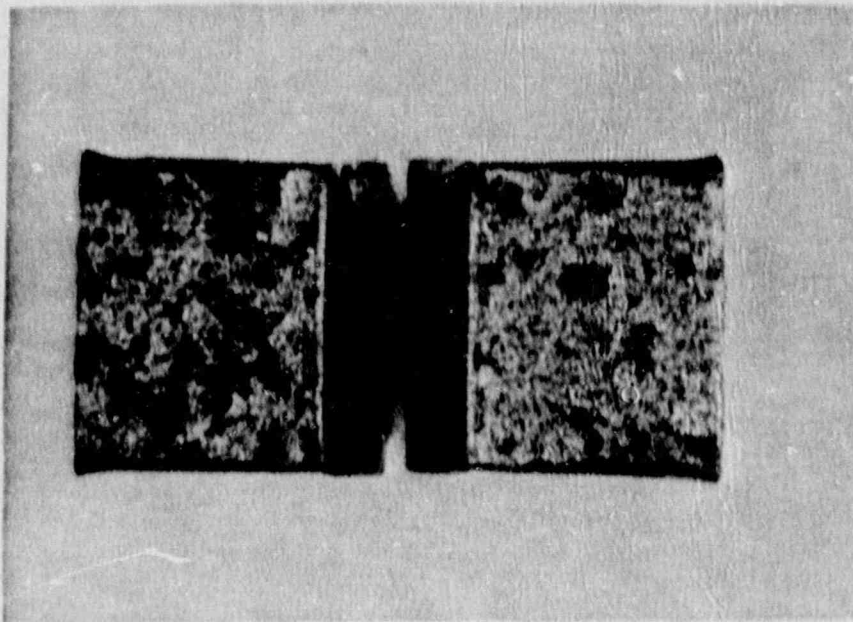
BASE: 7LU
TEMP: -30°F
ENERGY: 8.0 ft-lb

MLE: 11
% SHEAR: 7



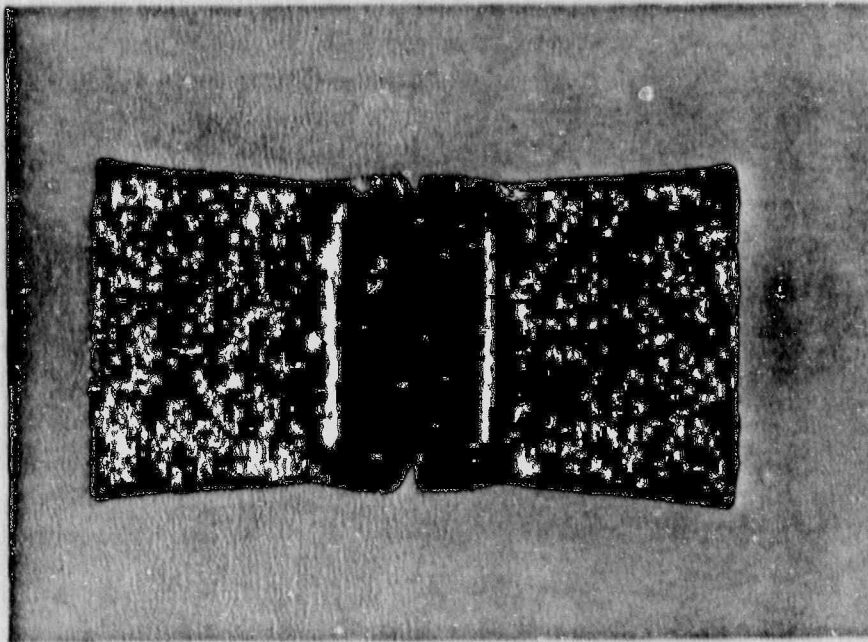
BASE: 7T6
TEMP: -20°F
ENERGY: 13.5 ft-lb

MLE: 13
% SHEAR: 9



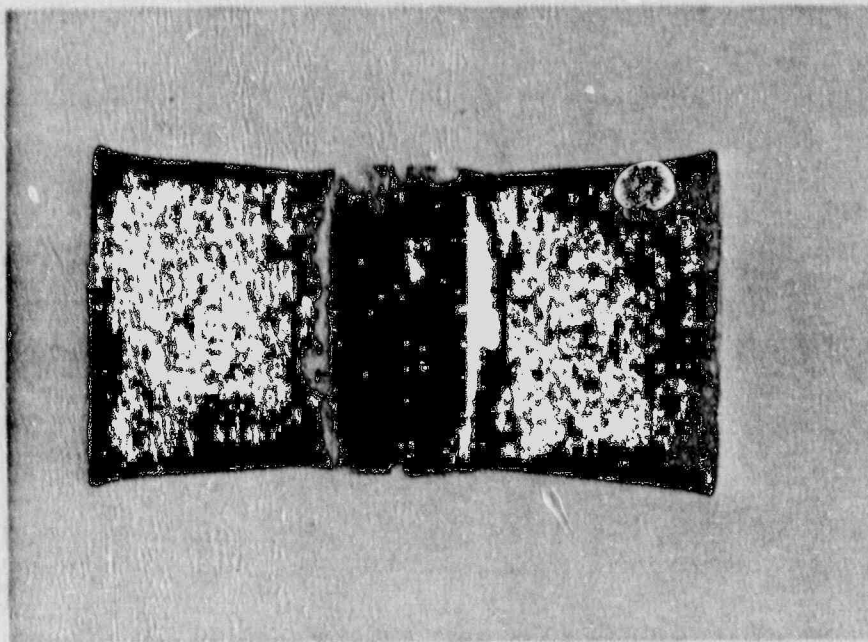
BASE: 7TB
TEMP: -10°F
ENERGY: 15.5 ft-lb

MLE: 14
% SHEAR: 8



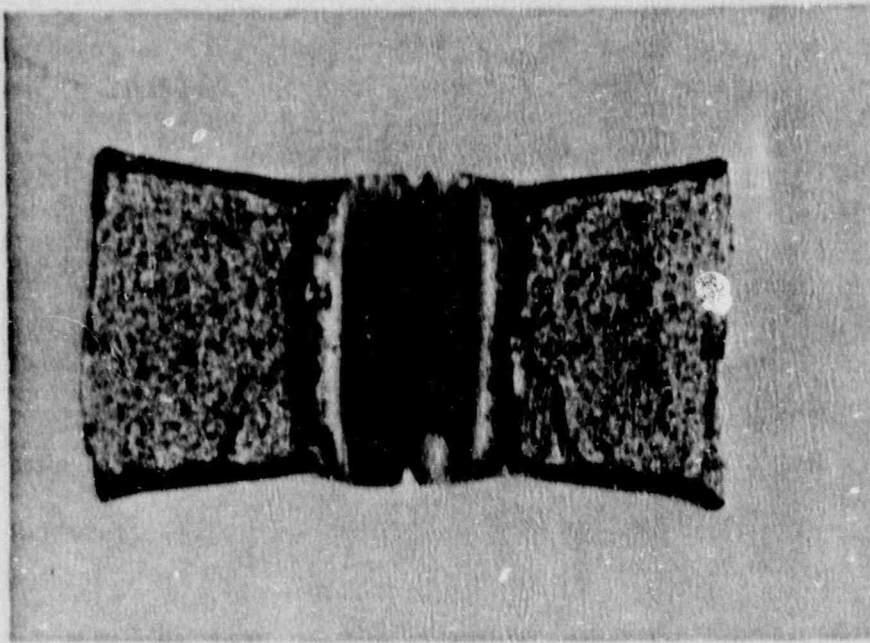
BASE: 7MU
TEMP: 0°F
ENERGY: 43.5 ft-lb

MLE: 34
% SHEAR: 16



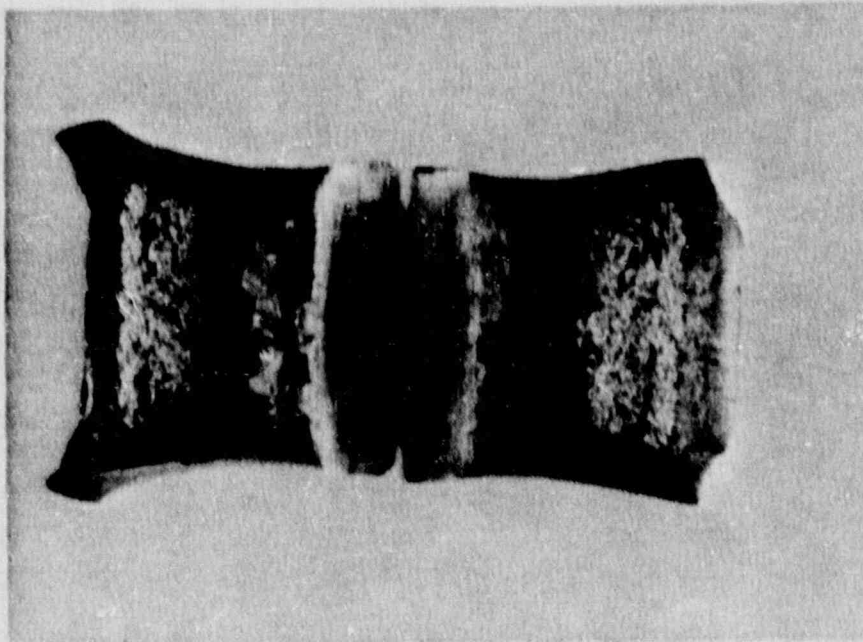
BASE: 7M5
TEMP: 20°F
ENERGY: 46.0 ft-lb

MLE: 42
% SHEAR: 22



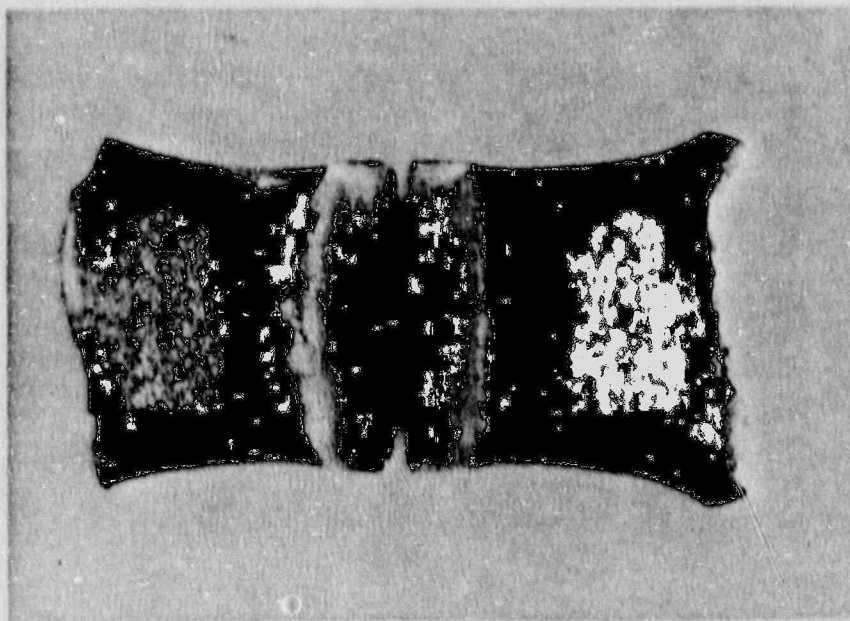
BASE: 7PP
TEMP: 40°F
ENERGY: 65.0 ft-lb

MLE: 50
% SHEAR: 23



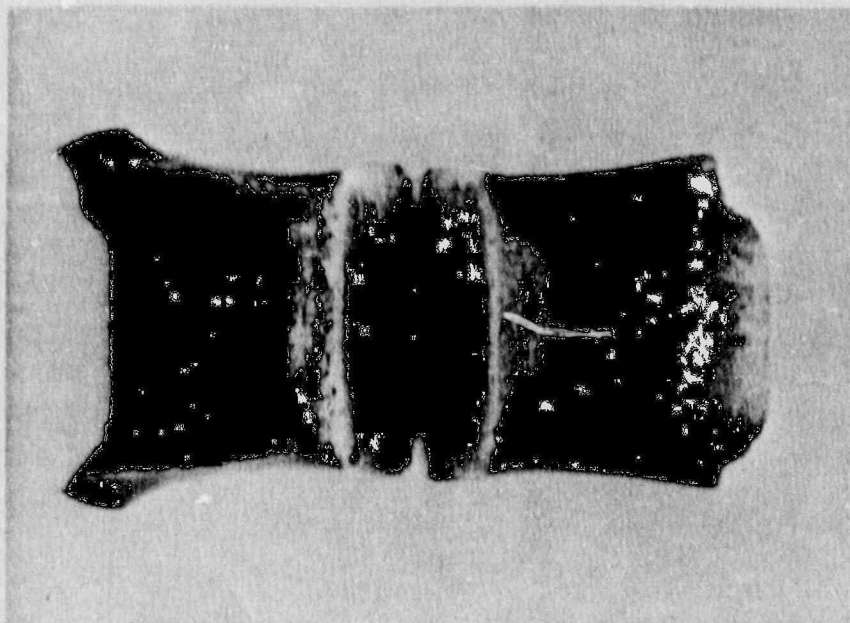
BASE: 7M7
TEMP: 80°F
ENERGY: 112.0 ft-lb

MLE: 88
% SHEAR: 73



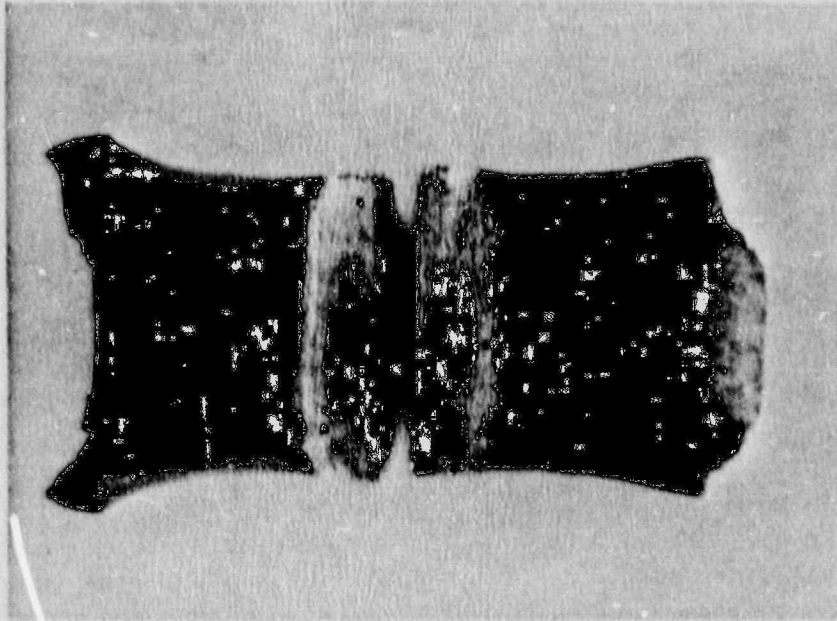
BASE: 7P2
TEMP: 120°F
ENERGY: 102.5 ft-lb

MLE: 70
% SHEAR: 67



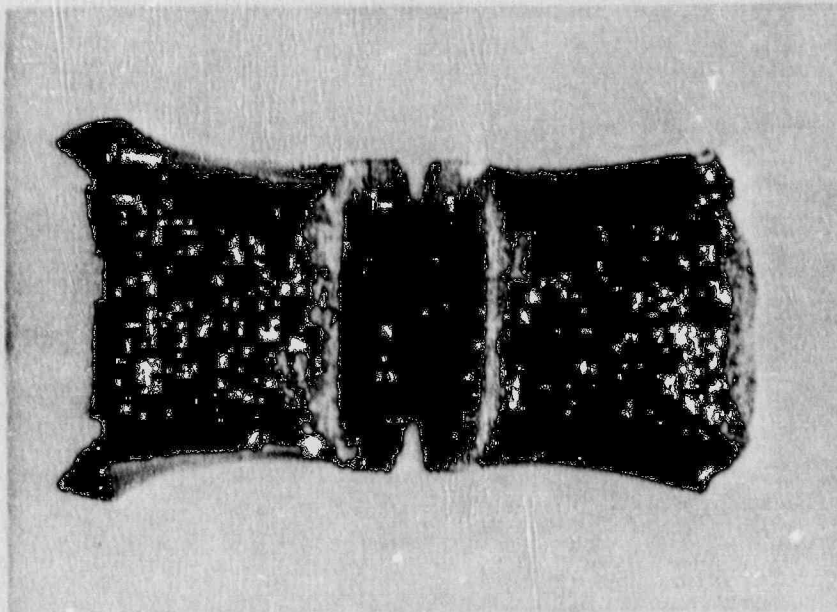
BASE: 7MJ
TEMP: 160°F
ENERGY: 129.0 ft-lb

MLE: 86
% SHEAR: 100



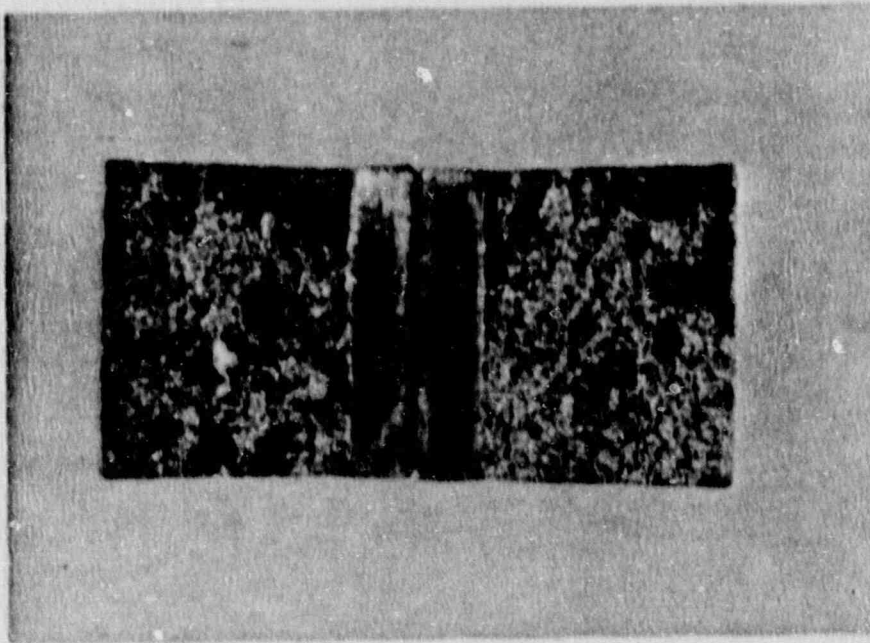
BASE: 7MB
TEMP: 200°F
ENERGY: 121.0 ft-lb

MLE: 89
% SHEAR: 100



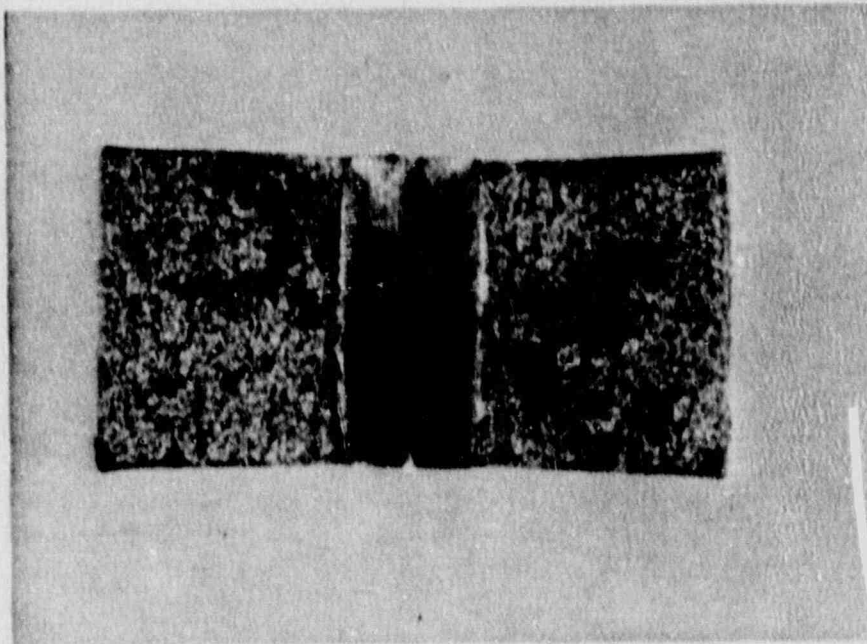
BASE: 7PY
TEMP: 300°F
ENERGY: 129.0 ft-lb

MLE: 88
% SHEAR: 100



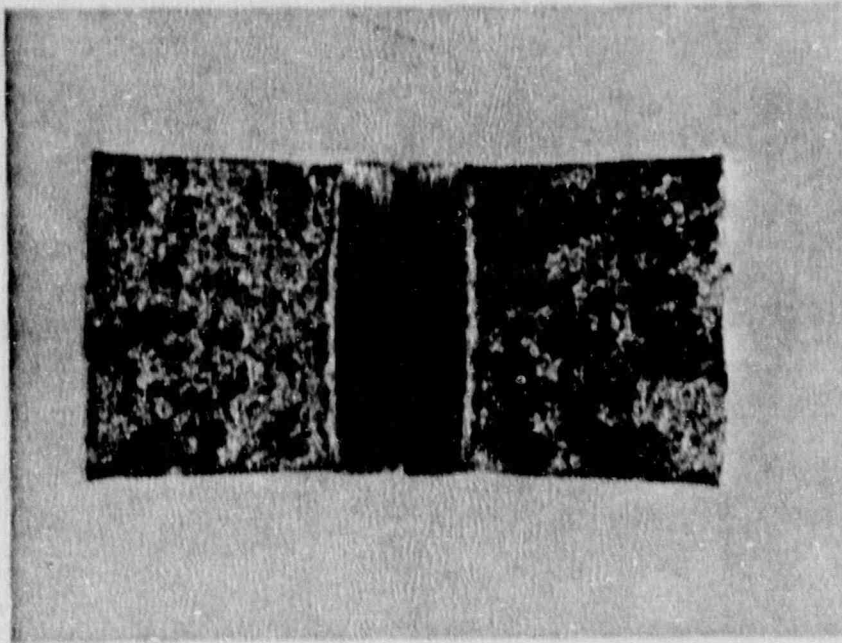
WELD: 7TJ
TEMP: -40°F
ENERGY: 11.0 ft-lb

MLE: 9
% SHEAR: 4



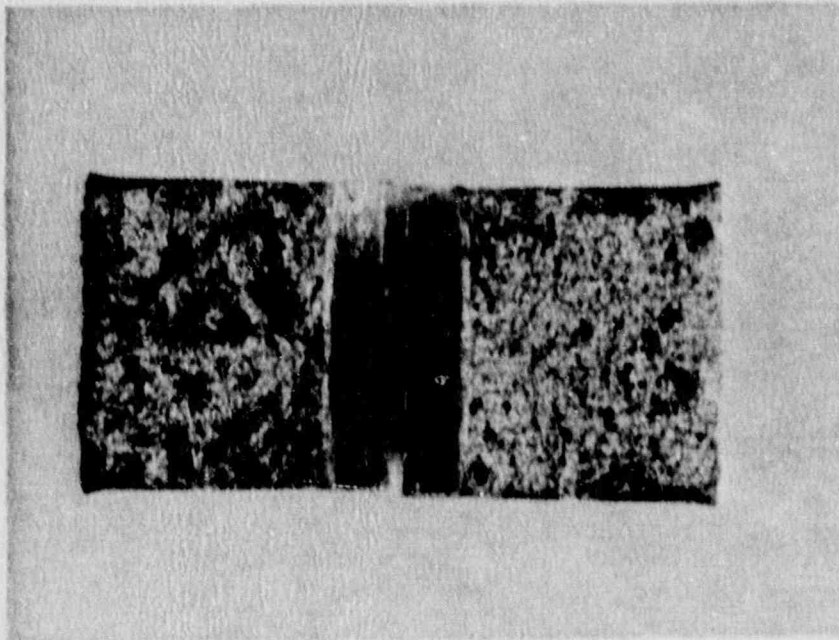
WELD: 7TL
TEMP: -20°F
ENERGY: 18.0 ft-lb

MLE: 16
% SHEAR: 3



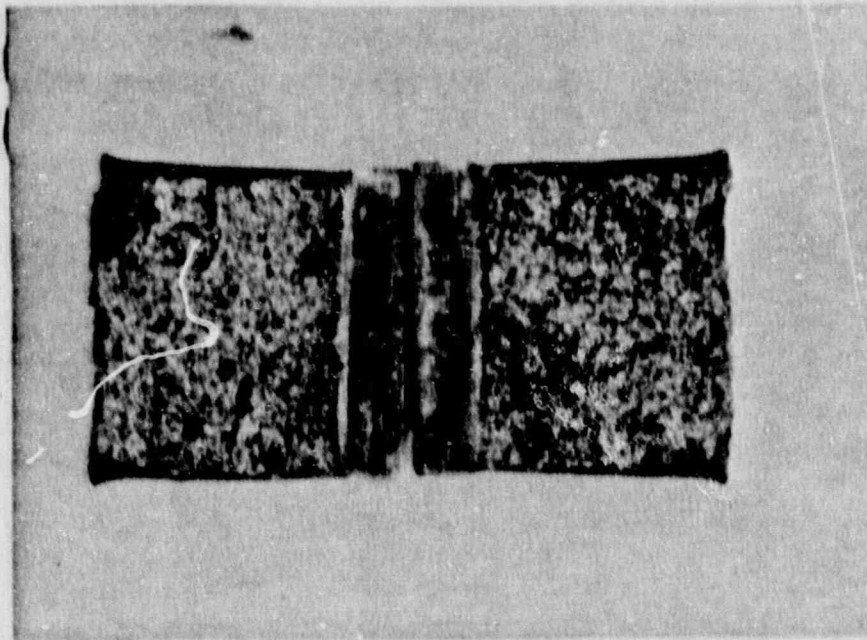
WELD: 7UA
TEMP: -10°F
ENERGY: 21.5 ft-lb

MLE: 20
% SHEAR: 6



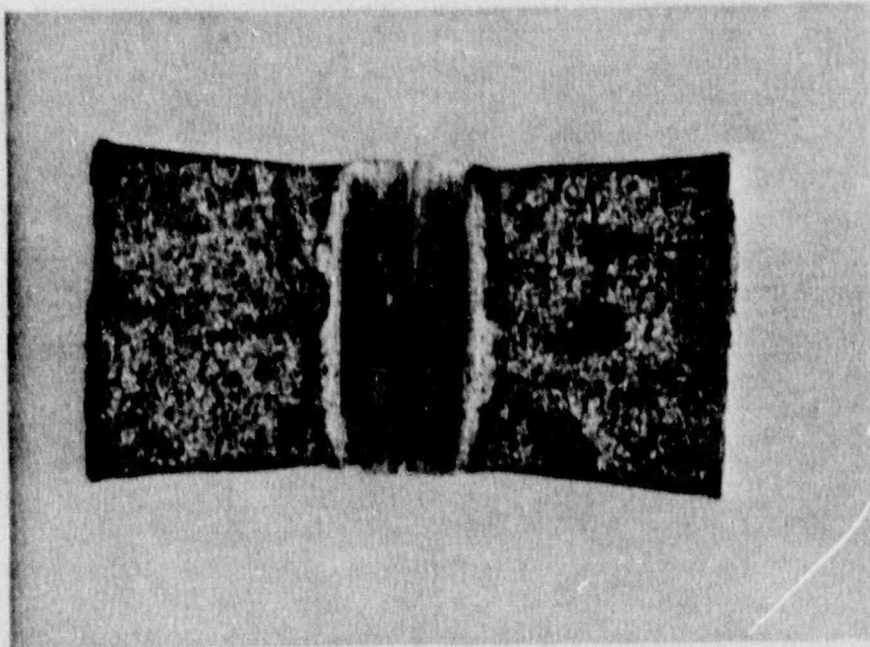
WELD: 7TK
TEMP: 0°F
ENERGY: 12.0 ft-lb

MLE: 14
% SHEAR: 3



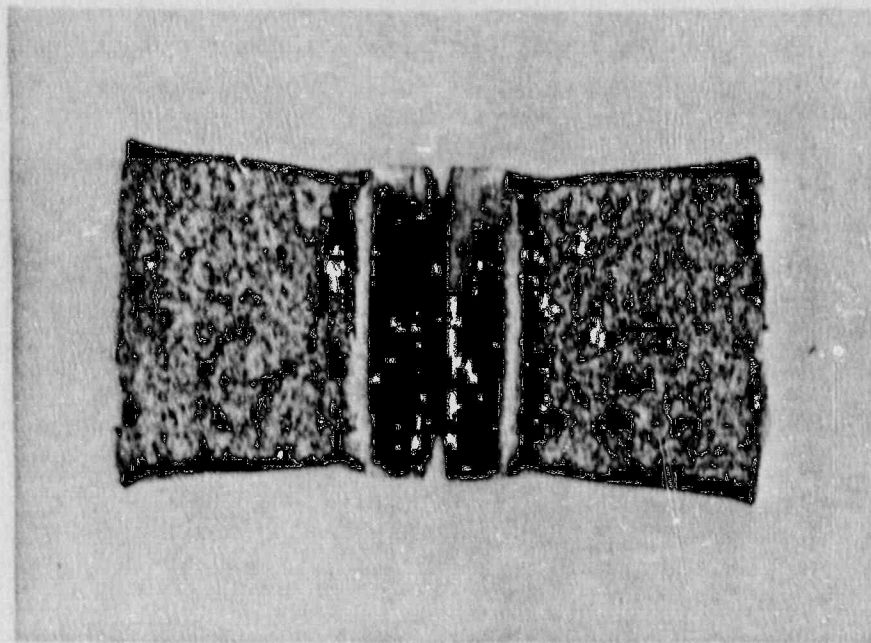
WELD: 7UU
TEMP: 10°F
ENERGY: 20.0 ft-lb

MLE: 20
% SHEAR: 15



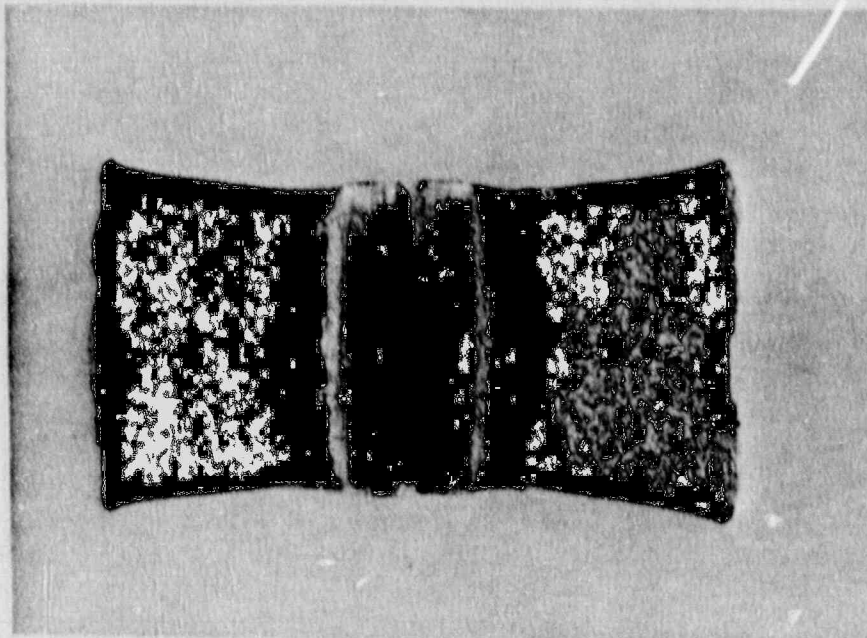
WELD: 7TU
TEMP: 20°F
ENERGY: 38.5 ft-lb

MLE: 35
% SHEAR: 11



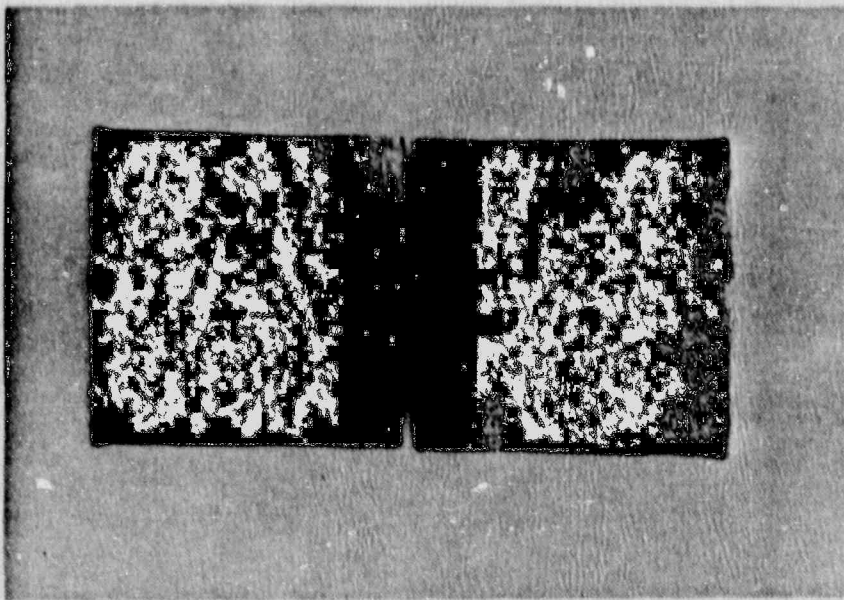
WELD: 7UP
TEMP: 40°F
ENERGY: 50.0 ft-lb

MLE: 42
% SHEAR: 23



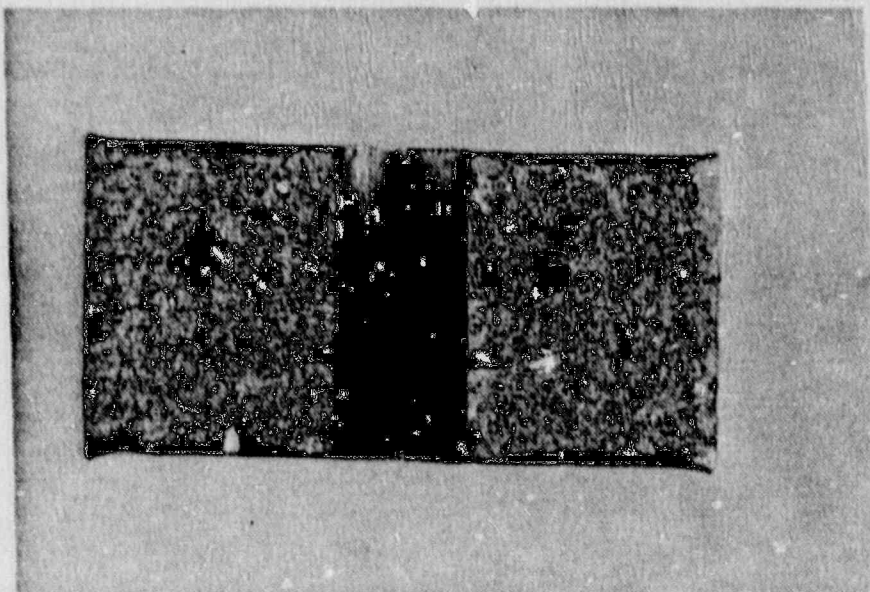
WELD: 7TD
TEMP: 80°F
ENERGY: 61.5 ft-lb

MLE: 56
% SHEAR: 32



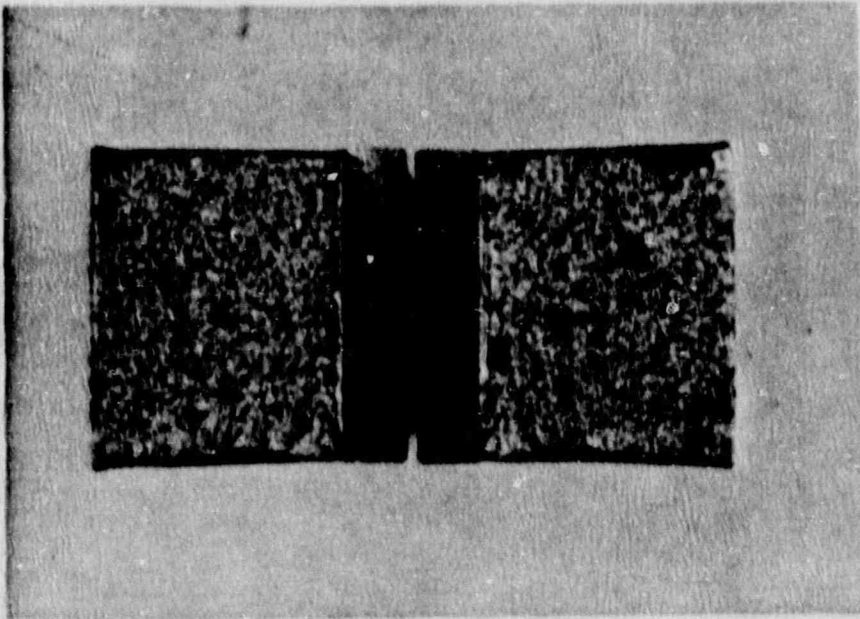
BASE: 7P1
TEMP: -40°F
ENERGY: 8.0 ft-lb

MLE: 6
% SHEAR: 3



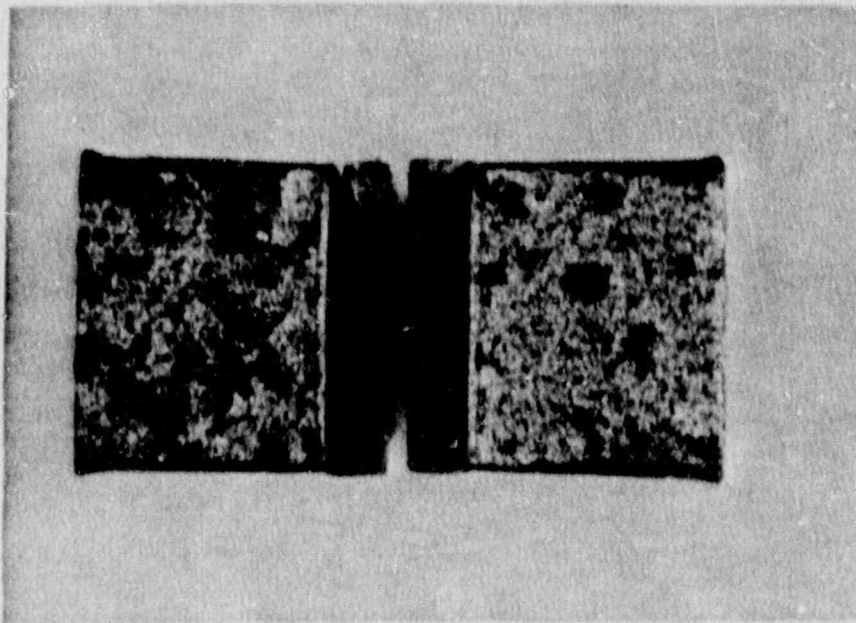
BASE: 7LU
TEMP: -30°F
ENERGY: 8.0 ft-lb

MLE: 11
% SHEAR: 7



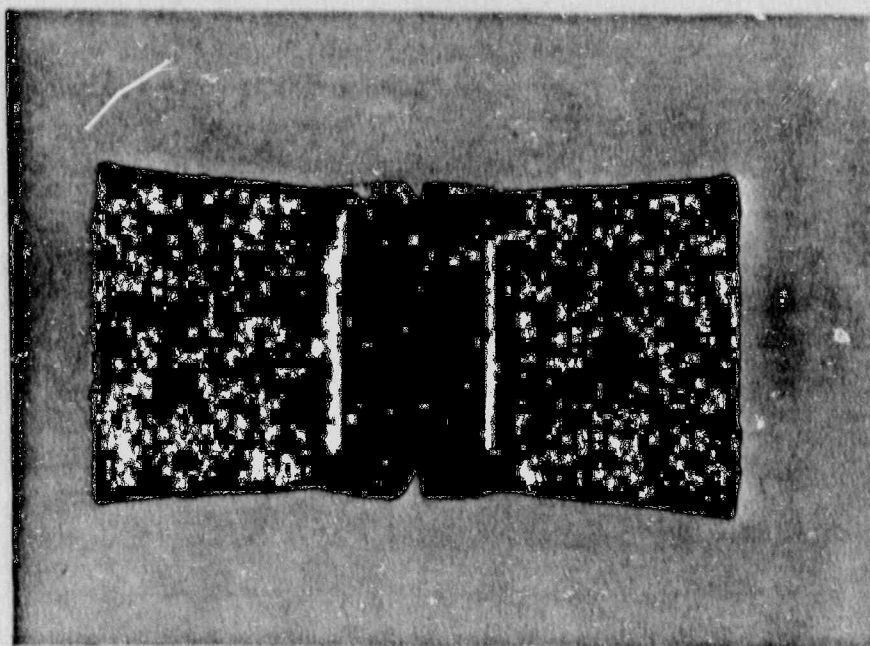
BASE: 7T6
TEMP: -20°F
ENERGY: 13.5 ft-lb

MLE: 13
% SHEAR: 9



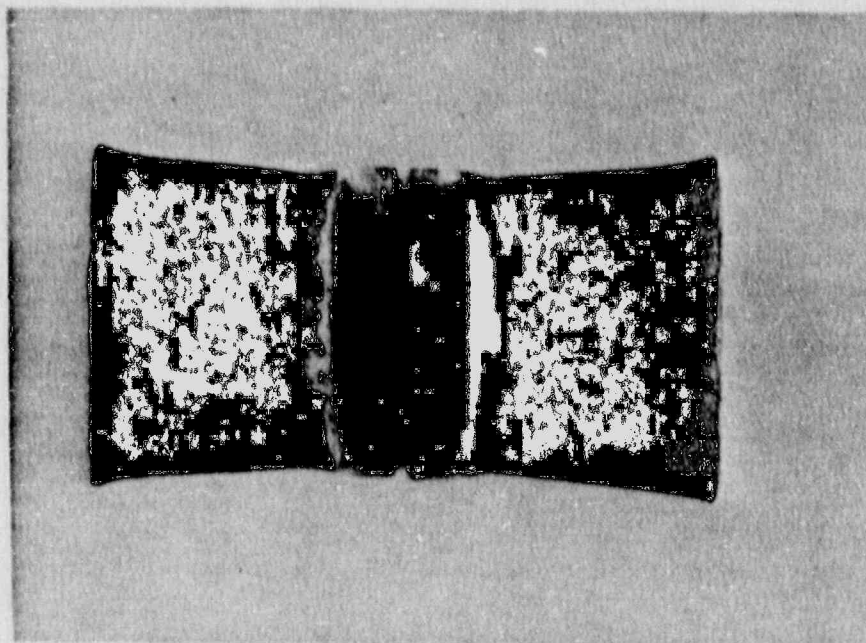
BASE: 7TB
TEMP: -10°F
ENERGY: 15.5 ft-lb

MLE: 14
% SHEAR: 8



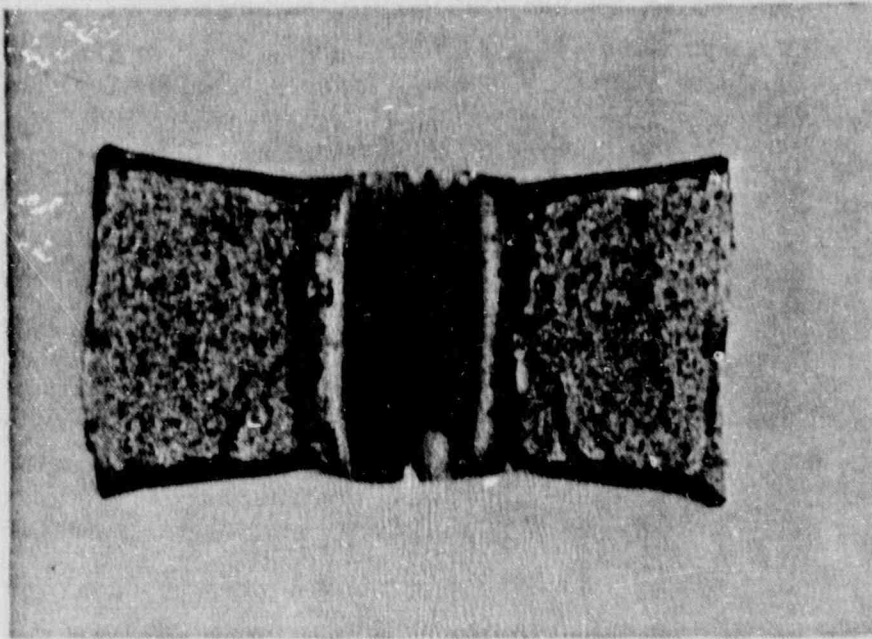
BASE: 7MU
TEMP: 0°F
ENERGY: 43.5 ft-lb

MLE: 34
% SHEAR: 16



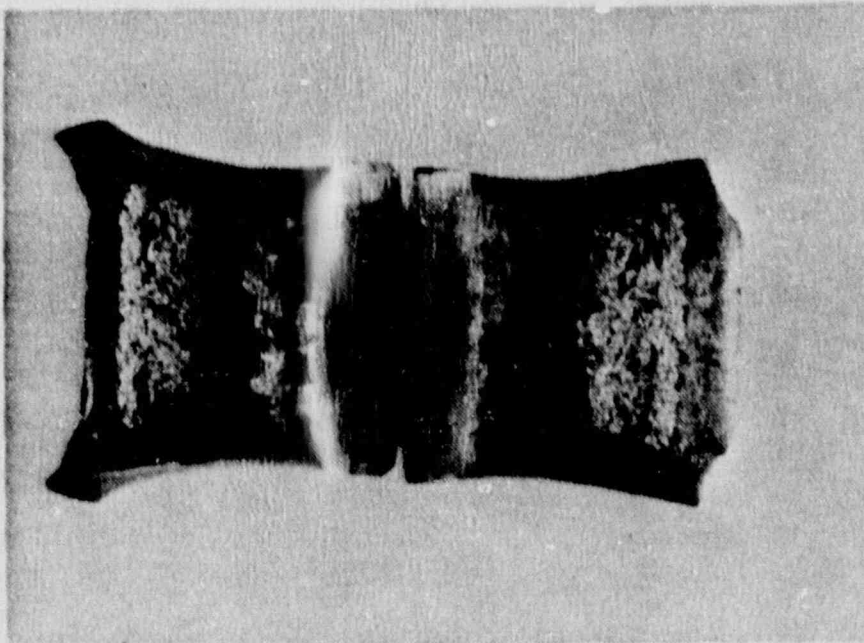
BASE: 7M5
TEMP: 20°F
ENERGY: 46.0 ft-lb

MLE: 42
% SHEAR: 22



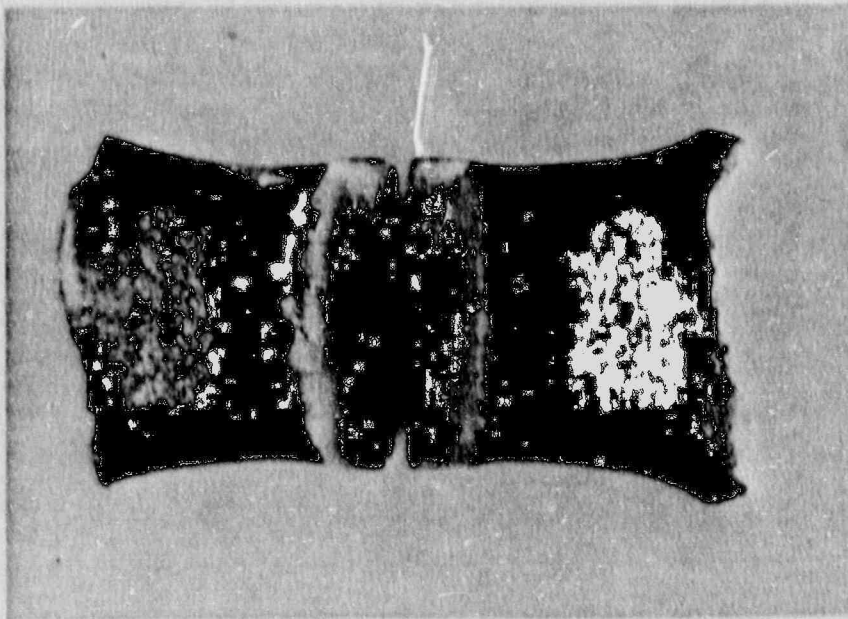
BASE: 7PP
TEMP: 40°F
ENERGY: 65.0 ft-lb

MLE: 60
% SHEAR: 23



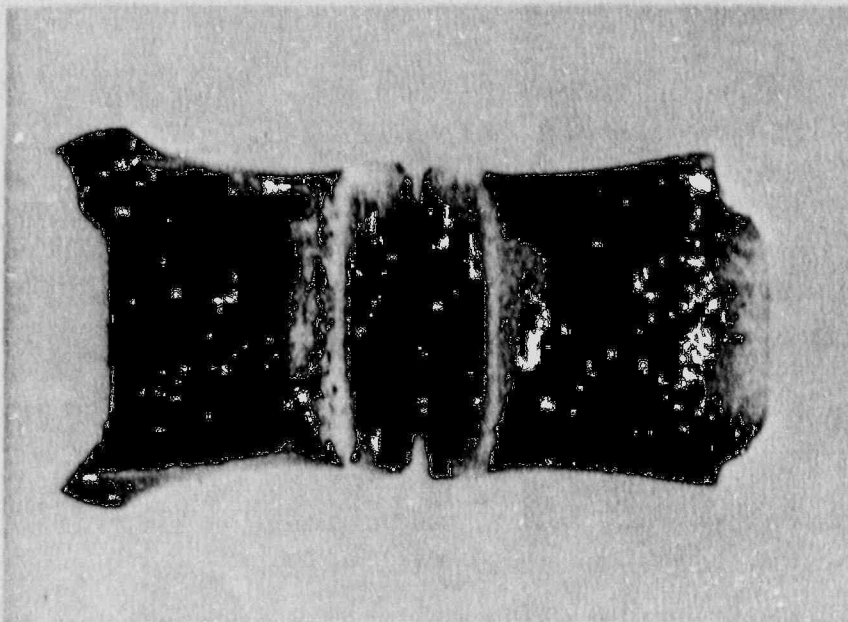
BASE: 7M7
TEMP: 80°F
ENERGY: 112.0 ft-lb

MLE: 88
% SHEAR: 73



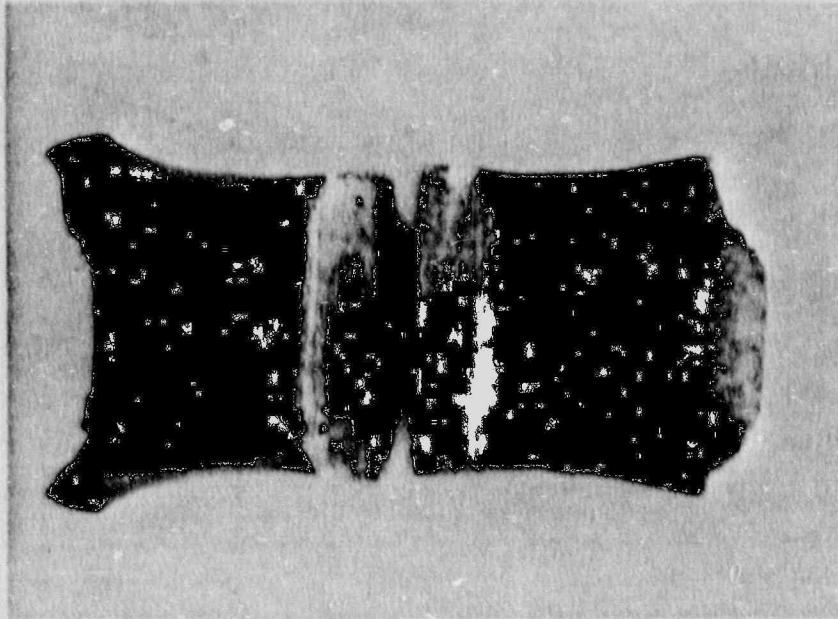
BASE: 7P2
TEMP: 120°F
ENERGY: 102.5 ft-lb

MLE: 70
% SHEAR: 87



BASE: 7MJ
TEMP: 160°F
ENERGY: 125.0 ft-lb

MLE: 86
% SHEAR: 100



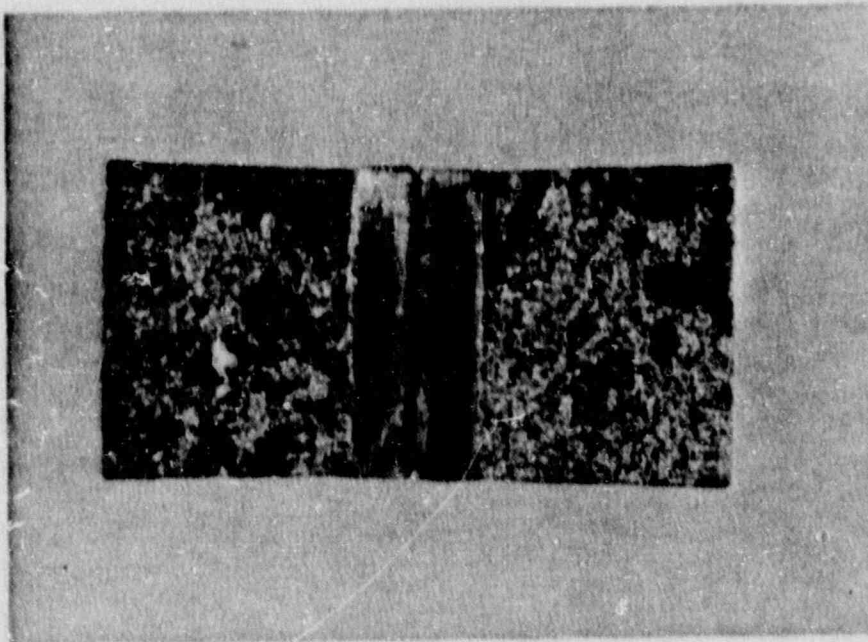
BASE: 7MB
TEMP: 200°F
ENERGY: 121.0 ft-lb

MLE: 89
% SHEAR: 100



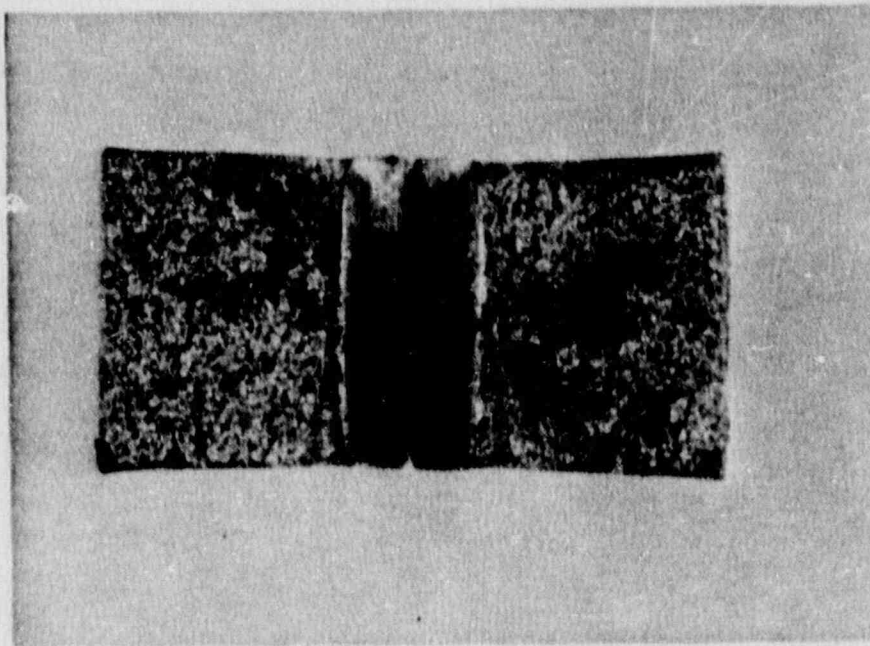
BASE: 7PY
TEMP: 300°F
ENERGY: 128.0 ft-lb

MLE: 88
% SHEAR: 100



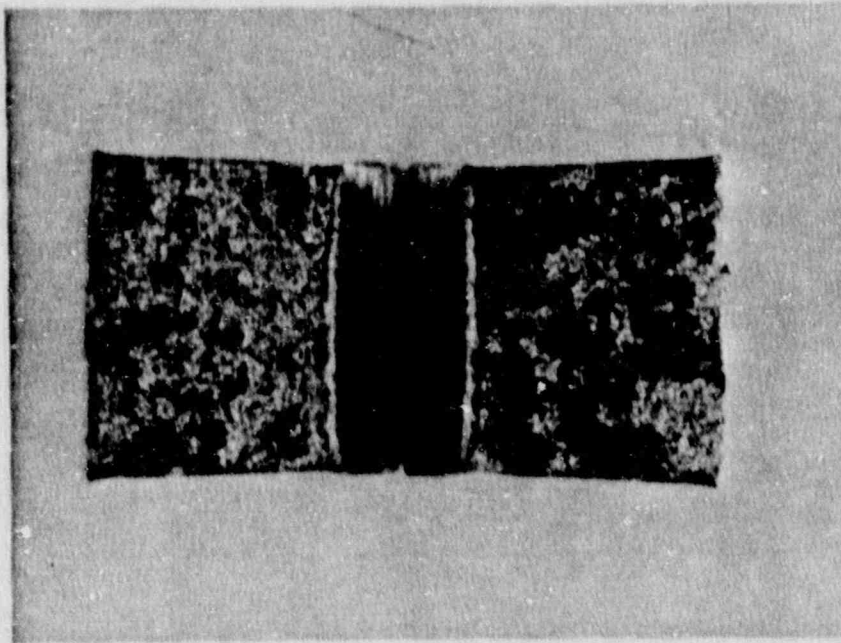
WELD: 7TJ
TEMP: -40°F
ENERGY: 11.0 ft-lb

MLE: 9
% SHEAR: 4



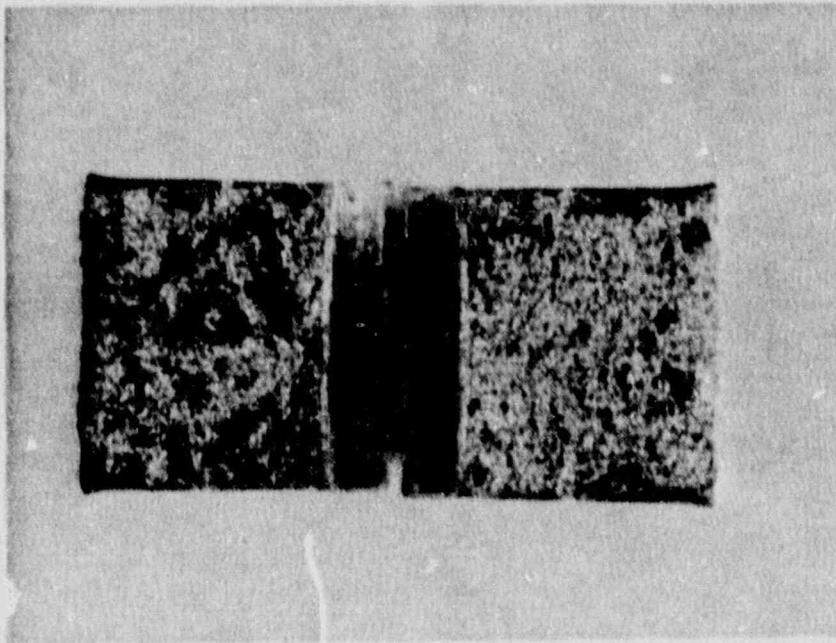
WELD: 7TL
TEMP: -20°F
ENERGY: 18.0 ft-lb

MLE: 16
% SHEAR: 3



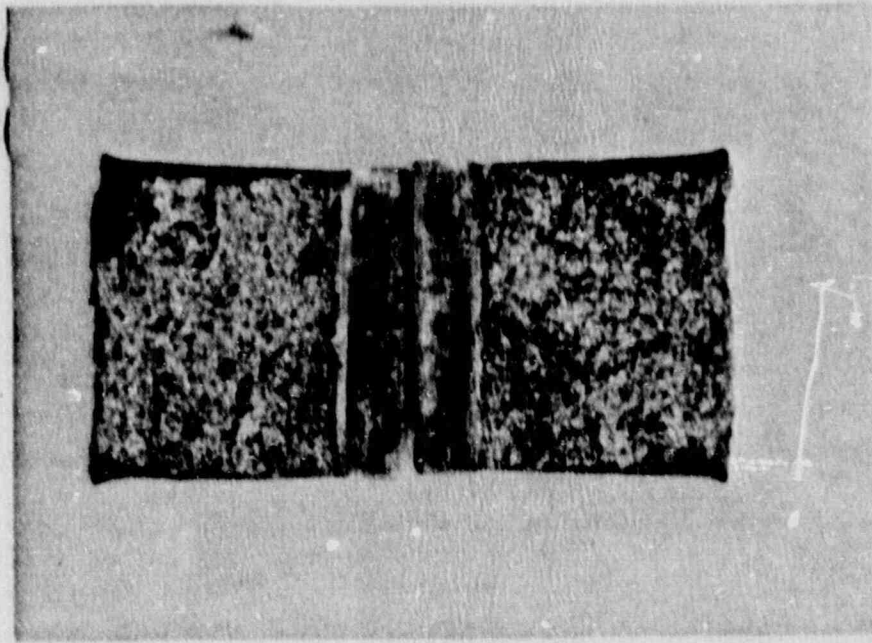
WELD: 7UA
TEMP: -10°F
ENERGY: 21.5 ft-lb

MLE: 20
% SHEAR: 6



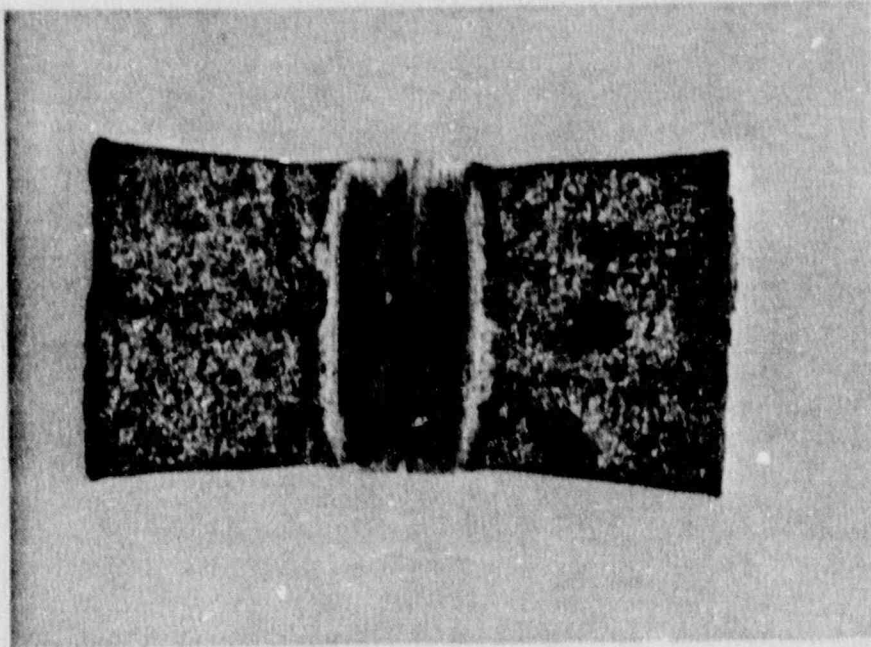
WELD: 7TK
TEMP: 0°F
ENERGY: 12.0 ft-lb

MLE: 14
% SHEAR: 3



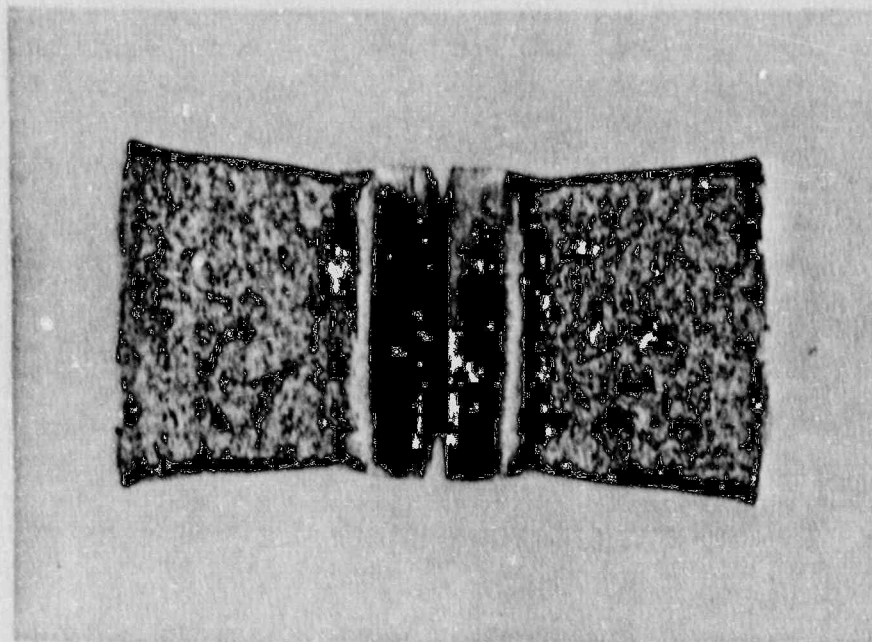
WELD: 7UU
TEMP: 10°F
ENERGY: 20.0 ft-lb

MLE: 20
% SHEAR: 15



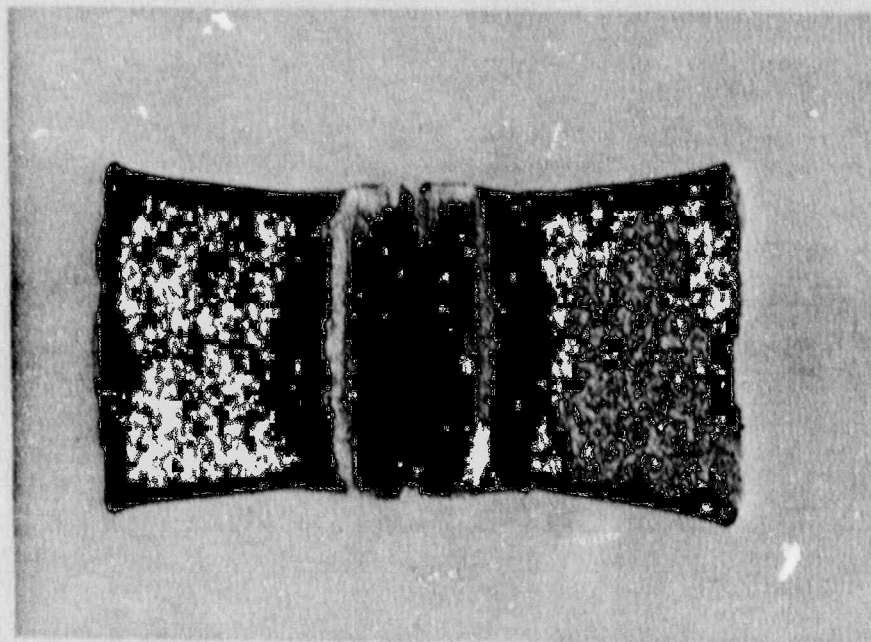
WELD: 7TU
TEMP: 20°F
ENERGY: 38.5 ft-lb

MLE: 35
% SHEAR: 11



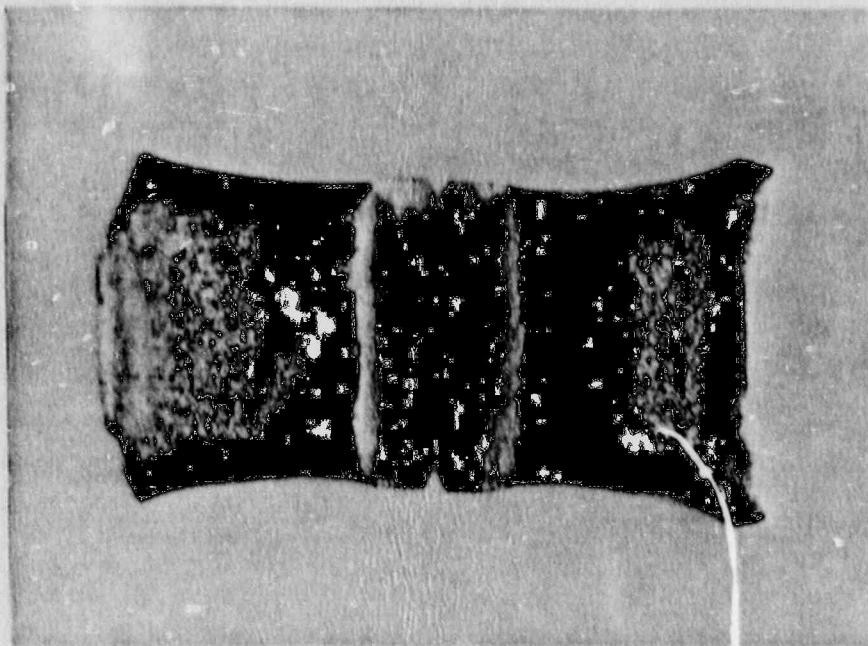
WELD: 7UP
TEMP: 40°F
ENERGY: 50.0 ft-lb

MLE: 42
% SHEAR: 23



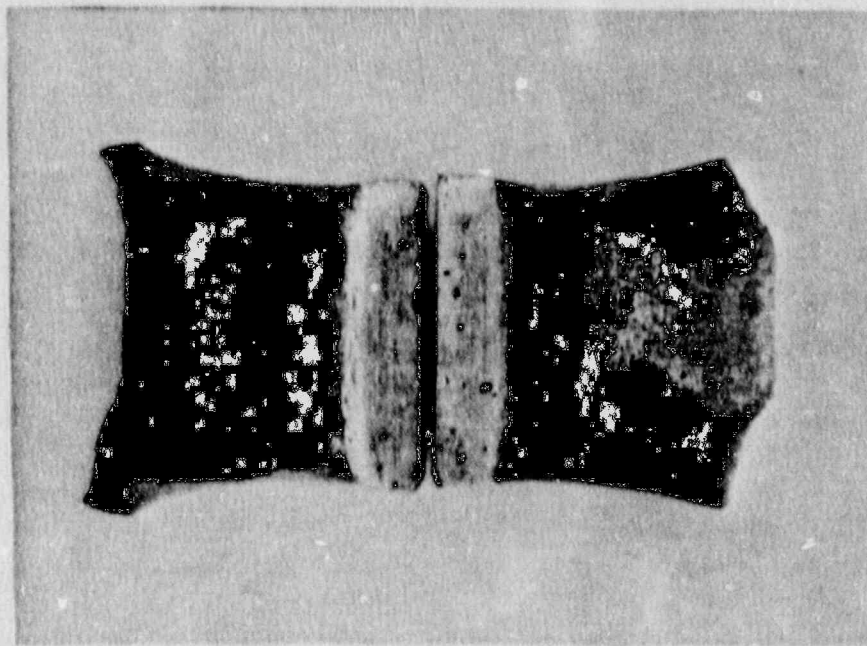
WELD: 7TD
TEMP: 80°F
ENERGY: 61.5 ft-lb

MLE: 56
% SHEAR: 32



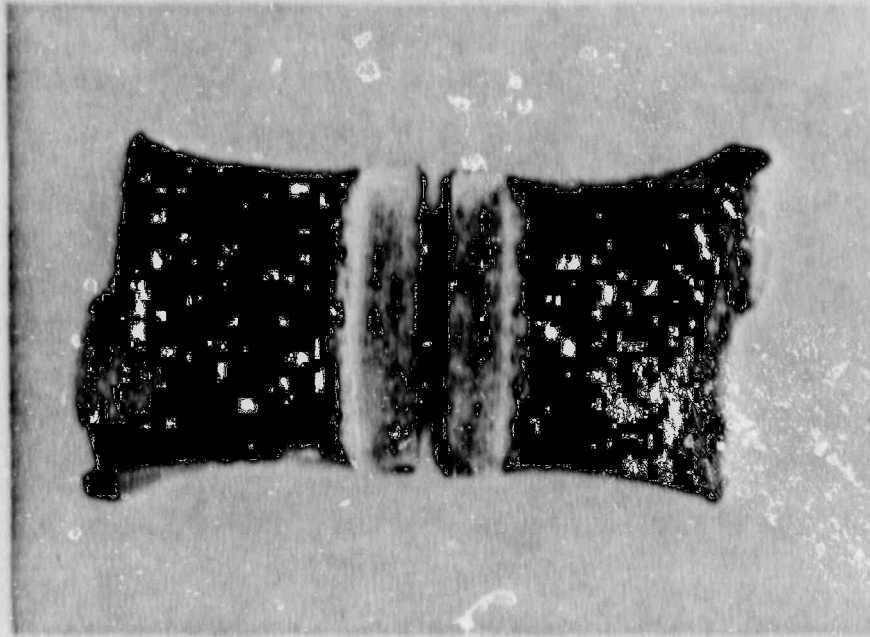
WELD: A11
TEMP: 120°F
ENERGY: 80.5 ft-lb

MLE: 73
% SHEAR: 76



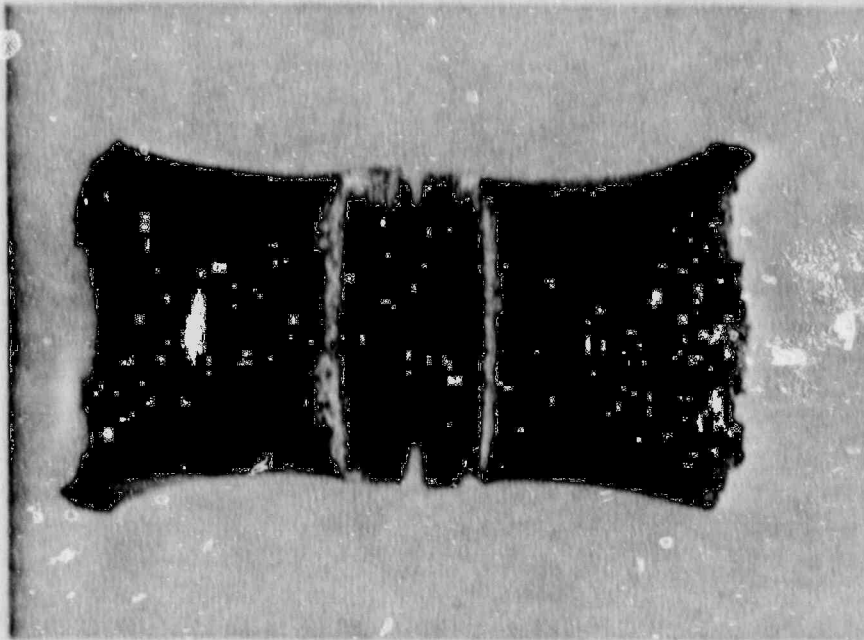
WELD: A15
TEMP: 180°F
ENERGY: 96.5 ft-lb

MLE: 74
% SHEAR: 84



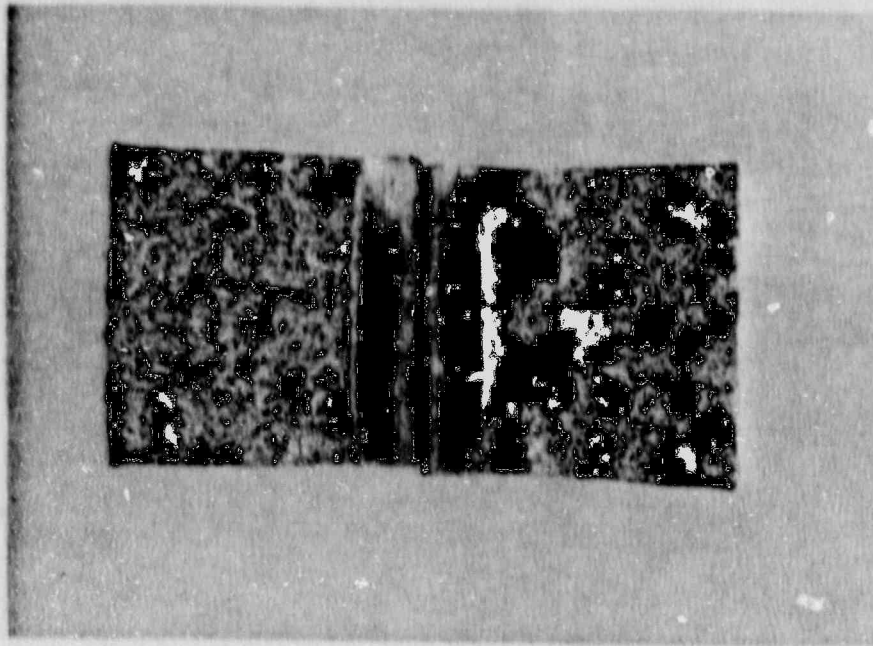
WELD: 7YD
TEMP: 200°F
ENERGY: 100.5 ft-lb

MLE: 85
% SHEAR: 100



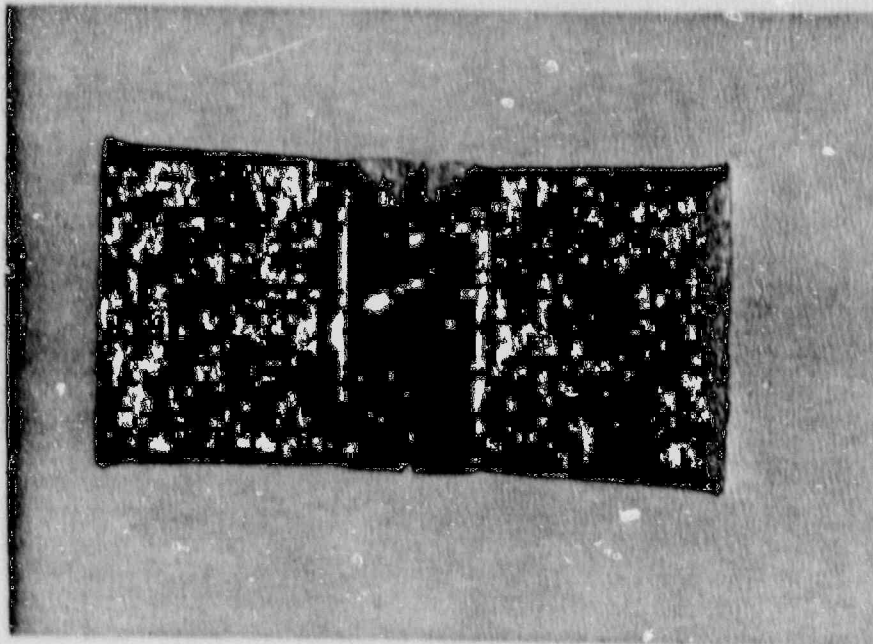
WELD: A14
TEMP: 300°F
ENERGY: 96.0 ft-lb

MLE: 81
% SHEAR: 100



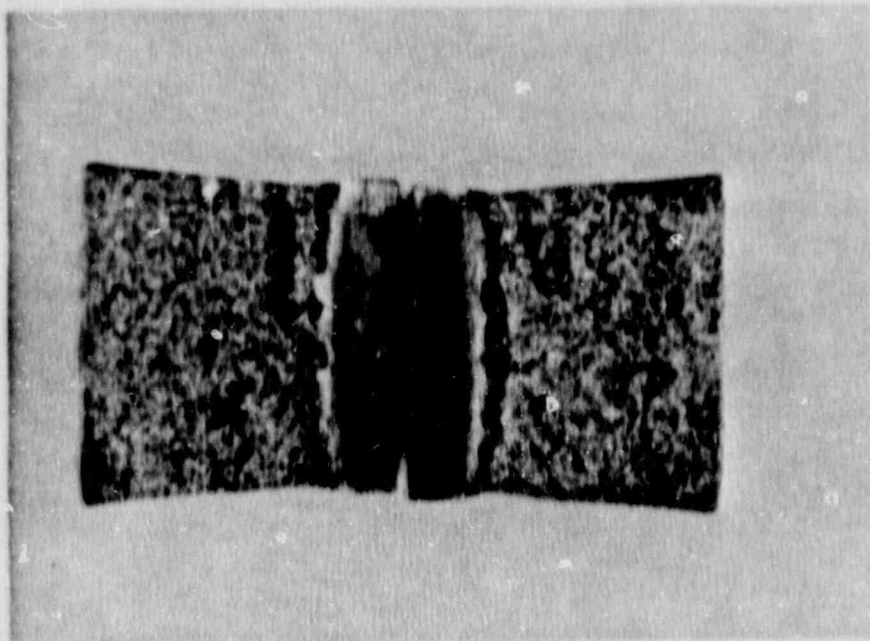
HAZ: A27
TEMP: -40°F
ENERGY: 16.5 ft-lb

MLE: 16
% SHEAR: 2



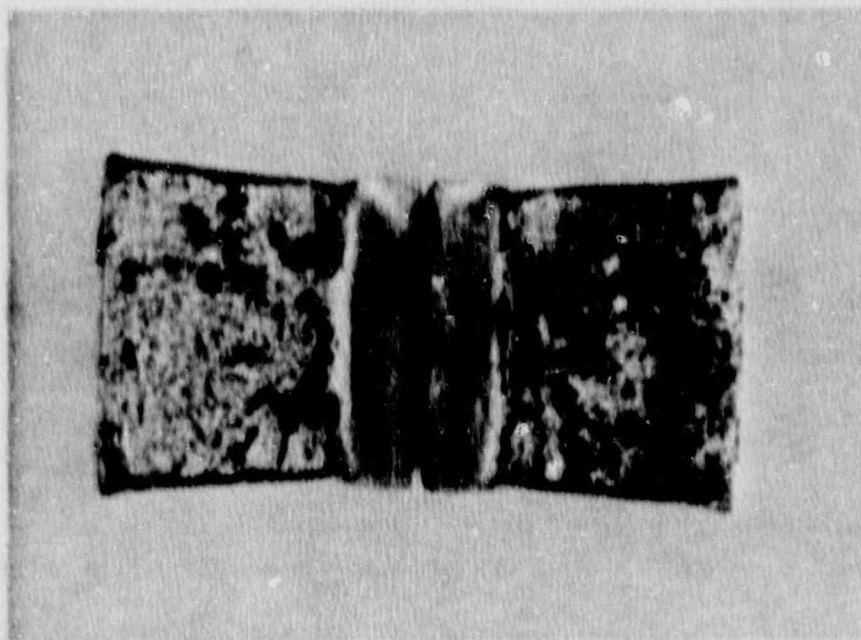
HAZ: A1C
TEMP: -30°F
ENERGY: 23.5 ft-lb

MLE: 20
% SHEAR: 12



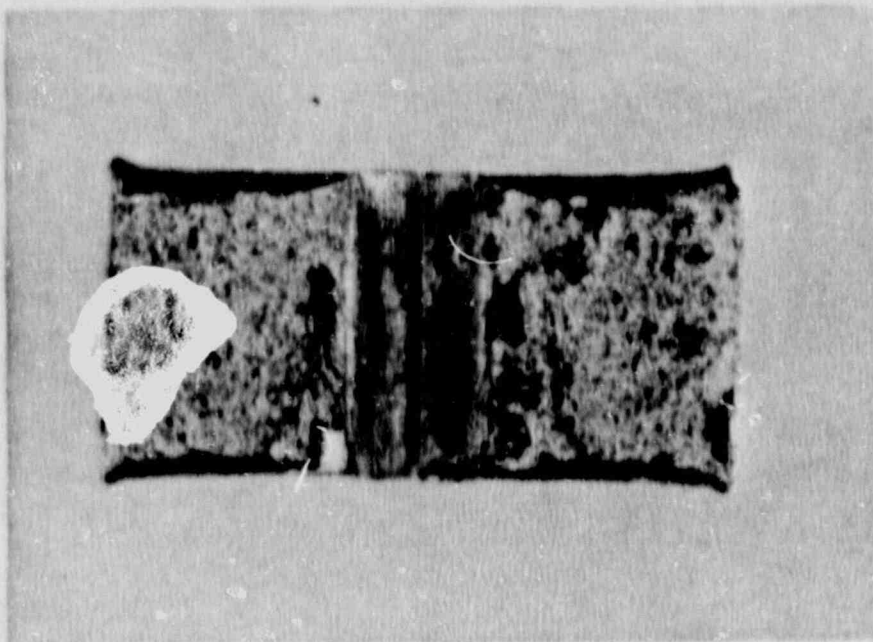
HAZ: A1E
TEMP: -20°F
ENERGY: 37.5 ft-lb

MLE: 34
% SHEAR: 8



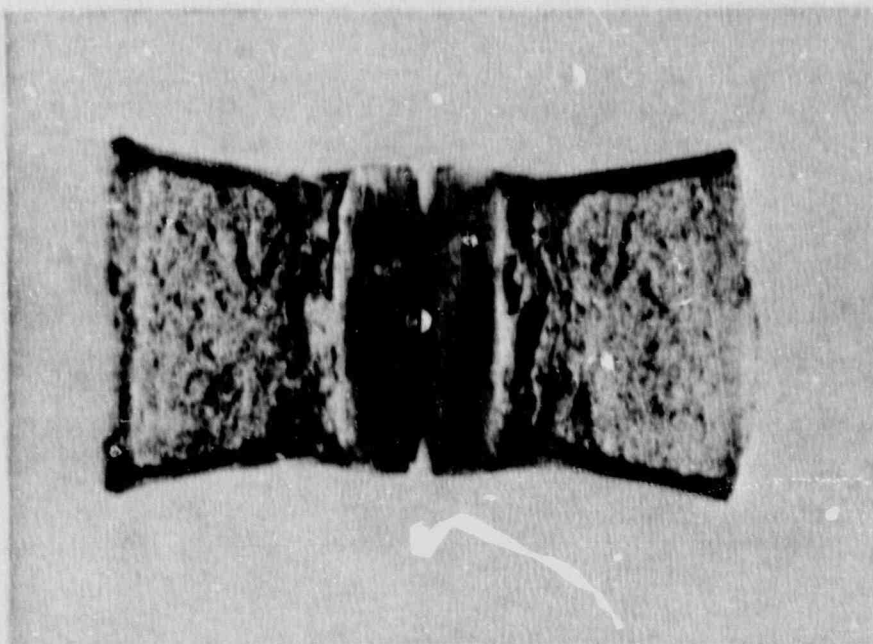
HAZ: A1L
TEMP: -10°F
ENERGY: 41.5 ft-lb

MLE: 31
% SHEAR: 16



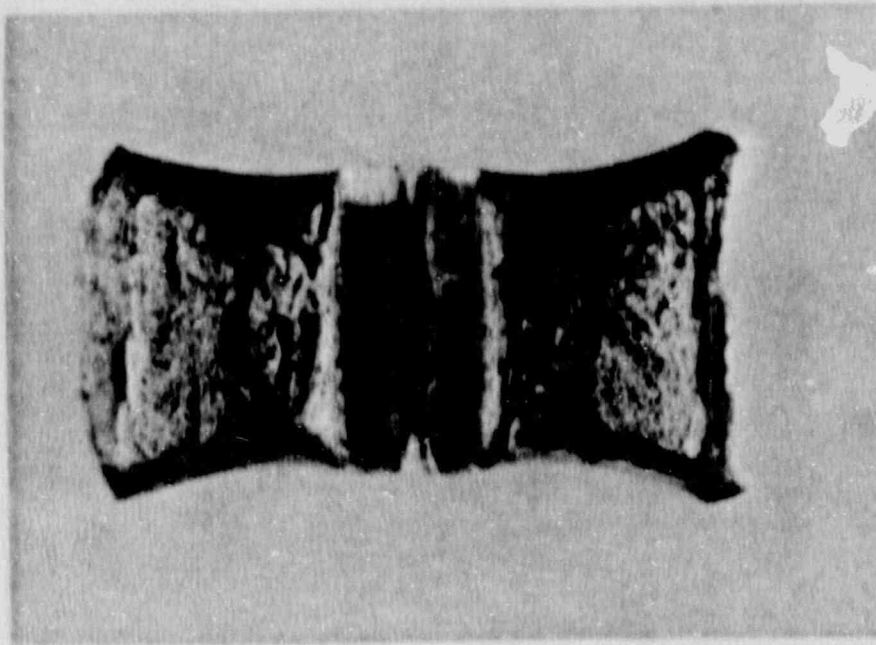
HAZ: A1K
TEMP: 0°F
ENERGY: 21.5 ft-lb

MLE: 21
% SHEAR: 19



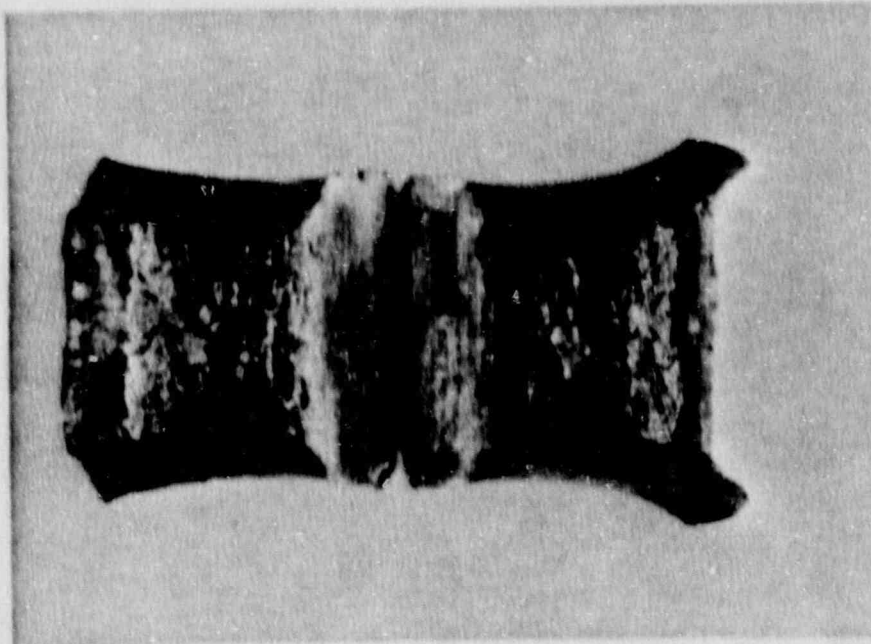
HAZ: A3A
TEMP: 20°F
ENERGY: 83 ft-lb

MLE: 60
% SHEAR: 40



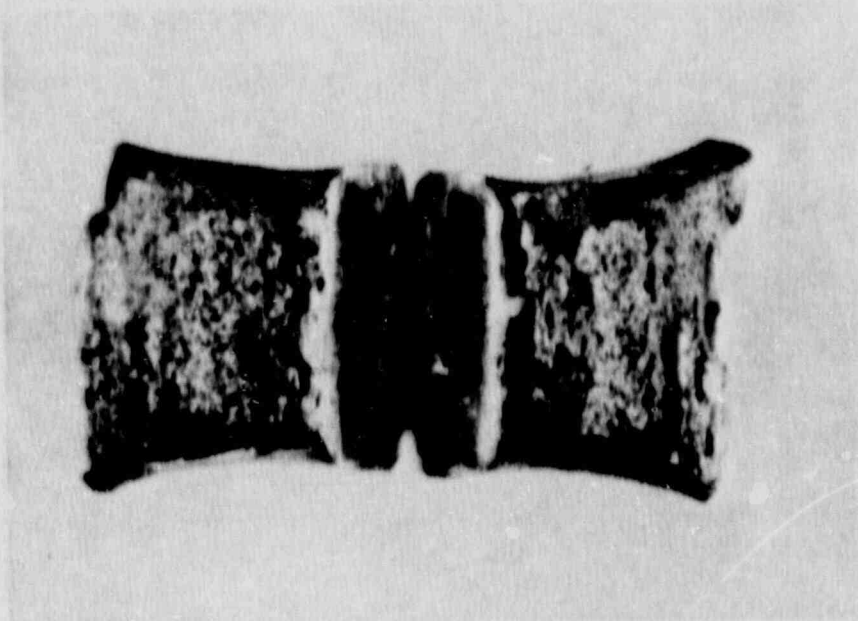
HAZ: A22
TEMP: 40°F
ENERGY: 111.5 ft-lb

MLE: 83
% SHEAR: 47



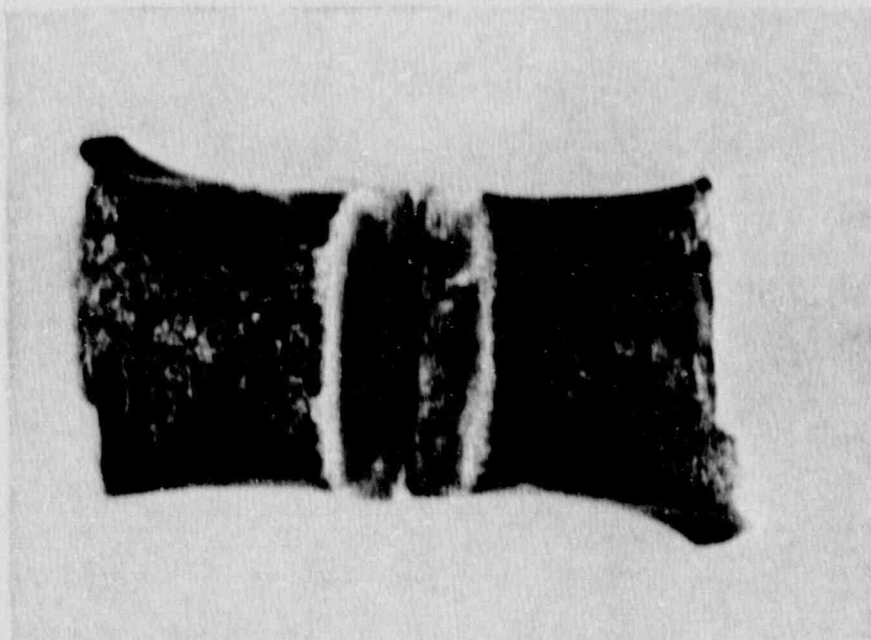
HAZ: A2E
TEMP: 80°F
ENERGY: 125.0 ft-lb

MLE: 91
% SHEAR: 82



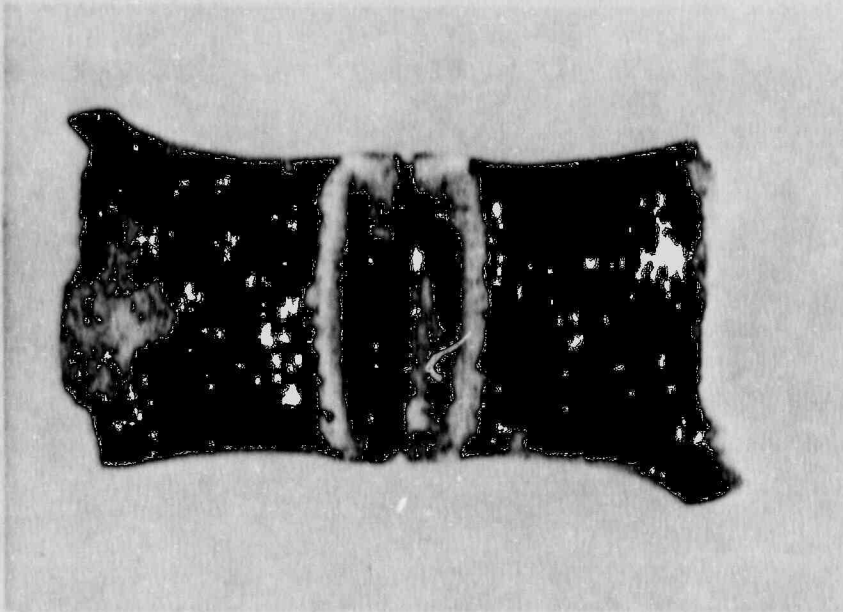
HAZ A23
TEMP: 120°F
ENERGY: 99.0 ft-lb

MLE: 70
% SHEAR: 81



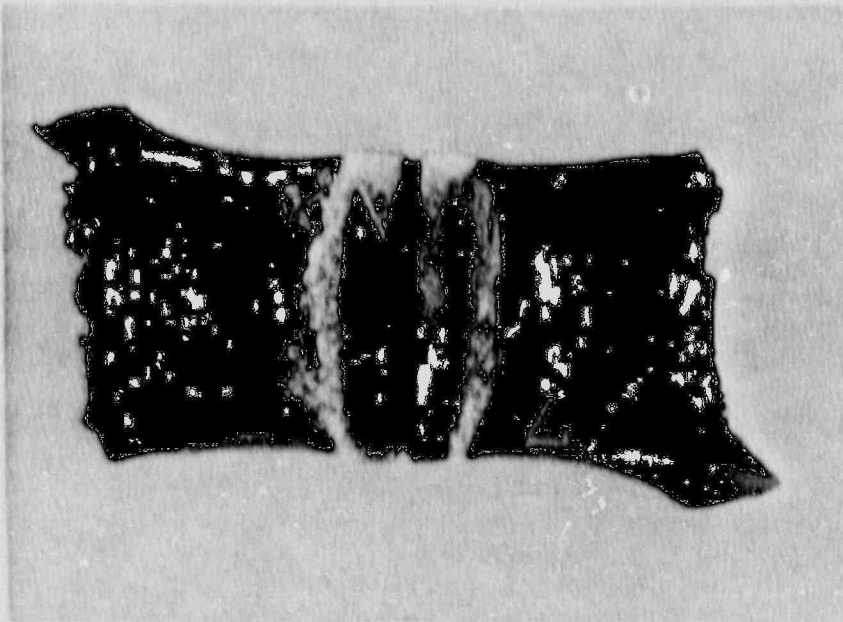
HAZ A1D
TEMP: 160°F
ENERGY: 103.0 ft-lb

MLE: 87
% SHEAR: 100



HAZ: A1J
TEMP: 200°F
ENERGY: 107.0 ft-lb

MLE: 88
% SHEAR: 100



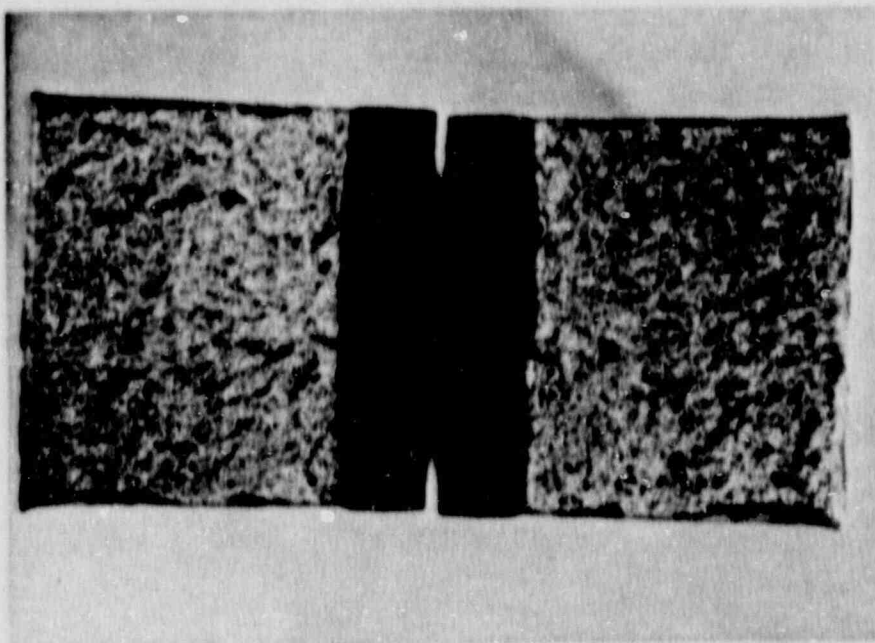
HAZ: A2T
TEMP: 300°F
ENERGY: 162.0 ft-lb

MLE: 86
% SHEAR: 100

APPENDIX B

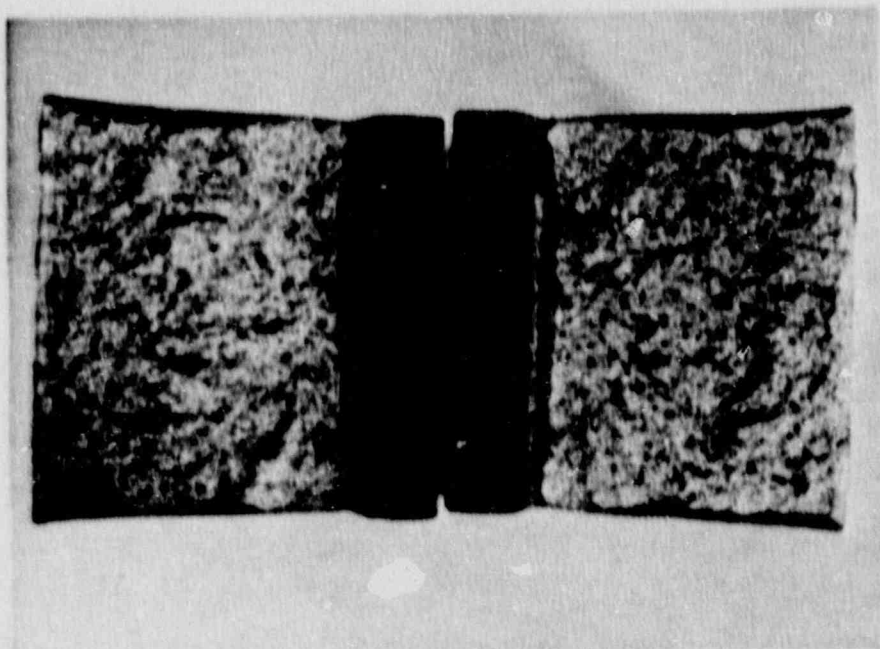
UNIRRADIATED CHARPY SPECIMEN FRACTURE SURFACE PHOTOGRAPHS

Photographs of each Charpy specimen fracture surface were taken per the requirements of ASTM E185-82. The pages following show the fracture surface photographs along with a summary of the Charpy test results for each specimen. The pictures are arranged with the materials in the order of base and weld.



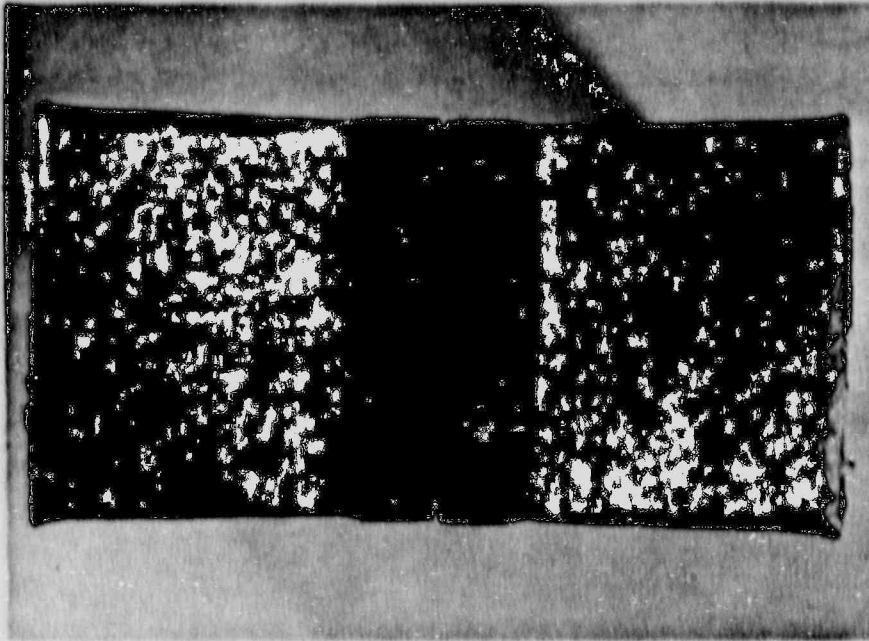
BASE: 7PC
TEMP: -40°F
ENERGY: 10.5 ft-lb

MLE: 9
% SHEAR: 0



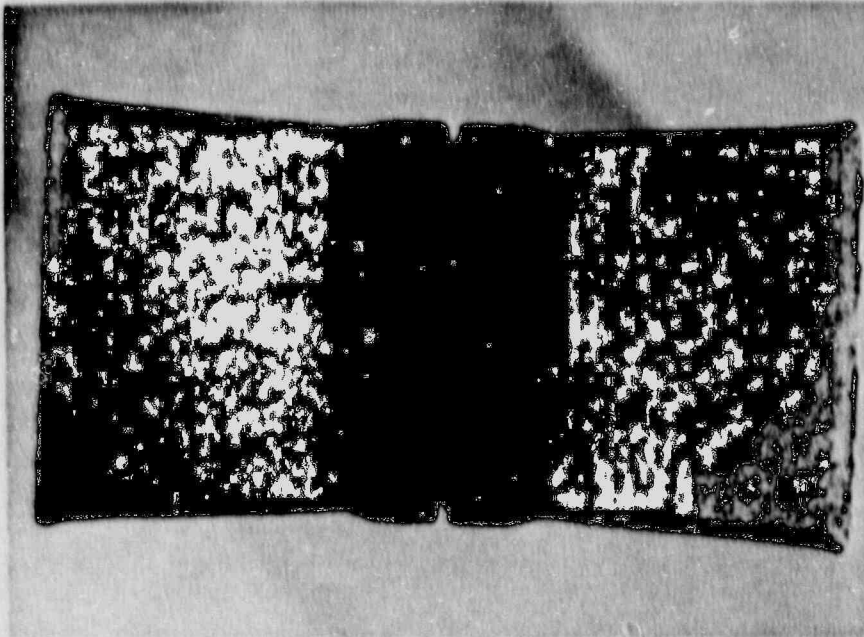
BASE: 7LY
TEMP: -40°F
ENERGY: 24.5 ft-lb

MLE: 17
% SHEAR: 0



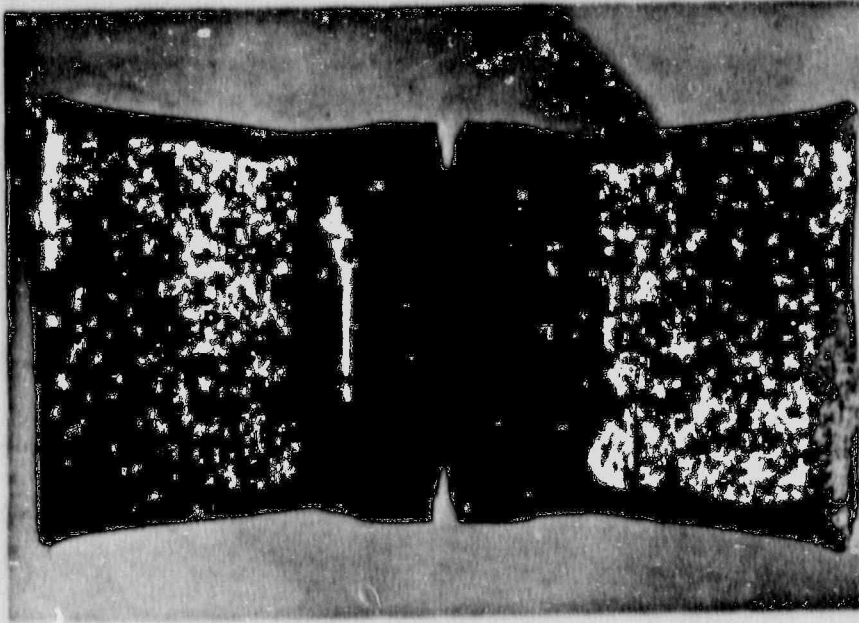
BASE: 7MT
TEMP: -20°F
ENERGY: 18.5 ft lb

MLE: 16
% SHEAR: 16



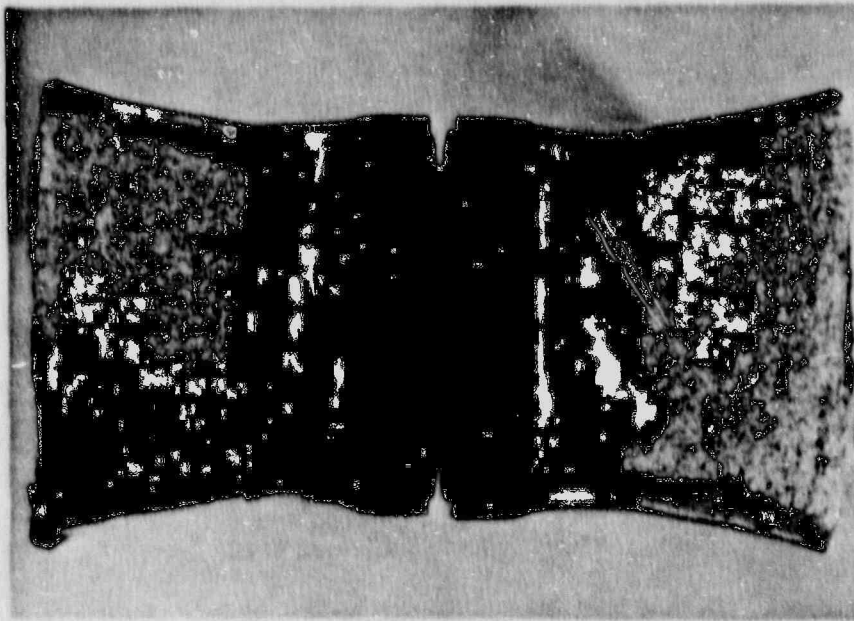
BASE: 7MY
TEMP: 0°F
ENERGY: 34 ft lb

MLE: 26
% SHEAR: 15



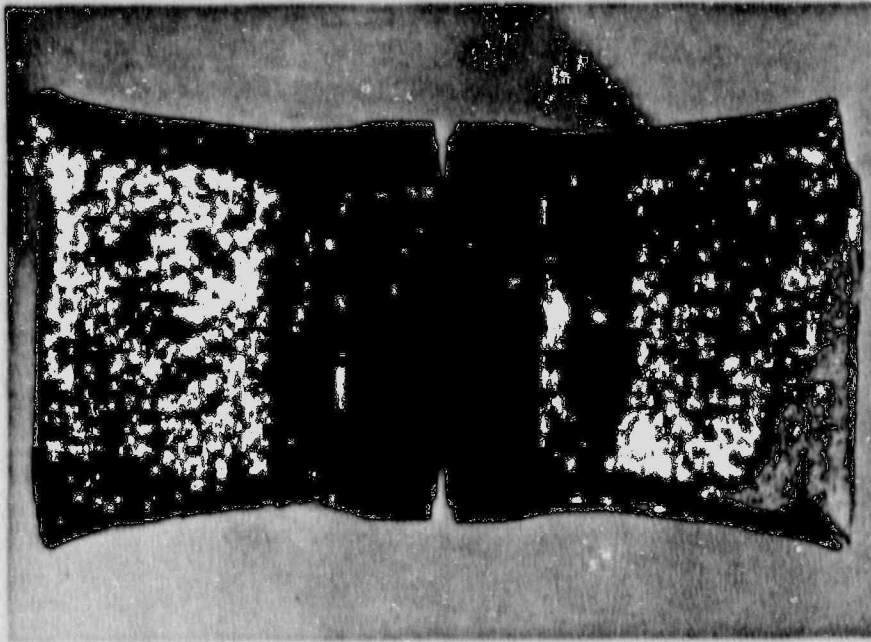
BASE: 7P4
TEMP: 20°F
ENERGY: 60.5 ft-lb

MLE: 44
% SHEAR: 27



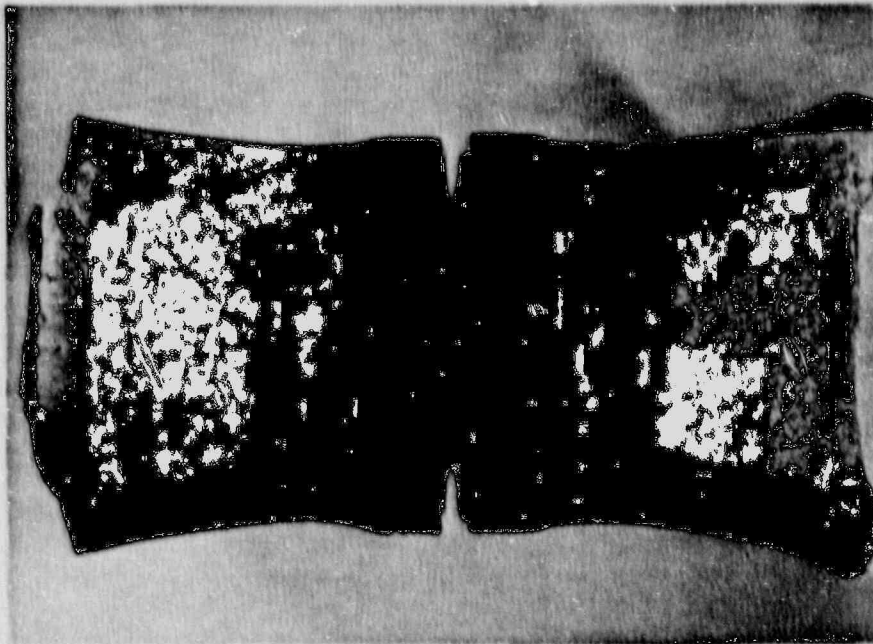
BASE: 7M3
TEMP: 40°F
ENERGY: 85 ft-lb

MLE: 62
% SHEAR: 39



BASE: 7M2
TEMP: 60°F
ENERGY: 72 ft-lb

MLE: 62
% SHEAR: 38



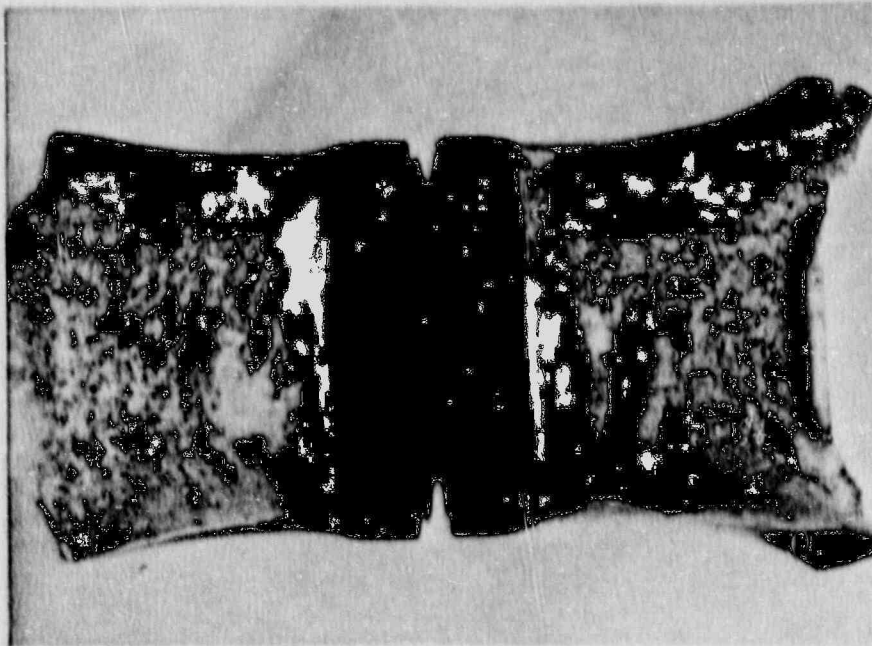
BASE: 7P7
TEMP: 80°F
ENERGY: 98.5 ft-lb

MLE: 70
% SHEAR: 67



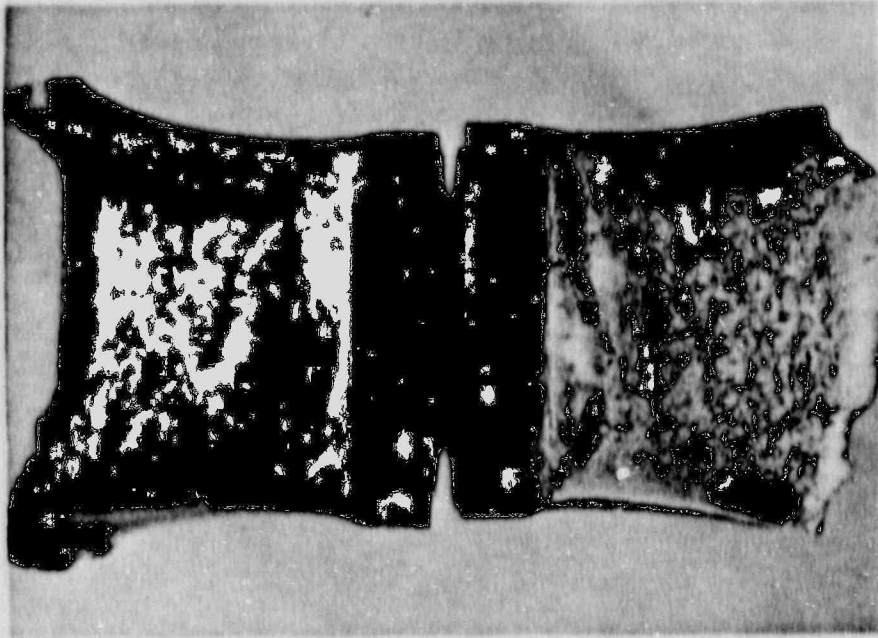
BASE: 7MD
TEMP: 120°F
ENERGY: 117.5 ft-lb

MLE: 87
% SHEAR: 83



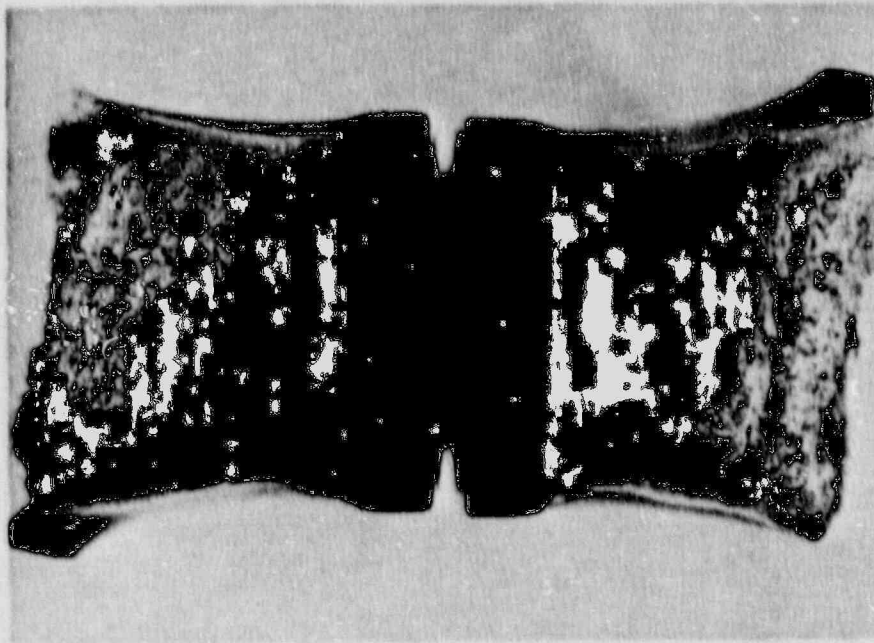
BASE: 7PB
TEMP: 160°F
ENERGY: 130.0 ft-lb

MLE: 81
% SHEAR: 100



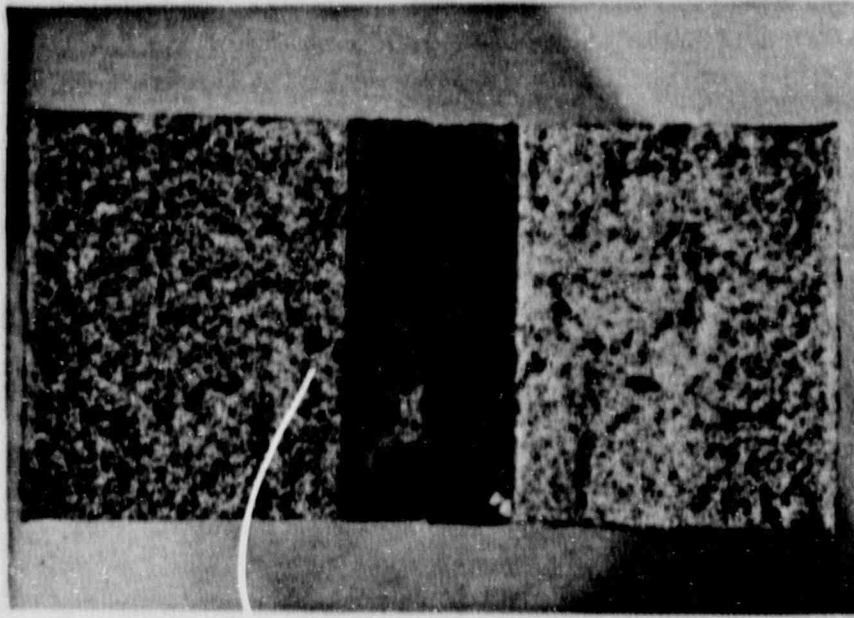
BASE: 7MM
TEMP: 200°F
ENERGY: 130.0 ft-lb

MLE: 80
% SHEAR: 100



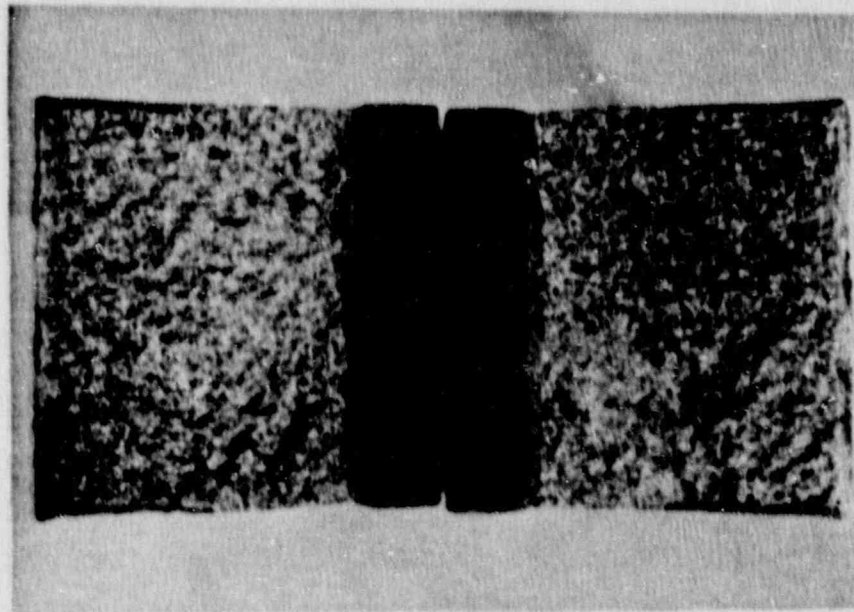
BASE: 7PD
TEMP: 300°F
ENERGY: 143.5 ft-lb

MLE: 83
% SHEAR: 100



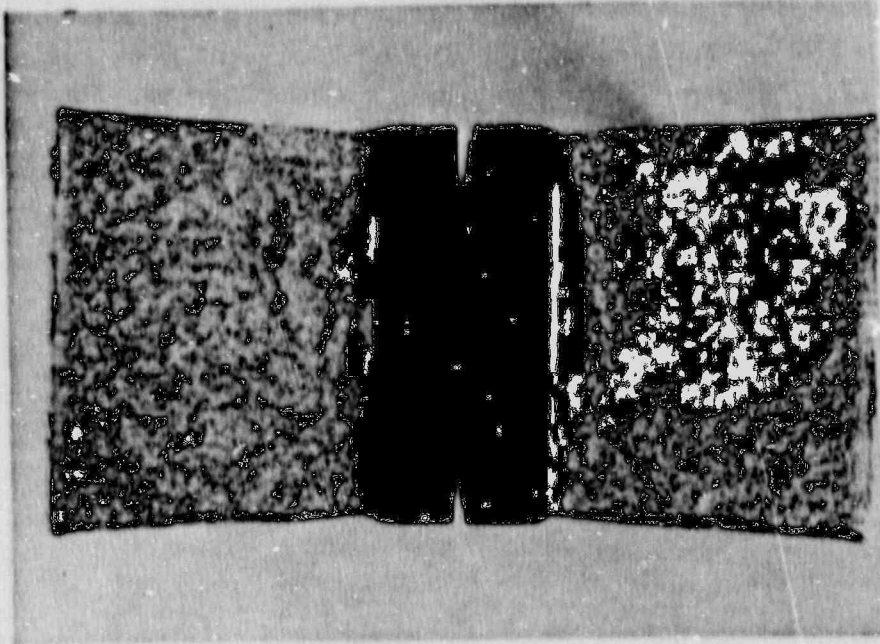
WELD: 7TE
TEMP: -40°F
ENERGY: 6.5 ft-lb

MLE: 3
% SHEAR: 0



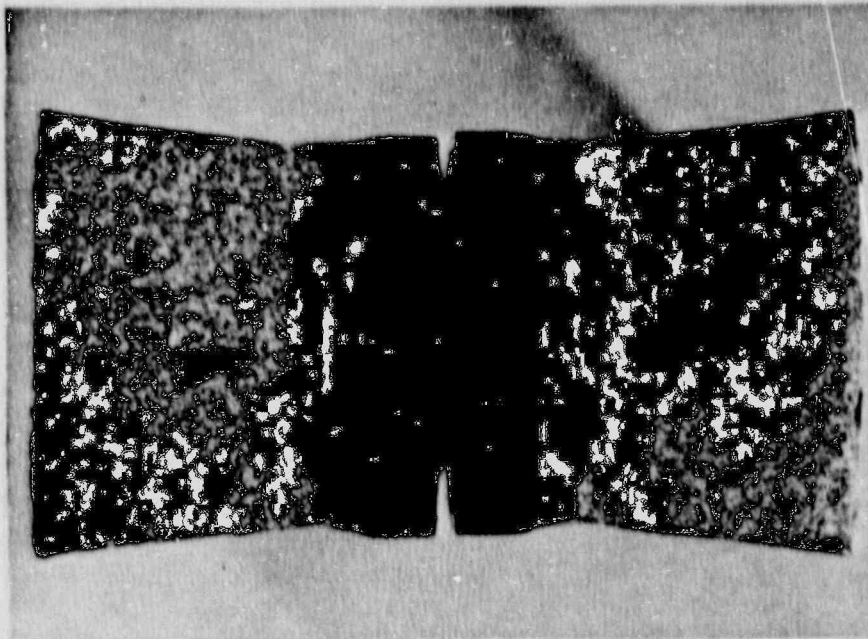
WELD: 7U1
TEMP: -20°F
ENERGY: 17.5 ft-lb

MLE: 18
% SHEAR: 6



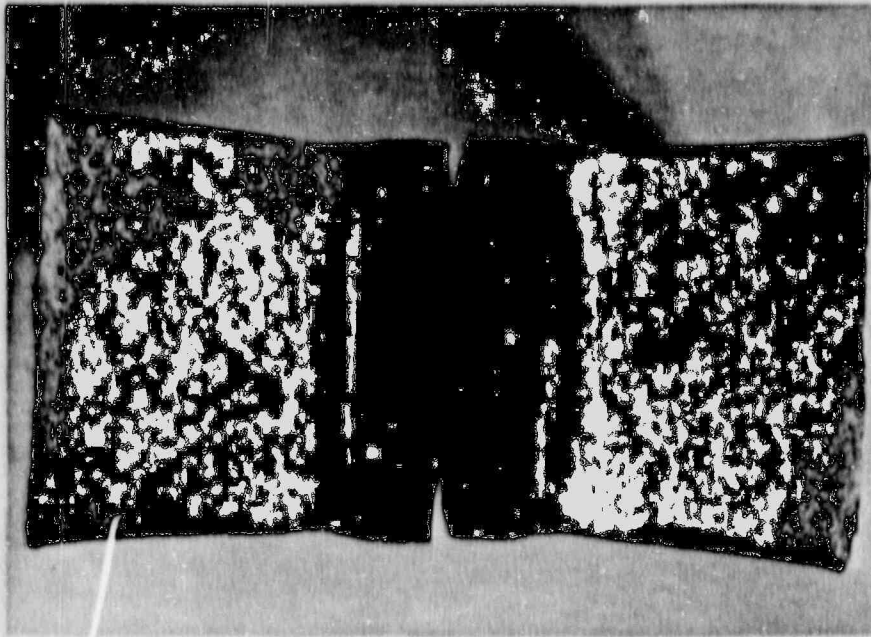
WELD: 7U6
TEMP: 0°F
ENERGY: 29.0 ft-lb

MLE: 21
% SHEAR: 11



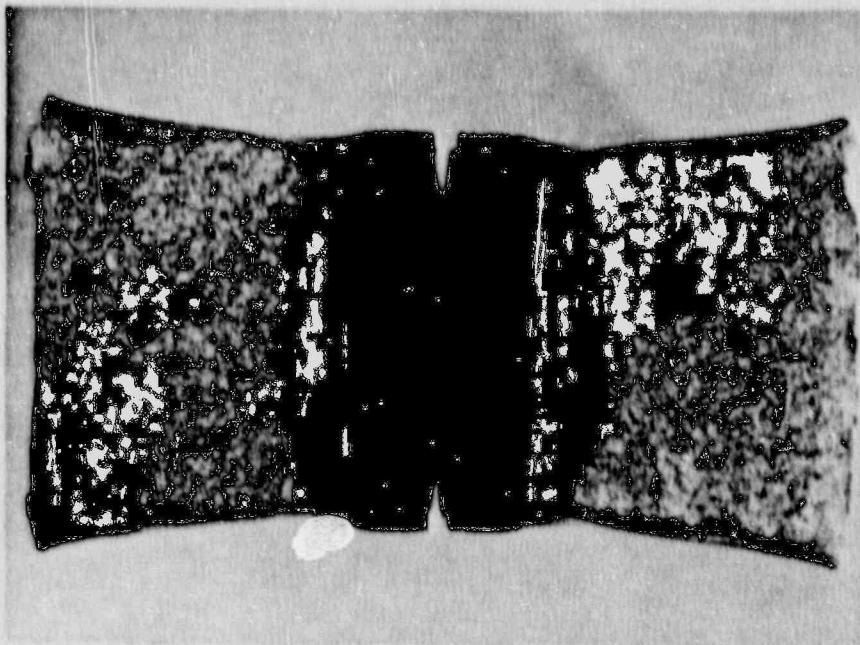
WELD: 7U2
TEMP: 0°F
ENERGY: 48.0 ft-lb

MLE: 42
% SHEAR: 15



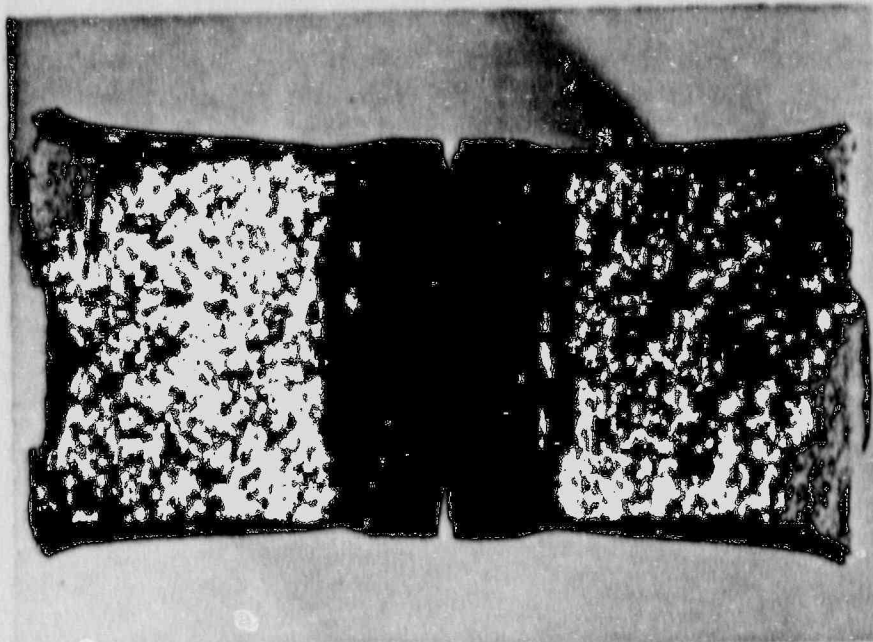
WELD: 7U3
TEMP: 20°F
ENERGY: 39.5 ft-lb

MLE: 31
% SHEAR: 14



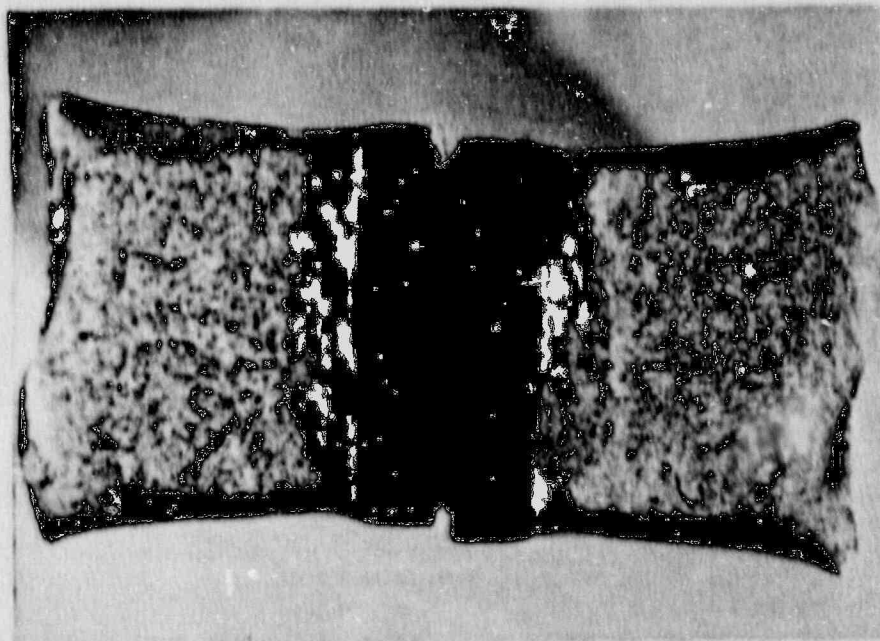
WELD: 7TP
TEMP: 40°F
ENERGY: 56.5 ft-lb

MLE: 46
% SHEAR: 22



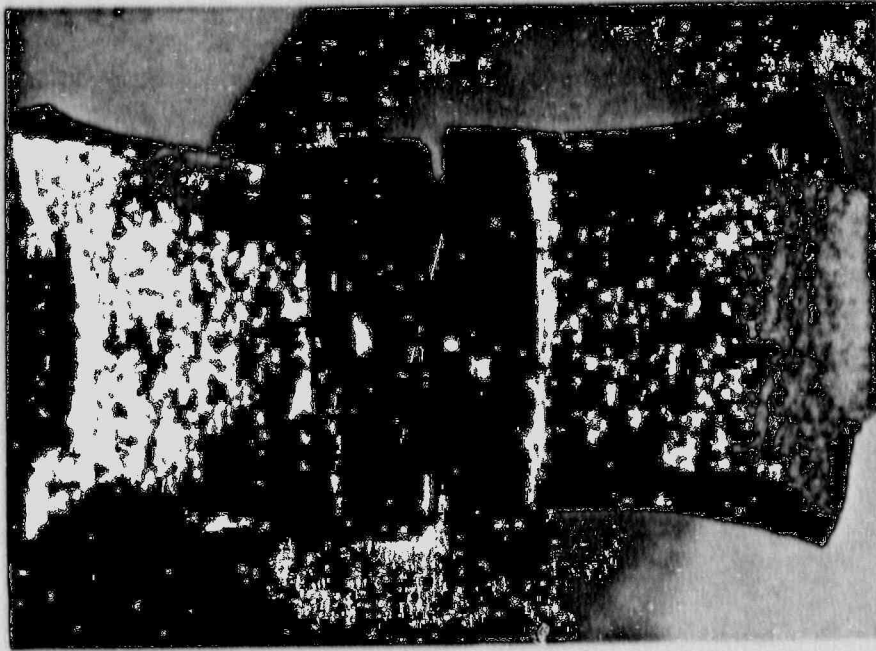
WELD: 7TM
TEMP: 80°F
ENERGY: 44.0 ft-lb

MLE: 39
% SHEAR: 39



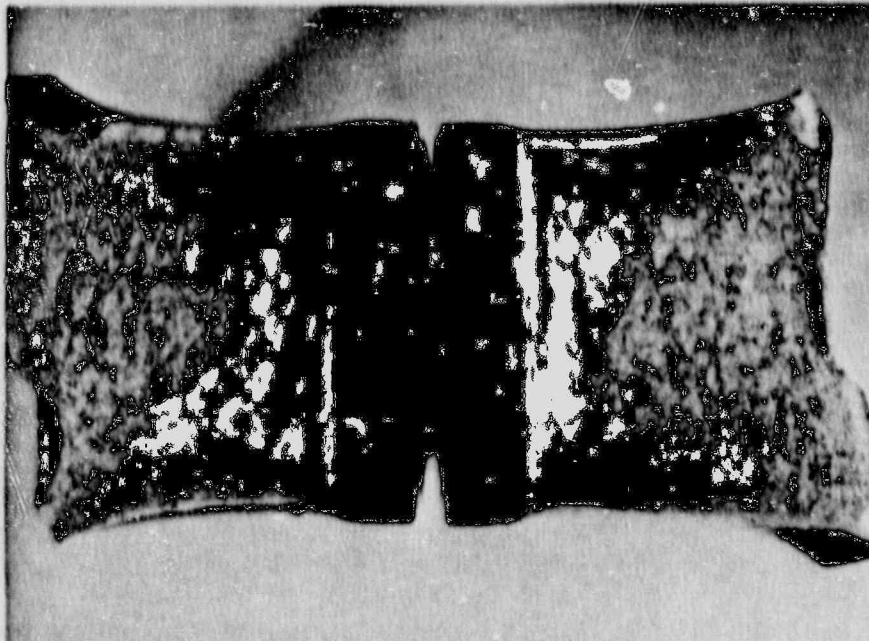
WELD: 7U4
TEMP: 80°F
ENERGY: 54.0 ft-lb

MLE: 41
% SHEAR: 41



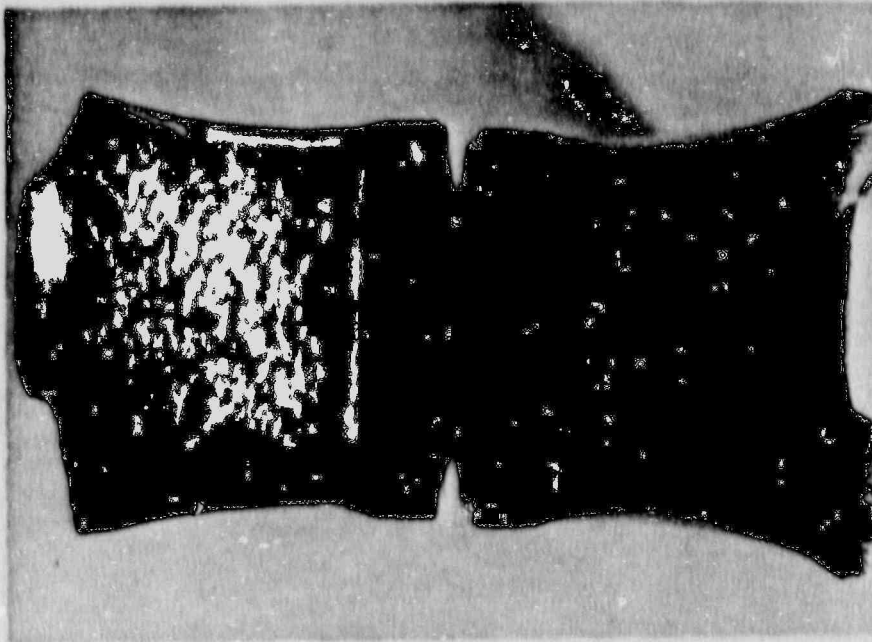
WELD: 7TT
TEMP: 120°F
ENERGY: 82.0 ft-lb

MLE: 70
% SHEAR: 77



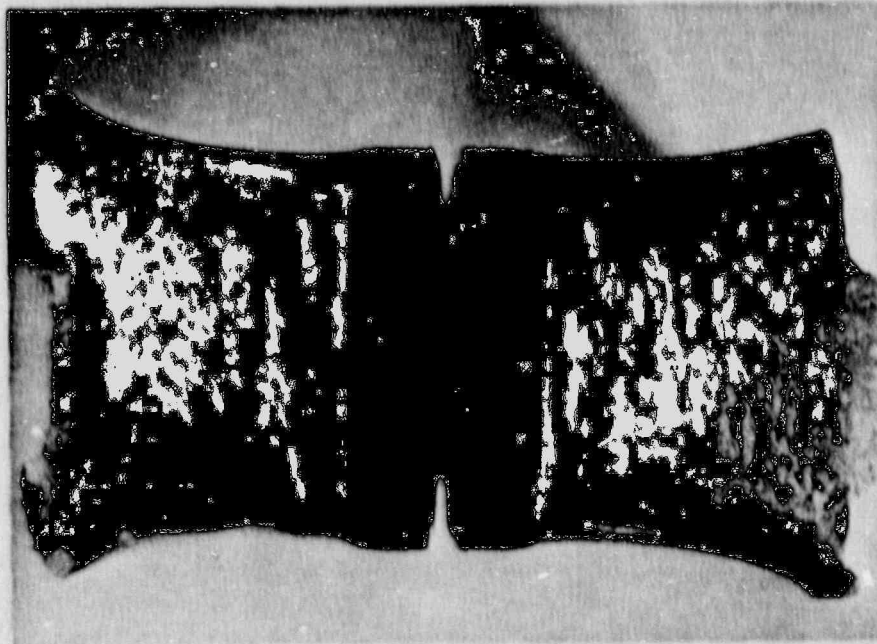
WELD: 7U5
TEMP: 180°F
ENERGY: 101.0 ft-lb

MLE: 77
% SHEAR: 100



WELD: 7TY
TEMP: 200°F
ENERGY: 106.5 ft-lb

MLE: 80
% SHEAR: 100



WELD: 7U7
TEMP: 300°F
ENERGY: 104.0 ft-lb

MLE: 79
% SHEAR: 100

APPENDIX C
BASIS FOR CONSERVATIVE RT_{NDT}

The values of initial RT_{NDT} used in this analysis were, in most cases, based on 30 ft-lb impact energy verification testing, with longitudinal Charpy specimens used for plate, as was standard practice at the time of vessel fabrication. The calculations of initial RT_{NDT} values in Section 3 are based on a GE procedure which establishes conservative values of RT_{NDT} from the fabrication test data. These RT_{NDT} values are expected to be conservative compared to results that would be obtained from current test methods.

For beltline materials, the methods of calculating adjusted RT_{NDT} in Regulatory Guide 1.99, Revision 2 (Rev 2) include a Margin term to be added to the calculated value, ΔRT_{NDT} . The Margin term includes a component for uncertainty in initial RT_{NDT}, σ_I . Rev 2 discusses determination of σ_I for two categories of initial RT_{NDT}, measured values and generic mean values. For generic mean values, σ_I is simply the standard deviation calculated for the data set used to compute the mean. For measured values, requirements for determination of σ_I are somewhat vague. Rev 2 states, "If a measured value of initial RT_{NDT} for the material in question is available, σ_I is to be estimated from the precision of the test method."^a GE's position for RT_{NDT} values derived from measured data, as is the case for the Unit 3 beltline materials, is that σ_I is zero, as explained in the next paragraph.

^a In the Rev 2 draft which was circulated after editing to incorporate public comments, the text stated, " σ_I , the standard deviation for the initial RT_{NDT}, may be taken as zero if a measured value of initial RT_{NDT} for the material in question is available."

The Charpy curves fit to surveillance data, which ultimately provided the ΔRT_{NDT} data for development of Rev 2, were best-estimate fits. An idealized example is provided as Curve 1 in Figure C-1. However, the ASME Code approach to determining RT_{NDT} is based on the lowest value of three specimens exceeding the required limits of impact energy and lateral expansion. A visualization of a Charpy curve drawn on the basis of the Code RT_{NDT} approach is shown as Curve 2 in Figure C-1. In comparing Curves 1 and 2, it is clear that Curve 2, which is based on the lowest value rather than the mean value, provides a conservative estimate of initial RT_{NDT} . Therefore, the current ASME Code method of determining RT_{NDT} from measured data is conservative. Since the method used in Section 3 to calculate RT_{NDT} values is conservative compared to current ASME methods, $\sigma_I = 0^\circ F$ is appropriate.

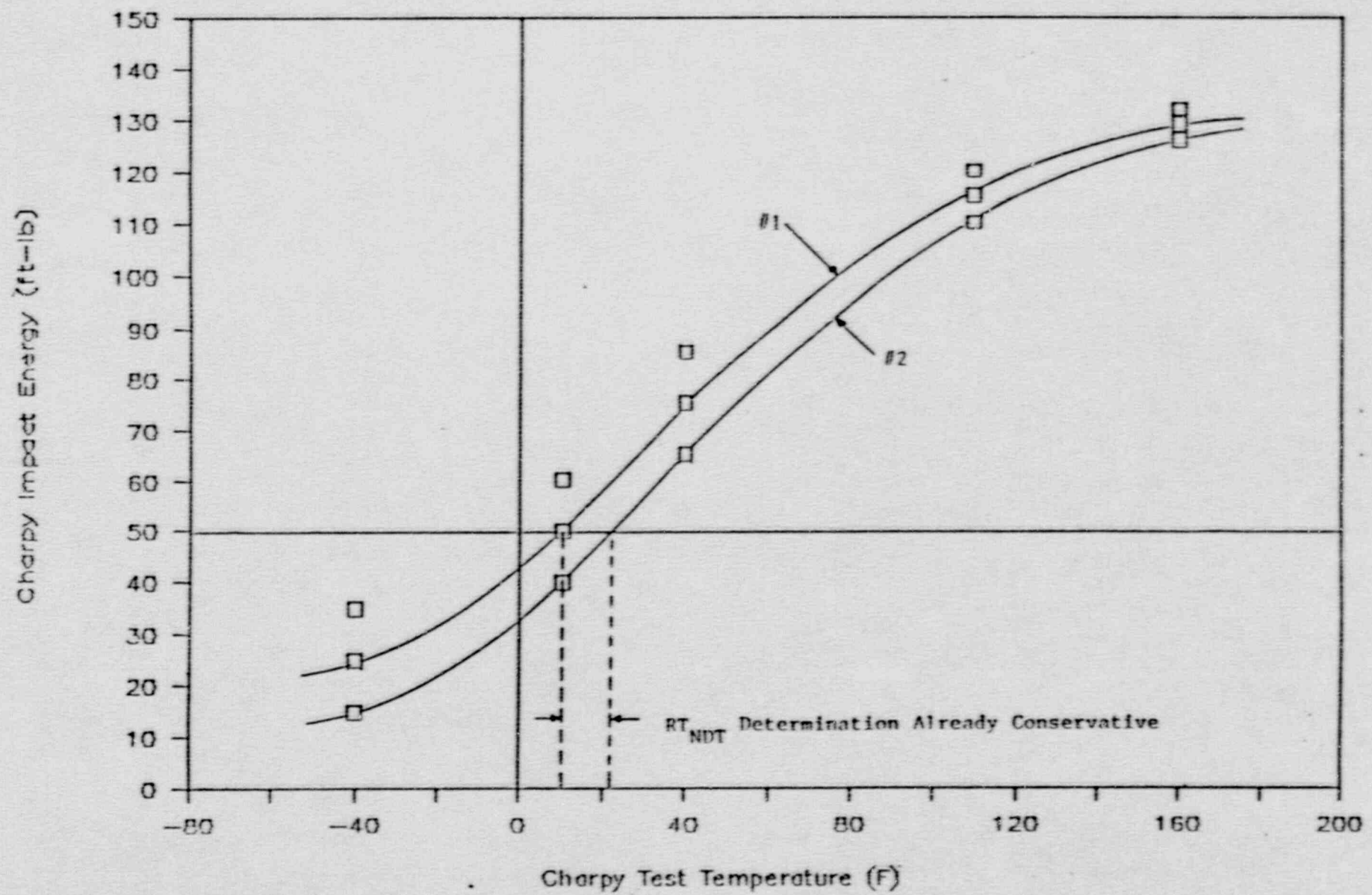


Figure C-1. Comparison of Surveillance Fit and RT_{NDT} Approach

*GE Nuclear Energy
175 Curtner Avenue
San Jose, CA 95125*